Comprehensive screening of persistent organic pollutants in industrial wastewater using GC and LC cyclic ion mobility-high resolution mass spectrometry

By

© Meera Johannah Bissram

A thesis submitted to the School of Graduate Studies in partial fulfillment

of the requirements for the degree of

Master of Science

Department of Chemistry Memorial University of Newfoundland

St. John's, Newfoundland and Labrador, Canada

July 2023

Abstract

Industrial chemicals play an important role in all facets of modern society; from flame retardants in electronics and furniture to non-stick coatings in cookware and food packaging. However, despite their extensive applications and many desired benefits, chemicals are sometimes released during their lifecycle resulting in deleterious ecological and human health effects. Industrial wastewater effluents are rich in chemical pollutants, both known and unknown as well as legacy and emerging. In this study, a combination of screening strategies was used to analyze industrial wastewater samples from over 10 sectors in Ontario for halogenated persistent organic pollutants (POPs). Samples were characterized with both gas chromatographic and liquid chromatographic cyclic ion mobility mass spectrometry (GC/LC-cIM-MS) methods.

A novel non-target screening (NTS) technique utilizing GC-cIM-MS, capable of isolating unknown per- and polyfluoroalkyl substances (PFAS) and other halogenated compounds based on the ratio of their mass and collision cross section (CCS) values, was recently developed in our group. When the combined dataset from GC-cIM-MS analysis of the wastewater samples was subjected to this novel filtering strategy, 344 potentially brominated, chlorinated or fluorinated chemical species were identified from the ~27,000 initially present. Following the application of a previously developed script tool (R code) and manual investigation, 44% of these ions were confirmed to be halogenated. Five compounds belonging to frequently detected classes were identified by suspect screening (e.g., polybrominated diphenyl ethers; PBDEs, polychlorinated biphenyls; PCBs, organophosphate flame retardants; OPFRs and perfluorosulfonamides; PFSMs).

Confirmed suspects represented a mere 14% of the halogenated ions (9% intensity) indicating that 86-91% of the halogenated content is truly “unknown”. A more in-depth look at these unknown ions revealed 19 suspected PFAS including 2 classes that were detected in the environment for the first time. Targeted analyses showed that legacy pollutants such as PBDEs, PCBs, polychlorinated naphthalenes (PCNs) and organochlorine pesticides (OCPs) were either not detected or present at low levels.

For characterization via LC-cIM-MS, wastewater samples were extracted using a tandem solid phase extraction (SPE) technique with weak anion exchange (WAX) and weak cation exchange (WCX) cartridges. LC-cIM-MS experiments revealed the presence of ~50,000 chemical species across all samples and filtering based on CCS and *m/z* yielded 937 likely brominated, chlorinated or fluorinated compounds. Further data reduction and mass defect analysis led to the discovery of roughly 300 potential PFAS by NTS. Only half of them were matched to a suspect screening database implying that the chemical identities of several PFAS in the Ontario environment are unknown. Multiply charged ions formed during electrospray ionization were found to be non-problematic when filtering data using CCS and *m/z*. As such, this novel way of data prioritization is a promising approach for PFAS discovery in complex samples when analyzed by LC-ESI-IM-MS. GC-APCI-IM-MS was also found to be a complementary technique for PFAS discovery since comparable numbers were identified using the same workflow.

Acknowledgements

I would like to thank my supervisor Dr. Jobst for his guidance in completing this master's degree. I am grateful to have had the opportunity to receive training on such an advanced and powerful instrument. My love and enthusiasm for mass spectrometry has flourished in these 2 years. It is with great appreciation that I acknowledge Drs. Katz, Bottaro, Reader, Pansare, Fridgen, Blundell and Burchell for the kindness and support they showed me in the final months of my program. It certainly made a world of difference during a difficult time. I extend my heartfelt thanks to Debbie Hickey for her assistance with administrative matters and Yvette Favaro for her excellent supervision during my tenure as a Teaching Assistant.

I would also like to express gratitude to my colleagues who have now become my close friends - Mahin, Xiaolei, Roshanak and Amber. I consider myself lucky to have had such smart, caring, and fun group members on this journey. I am beyond grateful to my parents, sisters (Kamini & Jessica), partner (Nox) and roommate (Andrea) for their love, encouragement, and roles as sounding boards. I could not have done it without you all. Special thanks to my uncle and aunt in Ontario whose support during my Canadian endeavors has been a constant source of motivation. Finally, none of this would be possible without the blessings of God. I sincerely thank him for giving me the health, determination, knowledge, and courage to achieve my goal.

Preface

This thesis is an original work by Meera Bissram. Conceptualization of the research topics in Chapters 2 and 3 was performed by the author, Dr. Karl Jobst, Sonya Kleywegt, Dr. André Simpson, and Dr. Myrna J. Simpson. For both these chapters I was responsible for methodology design and validation, data collection, formal analysis as well as composition of the manuscripts. Samiha Subah synthesized a standard that led to the confirmation of a tentatively identified PFAS in Chapter 2. Dr. Karl Jobst, Sonya Kleywegt, Dr. André Simpson, and Dr. Myrna J. Simpson reviewed and edited the manuscripts (Chapters 2 and 3). Dr. Frank Dorman contributed the gas chromatograph that was instrumental for data collection in Chapter 2. Finally, resources and supervision were provided by Dr. Karl Jobst who additionally performed project administration and acquisition of funds.

The research, of which this thesis is a part, was funded by the Canada Foundation for Innovation (CFI), the Natural Sciences and Engineering Research Council (NSERC), the Newfoundland and Labrador Department of Industry, Energy and Technology, and the Government of Ontario (Canada-Ontario Agreement grant #2505). Such support does not indicate endorsement by the Government of Ontario of the contents or conclusions of this contribution. The author would like to thank the following municipalities and staff for their support in collecting the wastewater samples used in this project: The Regional Municipality of Peel, The City of Sarnia and Katherine Gray, The City of Vaughan, Nima Javardi and Jordan Balch and The Regional Municipality of York and Fai-Chi Ng.

Furthermore, the author extends profound gratitude to Sonya Kleywegt for coordinating sample shipments and sharing her vast knowledge on Ontario wastewater policies.

Table of Contents

List of Tables

List of Figures

List of Abbreviations and Symbols

Abbreviation/Symbol	Description
$Å^2$	Square angströms
AC	Alternating current
ADONA	Ammonium 4,8-dioxa-3H-perfluorononanoate
APCI	Atmospheric pressure chemical ionization
APPI	Atmospheric pressure photoionization
ASE	Accelerated solvent extraction
BAF	Bio-accumulation factor
BCF	Bio-concentration factor
°C	Degree Celsius
CCS	Collision cross sections
CID	Collision induced dissociation
cIM	Cyclic ion mobility
Cl/Br	Chlorinated/brominated
Cl-PFESA	Chlorinated polyfluoroalkyl ether sulfonates
2D-HCA	Two-dimensional hierarchical cluster analysis
DC	Direct current
DCM	Dichloromethane
DDA	Data-dependent acquisition
DF	Detection frequency
DIA	Data-independent acquisition
DT	Drift time
DTIMS	Drift tube ion mobility spectrometry
ECD	Electron capture detector
EI	Electron ionization
ESI	Electrospray ionization
eV	Electron volt
FOSAs	Perfluorooctane sulfonamide

FOSEs	Perfluorooctane sulfonamidoethanols
FTEOs	Fluorotelomer ethoxylates
FTOHs	Fluorotelomer alcohols
FTSAs	Fluorotelomer sulfonic acids
GC	Gas chromatography
HBCD	Hexabromocyclododecane
HCl	Hydrochloric acid
He	Helium
HFPO-DA	Hexafluoropropylene oxide dimer acid
HPLC	High performance liquid chromatography
HRMS	High resolution mass spectrometry
HRMS/MS	High resolution tandem mass spectrometry
IE	Ionization energy
IM	Ion mobility
IMS	Ion mobility spectrometry
IS	Internal standards
IUPAC	International Union of Pure and Applied Chemistry
K_{ow}	Octanol water partition coefficient
L	Liter
LLE	Liquid liquid extraction
LOD	Limits of detection
LOQ	Limits of quantification
LRMS	Low resolution mass spectrometry
LRTP	Long range transport potential
m	Meter
mm	Millimeter
MD	Mass defect
MDL	Method detection limit
MISA	Municipal Industrial Strategy for Abatement

mL	Milliliter
MP	Mobile phase
ms	Millisecond
MS	Mass spectrometry
MS/MS (or MS^2)	Tandem mass spectrometry
m/z	Mass to charge ratio
N_2	Molecular nitrogen
NaOH	Sodium hydroxide
ng	Nanogram
ng/L	Nanogram per liter
N-EtFOSAA	*N*-Ethyl perfluorooctane sulfonamido acetic acid
NIST	National Institute of Standards and Technology
N-MeFOSAA	*N*-Methyl perfluorooctane sulfonamido acetic acid
NTS	Non-target screening
OCPs	Organochlorine pesticides
OPFRs	Organophosphate flame retardants
Pa	Pascal
PBDEs	Polybrominated diphenyl ethers
PCBs	Polychlorinated biphenyls
PCDD/Fs	Polychlorinated dibenzo-p-dioxins and dibenzofurans
PFAAs	Perfluoroalkyl acids
PFAS	Per- and polyfluoroalkyl substances
PFCAs	Perfluorocarboxylic acids
PFHxS	Perfluorohexane sulfonic acid
PFOA	Perfluorooctanoic acid
PFOS	Perfluorooctane sulfonic acid
PFSAs	Perfluorosulfonic acids
pg/m^3	Picogram per meter cube

pg/µL	Picogram per microliter
POPs	Persistent organic pollutants
POSF	Perfluorooctane sulfonyl fluoride
PTFE	Poly(tetrafluoroethylene)
ppm	Parts per million
QqQ	Triple quadrupole
Q-TOF	Quadrupole-time-of-flight
RF	Radio frequency
RSD	Relative standard deviation
RT	Retention time
s	Second
SC	Stockholm Convention
SCFPs	Side-chain fluorinated polymers
SP	Stationary phase
SPE	Solid phase extraction
TDCPP	Tris(1,3-dichloro-2-propyl)phosphate
TOF	Time-of-flight
TPs	Transformation products
TWs	Traveling waves
TWIMS	Traveling-wave ion mobility spectrometry
µA	Microamp
µL	Microliter
µm	Micrometer
UHPLC	Ultra-high performance liquid chromatography
UNEP	United Nations Environment Programme
UP	Ultra-pure
U.S. EPA	United States Environmental Protection Agency
V	Volt
VP	Vapor pressure

v/v	Volume/volume
WAX	Weak anion exchange
WCX	Weak cation exchange
WWTPs	Wastewater treatment plants
XICs	Extracted ion chromatograms

Chapter 1. Introduction

1.1. Persistent Organic Pollutants (POPs)

1.1.1. Definition

Persistent organic pollutants are defined as "organic compounds that are resistant to environmental degradation through chemical, biological, and photolytic processes". They are characterized by their ability to persist in the environment for extended periods, bioaccumulate in humans and animals, undergo long-range transport and exhibit toxicity towards humans and the environment.[1] The Stockholm Convention (SC) is a global treaty under the United Nations Environment Programme (UNEP) that was adopted in 2001 with the goal of protecting humans and the environment from harmful chemicals by restricting or eliminating their production and release into the environment.[2] Currently, there are 31 chemicals or classes of chemicals listed in the SC most of which are polyhalogenated compounds. They include several organochlorine pesticides (OCPs) (e.g., dichlorodiphenyltrichloroethane and dieldrin), chemicals produced for industrial use (e.g., polychlorinated biphenyls (PCBs), polybrominated diphenyl ethers (PBDEs) and some per- and polyfluoroalkyl substances (PFAS) and those unintentionally produced (polychlorinated dibenzo-p-dioxins and dibenzofurans (PCDD/Fs)).[3] Figure 1.1 illustrates some of these examples.

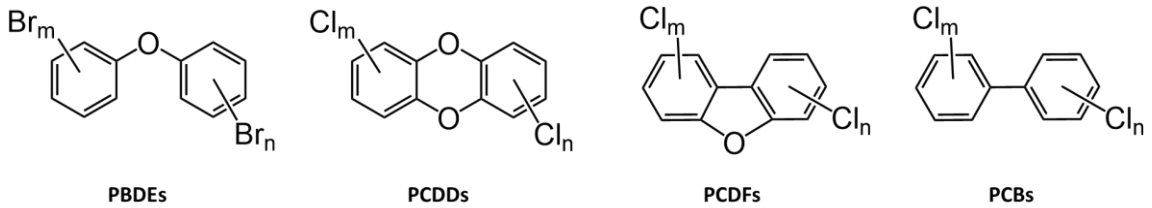

Figure 1.1. The chemical structures of some common persistent organic pollutants.

According to Annex D of the SC, for a chemical to be considered persistent it must possess a half-life of more than 2 months in water or greater than 6 months in soil or sediment. Fulfilling any one of these criteria in any medium satisfies the requirement.[3] Since most POPs are halogenated, their persistence can be attributed to the high bond strength of the carbon-halogen bonds.[4] POPs can have half-lives of several years, even decades in different environmental media. For instance, PCB congeners have estimated half-lives ranging from 3-38 years in soil and sediments and 0.2-27 years in water.[5] Due to their lipophilic and hydrophobic character, POPs tend to preferentially bind to the lipids of organisms rather than the aqueous medium inside cells.[6] They bioaccumulate in fatty tissues where the metabolism rate is low and eventually biomagnify or become concentrated as they move through the food chain. For the bioaccumulation criteria to be met under the SC, the bio-concentration factor (BCF) or bio-accumulation factor (BAF) in aquatic species for the chemical must be greater than 5,000. If neither of these are available, the log of the octanol water partition coefficient (log K_{ow}) will be considered and must be greater than 5.[3]

As a result of their persistence, POPs undergo a phenomenon known as long-range transport where they are distributed throughout the planet, including regions where they have never been used. Their semi-volatile nature facilitates transport via the atmosphere[7] but distribution through the aquatic environment is also possible, especially for more polar POPs like PFAS.[8, 9] A half-life greater than 2 days in air is the criterion required by the SC for a chemical that migrates through the atmosphere.[3] Atmospheric half-lives on the order of years have been noted for many POPs in the Antarctic.[10] Concerning levels of the

chemical must also be found in locations far from the source of release.[3] Relatively high average air concentrations of 83 to 120 and 60 to 80 pg/m^3 have been measured for the OCPs hexachlorobenzene and α-hexachlorocyclohexane in the Arctic.[11] As these substances have never been used in these polar areas, their presence there illustrates long range transport potential (LRTP).[7] Atmospheric transport of POPs to the cold Arctic and Antarctic regions usually occurs via a process called the "grasshopper effect" in which repeated cycles of warm volatilization and cold deposition cause POPs to move away from tropical and temperate climates to colder regions.[12] Wania and Mackay[12] proposed 4 categories to describe the global atmospheric transport behavior of POPs according to their

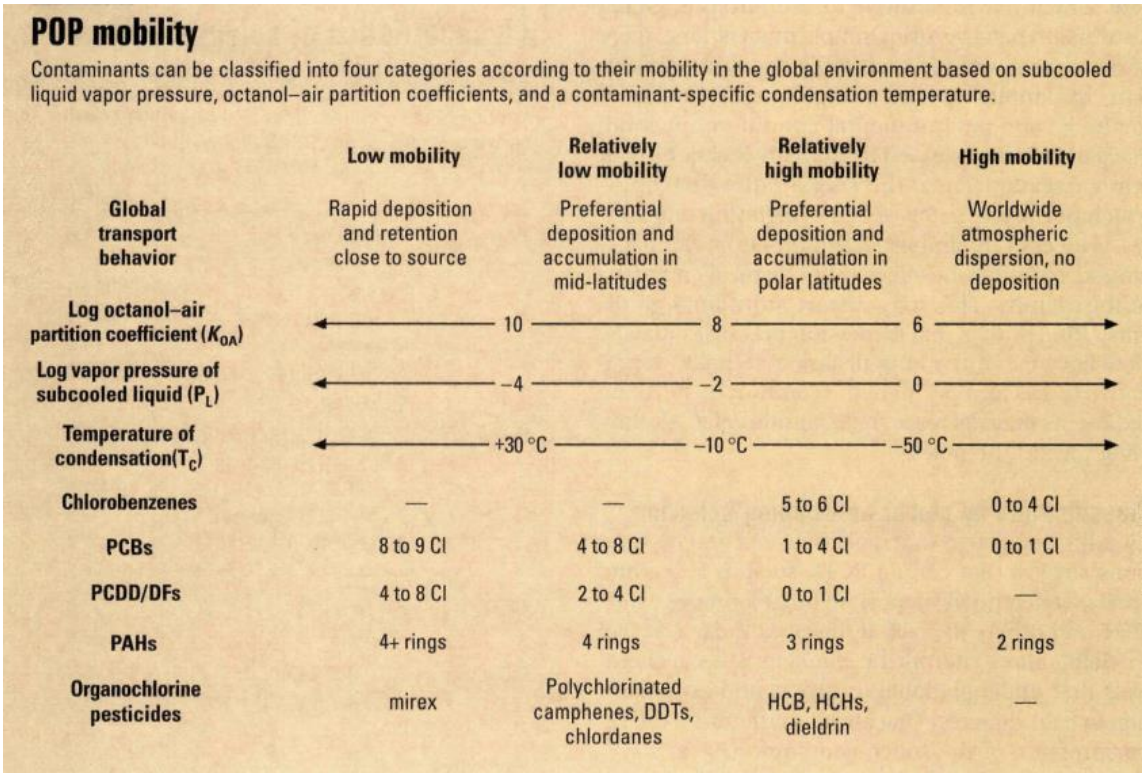

Figure 1.2. Classification of global transport behavior of POPs according to their mobility. Reprinted with permission from Wania and Mackay.[12] Copyright © 1996, American Chemical Society.

mobility. One factor influencing this classification is vapor pressure (VP). Highly volatile compounds with high VP (>1 Pa) do not readily condense at ambient temperatures and are therefore classified as having high mobility with consequent worldwide atmospheric circulation. Those with lower mobility are subject to temperature dependent deposition at varying latitudes.[12] Figure 1.2 displays the other 3 categories of mobility as well as other factors upon which the classification is based.

The final criterion that must be met under the SC for a chemical to be considered a POP is that it should cause adverse effects to human health or to the environment.[3] Numerous POPs have been identified as endocrine disrupting chemicals meaning that they interfere with the normal functioning of endogenous hormones.[13] They also cause complications such as learning disabilities, birth defects, cancer, reproductive problems and behavioral, neurological, and immune system disorders in wildlife species and humans.[6] POPs can have long half-lives between 5-15 years in humans.[13] Moreover, for most POPs, the bioaccumulation in an organism increases with age.

As a result of the SC and other control efforts, there has been a worldwide decrease in the environmental concentrations of legacy POPs.[14] However, within the last 2 decades, hundreds to thousands of chemicals that have the potential to be POPs have been identified through *in silico* screening of chemical inventories. The results suggest that more than half of these chemicals are halogenated,[15] a cause for concern due to the extensive problems already documented for legacy halogenated POPs. Initially there were 12 categories of POPs included on the original SC list in 2001.[2] Since then, several additions have been

made and a continuance of this trend can be expected as research into emerging chemicals with POP-like characteristics progresses.

1.1.2. Per- and polyfluoroalkyl substances (PFAS)

PFAS are a family of chemicals (>5000) that have been in production and use for over half a century.[16] Due to the high polarity and strength of the carbon-fluorine bonds, PFAS possess unique physicochemical attributes such as high thermal and chemical stability,[17] surfactant properties as well as resistance to oil and water. These desirable properties have resulted in their widespread use in industrial and consumer products including cosmetics, textiles, food packaging, pesticide formulations and firefighting foams.[18] However, the same characteristics that make PFAS valuable, also contribute to their omnipresence and persistence in the environment and biota.[19] The chemical structures of some well-known classes of PFAS including perfluorocarboxylic acids (PFCAs) and perfluorosulfonic acids (PFSAs) are illustrated in Figure 1.3. PFCAs and PFSAs belong to a broader family called perfluoroalkyl acids (PFAAs). "Long-chain" PFAAs refer to PFCAs containing eight or more carbons and PFSAs with six or more carbons.[20]

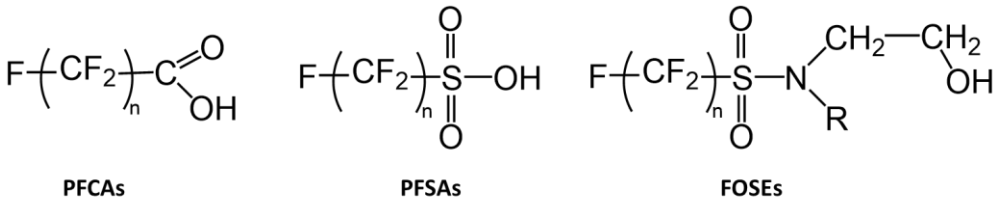

Figure 1.3. The chemical structures of some well-known classes of PFAS.

One of the earliest detections of PFAS in human blood occurred in 1976.[21] However, it was not until 2001 that the extent of global contamination was shown for perfluorooctane sulfonic acid (PFOS) in wildlife.[22] Current evidence demonstrates the

presence of several other PFAS in the blood of humans and animals worldwide.[23] Concerns about the potential environmental and human health impacts of certain long-chain PFAAs have led to voluntary industrial phase-outs and various domestic, regional or international restrictions and regulations to reduce environmental releases of these compounds.[20, 24] In particular, PFOS, perfluorooctanoic acid (PFOA) and perfluorohexane sulfonic acid (PFHxS) (together with their salts and related compounds) were added to the SC in 2009, 2019 and 2022, respectively.[25] The results obtained by Land et al.[23] suggest that these efforts have resulted in a decline or leveling off of concentrations for these chemicals in humans. However, an increase in the concentrations of other long chain PFCAs (C9-C14) was noted for most matrices and regions studied and was attributed to increased use of alternative PFAS.

The persistent nature of PFAS is due to the perfluoroalkyl ($C_nF_{2n+1}-$) and perfluoroether ($C_nF_{2n+1}-O-C_mF_{2m+1}-$) moieties that are resistant to degradation under natural conditions. Although certain PFAS may undergo partial degradation in the environment and biota, they will inevitably transform into end products such as perfluoroalkyl or perfluoroalkyl(poly)ether acids, which are highly stable and persistent.[18] Due to their persistence and water solubility, PFAS can be directly transported to remote environments such as the Arctic by oceanic currents.[8, 26, 27] Another important long-range transportation pathway is the atmospheric transport of neutral and volatile PFAS such as fluorotelomer alcohols (FTOHs), perfluorooctane sulfonamidoethanols (FOSEs) and perfluorooctane sulfonamides (FOSAs).[28, 29] These airborne precursors can be degraded by

atmospheric oxidation to form PFAAs and then undergo wet and dry depositions in isolated regions.[29]

While neutral hydrophobic organic chemicals tend to accumulate in storage lipids, PFAAs show a preference for blood and liver, as well as other tissues.[30-32] Binding to proteins such as serum albumin and liver fatty acid binding protein is thought to be an important pathway in PFAAs bioaccumulation.[33] Since PFAAs differ from typical lipophilic POPs, traditional methods of assessing bioaccumulation potential using BCF or K_{ow} are either inadequate or inappropriate. For instance, the high solubility of PFOA was linked to a faster elimination through the gills of fish resulting in a low BCF of 1.8-27.[18] However, elimination from humans is slow and can take years.[18, 34] Due to their hydrophobic and lipophilic nature, direct measurement of the K_{ow} of PFAAs is impossible because they tend to form three immiscible layers when added to an octanol and water mixture.[35] As a result, alternative evidence must be considered to evaluate PFAAs bioaccumulation. The bioaccumulation potential of PFOS has been inferred from field evidence of PFOS biomagnification and trophic magnification.[36] Biomagnification factors (the concentration in an organism relative to its diet) between 10 and 4000 have been documented for many organisms worldwide with animals at higher trophic levels possessing higher PFOS concentrations than those at lower levels.[37] Several other PFASs have been shown to accumulate in food chains, including those in remote environments such as the Arctic.[38] Positive correlations have been observed between BCF/BAF and fluoroalkyl chain length for PFAAs.[39] In addition, PFSAs were typically found to be more bioaccumulative than PFCAs of an equivalent number of $–CF_2$ units. For emerging PFAS

F-53B (chlorinated polyfluoroalkyl ether sulfonate), BAFs higher than PFOS were reported for amphibians and fish in Chinese freshwater ecosystems.[40, 41]

Major PFAS exposure pathways for humans are directly through the consumption of contaminated food and drinking water. Other sources of exposure include air, indoor dust and personal care products.[42] For wildlife, point-source contamination of their habitats, dietary sources and even maternal transfer to fetuses are possible routes of exposure. Human epidemiological studies and research conducted in laboratories on animals reveal that exposure to certain PFAS is correlated with numerous negative health outcomes.[34] Toxicity studies have mainly focused on PFOS, PFOA, and some other long-chain PFAAs. However, fluorotelomers, shorter chain PFAAs, as well as replacement PFAS chemicals (such as GenX) have been the subject of recent attention.[43-45] In laboratory animal models, PFAS exposure has been linked to hepatotoxicity, tumor induction, developmental toxicity, immunotoxicity, neurotoxicity and endocrine disruption.[34] Similar results have been obtained in human epidemiological studies, with PFAAs exposure (primarily PFOA and PFOS) being associated with high cholesterol, adverse reproductive (decreased fertility), developmental (decreased fetal growth) and immunological (decreased vaccine response) effects.[36, 46, 47]

GenX chemicals have been in use since 2009. More than a decade later and there are still no epidemiological studies on health effects in humans.[44] A recent study by Arp et al.[48] has alluded to the fact that there are millions of PFAS chemicals in existence today. A delay clearly exists between pollutant discovery and research efforts into their potential human health impacts. Being able to efficiently detect and identify these unknown PFAS

is therefore of the utmost importance as it serves as the first step in evaluating the risk posed to humans and the environment and hence, informing regulation.

1.2. Instrumental analysis

Gas chromatography (GC) coupled to numerous traditional detectors such as the electron capture detector (ECD) was the technique of choice in POPs analysis for many years.[49] While ECD is still used as a screening tool[50] or for low cost routine detections,[2] unambiguous identification is not possible and misidentification easily occurs.[49] Mass spectrometry (MS) has been used for POPs analysis since the 1980s and has now become the most popular detection method. It enables the differentiation of co-eluting analytes with different masses as well as the use of the isotope dilution technique.[2] For the separation of isomeric compounds (e.g., PCBs and PCDD/Fs) that have very similar or even identical mass spectra, Reiner et al.[50] notes that chromatographic separation prior to mass spectrometric detection is crucial. GC coupled to high resolution mass spectrometry (GC-HRMS) is becoming routine for separation and quantification of POPs in environmental matrices due to its highly selective and sensitive nature.[49] However, it is worth noting that even GC-HRMS can fail to separate interferences from analytes or between analytes[2] especially in complex matrices containing hundreds of halogenated chemicals. Additional separation can be achieved using multidimensional chromatography (e.g. GC×GC)[51] or by an orthogonal technique such as ion mobility spectrometry.[52]

Liquid chromatography coupled with MS (LC–MS) has also been reported to a smaller extent in the analysis of legacy POPs, especially PBDEs and hexabromocyclododecane (HBCD).[2, 49, 51] On the other hand, LC-MS is the most widely

used technique for the quantitative and qualitative analysis of ionic PFAS such as PFAAs.[53] Most studies used LC coupled to tandem mass spectrometry (LC-MS-MS),[54-59] but HRMS methods have been employed as well.[60-62] GC-MS is usually used for the detection of neutral and volatile PFAS such as the FTOHs, FOSEs and FOSAs.[53] For the analysis of POPs in this thesis, both LC and GC were utilized. Chromatographic instruments were coupled to a cyclic ion mobility-mass spectrometer (cIM-MS). A schematic of this instrument is shown in Figure 1.4 with a discussion of the main components following in subsequent sections.

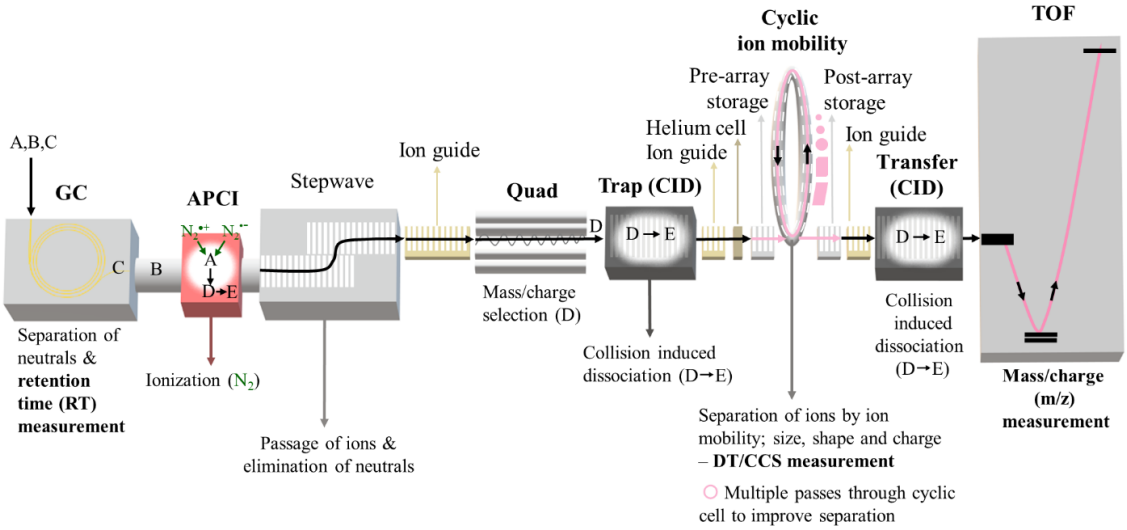

Figure 1.4. Schematic of the GC-APCI-cIM-MS used for instrumental analysis. For experimental work in Chapter 3, the GC is replaced with LC, and the APCI with ESI. Adapted with modifications from Amiri.[63]

1.2.1. Chromatographic separations

Chromatography is an extensively used and powerful method of separation for analytes in complex mixtures.[64] With this technique, components of a mixture are separated due to differences in migration rates as they are carried through a fixed stationary phase

(SP) by a mobile phase (MP). Differential migration occurs because the components are distributed to varying degrees in each of the two phases. Since the solute molecules can only move when they are in the MP, components that have a high distribution in the SP will move through the column more slowly than those with lower distributions, and thus have a longer retention time (RT).[64] Optimizing chromatographic separation lowers the requirements for detection, thereby enhancing the quality of analysis.[50]

1.2.1.1. Gas chromatography (GC)

GC is applicable to compounds that are (semi) volatile and thermally stable. The physicochemical properties of the majority of POPs make them ideal for GC analysis.[51] In GC the MP is an inert gas (e.g., hydrogen, helium or nitrogen) while the SP is usually a liquid adsorbed/bonded to the walls of an open tubular capillary column.[64] The sample is first vaporized and then injected onto the head of the chromatographic column. Analytes are transported through the column by the gaseous MP and selective retardation occurs based on the differential solubility of the analytes in the SP.[50] Separation occurs largely due to differences in the boiling point of compounds and interactions with the SP.[51] Judicious selection of SP, column dimensions, temperature program and MP flow rate are essential to achieving optimal separation.[50] For the separation of POPs, nonpolar and moderately polar SPs are generally used.[65] The SP used to perform experiments in this thesis was low polarity and consisted of 5% diphenyl, 95% dimethylpolysiloxane. General purpose columns such as this can be useful as an initial screen to identify potential contaminants of concern.[51] After separation in the GC column, analytes of different RTs emerge and are quickly transported to the ionization source.

1.2.1.2. Liquid chromatography (LC)

Compared to GC, LC enables the analysis of a wider range of contaminants with very different polarities and chemical properties.[66] LC is the method of choice for the analysis of POPs that are non-volatile, polar, thermally labile, or ionic in nature. However, unlike GC where the mobile phase is inert and does not interact with analyte molecules, LC separations are more complicated due to equilibria of analytes between both the SP and MP.[50] Separations can be performed in an isocratic manner with a single solvent or solvent mixture of constant composition or using gradient elution where two or more solvents of differing polarities are varied in composition during the separation.[64] The most commonly used form of LC for environmental analysis is reversed phase LC employing octadecyl (C18)-bonded silica and octyl (C8)-bonded silica SP.[51] Besides traditional high performance liquid chromatography (HPLC), ultra-high performance liquid chromatography (UHPLC) is also widely utilized for environmental separations. With UHPLC, sub-2μm particle sizes are used resulting in narrower peaks and thus better chromatographic resolution and increased peak capacity. Shorter run times are also possible facilitating high-throughput analyses.[67] Several ionization techniques are compatible with both HPLC and UHPLC including electrospray ionization (ESI), atmospheric pressure chemical ionization (APCI) and atmospheric pressure photoionization (APPI).[51] The experiments performed in this thesis employed UHPLC reversed phase C18 separation followed by ESI.

1.2.2. Ionization

After compounds elute from the GC or LC column they must be ionized or converted into gaseous analyte ions before mass spectrometric analysis can occur. There are two categories of ionization sources: *hard sources* and *soft sources*. With *hard sources* a significant amount of energy is transferred to analyte molecules leaving them in a highly excited energy state. Upon relaxation, bonds are broken yielding many fragments and thus providing useful structural information. On the other hand, s*oft sources* produce little fragmentation and thus supply important information about the molecular mass of analytes. Electron ionization (EI) is an example of a *hard* ionization technique where vaporized analyte molecules are bombarded with a beam of energetic electrons.[68] It is the most commonly used technique for the identification of POPs.[51] The mass spectra of organic pollutants generated by EI are highly reproducible and structure-diagnostic, making it possible to identify a pollutant through spectral library searches.[69] The ionization sources used in this thesis, APCI and ESI, are both classified as s*oft* ionization techniques. Their suitability to POPs analysis is discussed below.

1.2.2.1. Atmospheric Pressure Chemical Ionization (APCI)

There are 2 primary mechanisms that can cause ionization in the APCI source: charge transfer, which is favored by relatively non-polar compounds and protonation, which occurs with more polar compounds.[70] The first step of APCI involves the transport of the GC eluent through the transfer line to the corona pin by a high flow of make-up gas, typically nitrogen (N_2) gas. In both mechanisms, ionization of the N_2 make-up gas due to corona discharge leads to the creation of a plasma containing primary ions (e.g., $N_2^{\bullet+}$ and

$N_4^{\bullet+}$ in positive mode) and electrons. With charge transfer, collisions between these primary ions and organic compounds (M) produce $M^{\bullet+}$ molecular ions if the recombination energy of the primary ions exceeds the ionization energy (IE) of M. However, if water or other protic solvents (S) are present in the source, then they may undergo charge exchange to form $H_2O^{\bullet+}$ or $S^{\bullet+}$. Self-protonation can subsequently occur through the reaction: $S^{\bullet+} + S \rightarrow [S - H]^{\bullet} + SH^+$ resulting in the formation of H_3O^+ or SH^+. If the proton affinity of M exceeds that of S, it can abstract a proton from SH^+ yielding (quasi)molecular ions $[M+H]^+$.[69]

There are several advantages to using APCI in environmental analysis. When collisional cooling happens at atmospheric pressure, fragmentation is reduced and higher yields of (quasi)molecular ions are obtained.[69] Molecular formula determination for unknown compounds hinges on (quasi)molecular ions being detected.[71] Increased quantities of these ions also result in improved detection limits, which can be critical for the analysis of POPs present at low concentrations.[72] Another benefit of APCI is that it enables facile coupling of GC instruments to numerous types of advanced mass spectrometers.[69] Finally, diagnostic ion-molecule reactions that would be challenging to conduct with traditional GC-MS technology, can be easily facilitated by APCI source conditions.[69, 73]

1.2.2.2. Electrospray Ionization (ESI)

ESI is classified as a desorption ion source since it does not require volatilization of analyte molecules prior to ionization. Instead, it requires the formation of ions in solution prior to the transfer to the gas phase. ESI occurs at atmospheric pressure and can be used

to convert liquid samples that are nonvolatile or thermally unstable directly into gaseous ions for MS analysis.[68] In an ESI source, a stainless steel capillary needle is held at a high voltage (several kilovolts, positive or negative) relative to the walls of the surrounding chamber. A solution containing analyte molecules, often as an LC eluant, is sprayed from the capillary. The result is a mist of highly charged droplets having the same polarity as the capillary voltage. A high source temperature and/or a flow of drying gas is employed to assist with solvent evaporation. As charged droplets become smaller, their charge density increases until the electric field strength reaches a critical point where ions at the surface of the droplets are ejected into the gaseous phase.[74] It is not uncommon to observe protonated $[M+H]^+$ and deprotonated $[M-H]^-$ quasi(molecular) ions in positive and negative mode ESI, respectively. However, for analytes that do not have acidic or basic groups, adduct formation can be used to create ions of them. For instance, chloride adducts have been successfully used in negative mode ESI while sodium, lithium, ammonium, or other cationic species are often observed with ESI in the positive mode.[75] Negative mode ESI is the most widely used interface for the analysis of anionic PFAS in environmental samples.[53]

1.2.3. High resolution tandem mass spectrometry (HRMS/MS)

Once ions are generated by either APCI or ESI they are transported through the StepWave, which is an ion transfer device with a unique design that increases ion transmission from the source to the mass analyzer while reducing the passage of the high flow gas, excess solvent, and neutral species.[76] Ions are then focused by the ion guide and sent to the first mass analyzer – the quadrupole. The cyclic ion mobility-mass spectrometer

used in this thesis is a hybrid instrument consisting of quadrupole and time-of-flight (Q-TOF) mass analyzers coupled to a cyclic ion mobility cell.[77] Because there are two mass analyzers, it is considered a tandem mass spectrometer (HRMS/MS). It is also an HRMS system since the TOF mass analyzer can achieve a resolution of 100000.[77] Having such a high resolution allows the instrument to distinguish between peaks with much smaller mass differences[71] thereby reducing interferences. This is especially useful in the analysis of complex samples such as wastewater, which may contain huge numbers of organic contaminants and other matrix components. Another benefit of HRMS is that due to its high mass accuracy, it permits determination of elemental composition for detected ions. Furthermore, HRMS instruments offer high sensitivity (over a wide mass range) when operated in full scan mode thereby allowing femtogram levels of some trace contaminants to be determined.[16]

A quadrupole mass analyzer consists of four parallel cylindrical rods that act as electrodes. Each pair of diagonally placed rods is connected to an equal but opposite DC voltage and a variable radio frequency (RF) AC voltage is superimposed. This produces an electric field that moves ions forward in the space between the rods in an oscillating pattern. The AC and DC voltages on the rod are increased simultaneously while keeping the ratio constant to control ion trajectories within the rods. At any given point, only ions of a certain mass to charge ratio (*m/z*) will have an amplitude of oscillation that allows a stable path through the rods to the detector. All other ions will impact the rods and get neutralized.[68, 74]

In the TOF mass analyzer, the time taken for ions to travel a known distance, typically 1 m, is measured. Flight times are usually on the order of microseconds. Ions are

first accelerated by a pulsed electric field that pushes them in an orthogonal direction to their original trajectory. Accelerated ions enter a field-free drift-tube where separation by mass occurs as ions transit to the detector at the other end of the tube. Since all ions are expected to have the same kinetic energy, their velocities will depend on their masses such that lighter ions will travel faster and arrive at the detector in a shorter time than heavier ones. The measured flight times, t_F, can be used to obtain *m/z* values according to Equation 1.1 where L is the distance from the source to the detector, v is the velocity, e is the charge on an electron, m is the mass of the ion, z is the ion charge state and V is the applied voltage.[68]

$$t_F = \frac{L}{v} = L\sqrt{\frac{m}{2zeV}} \qquad \text{(Equation 1.1)}$$

The quadrupole can function as a mass filter transmitting only ions of a specific *m/z* or in RF only mode, enabling the passage of all ions.[78] In MS experiments, the quadrupole is set to RF-only mode to provide accurate mass full scan data of all ions generated in the ion source. In MS/MS (or MS^2) experiments, the quadrupole is operated in either mass filter mode or RF-only mode transmitting ions to a collision cell where they are bombarded with inert gas molecules (e.g., nitrogen or argon) resulting in fragmentation of precursor ions by a process known as collision induced dissociation (CID).[68] Accurate mass measurements of both product ions and unfragmented precursor ions are then made by the second mass analyzer, or TOF in this case, to obtain important structural information. Both the trap and transfer regions of the instrument (Figure 1.4) located before and after the cyclic ion mobility cell, respectively, can act as collision cells.[77] If CID is performed in the trap, mobilities of fragments, and thus collision cross sections (CCS), can be obtained

thereby assisting in structural elucidation.[73] When CID is done in the transfer region, as is the case for experiments in this thesis, both precursor and product ions have the same mobilities (and CCS), which can facilitate MS/MS spectral cleaning via drift time alignment.[79]

1.2.4. Cyclic Ion Mobility (cIM)

Ion mobility spectrometry (IMS) is a gas phase separation technique where ions travel through an ion mobility (IM) drift cell filled with an inert buffer gas (usually nitrogen or helium) under the influence of an electric field. Separation in the drift cell is based on an ion's mobility, which depends on its size, shape and charge.[80] As ions move through the drift cell in the direction of the electric field, they are slowed down by collisions with the buffer gas. For a given charge, ions with compact structures interact less with the buffer gas than ions with more extended structures and thus traverse the drift cell faster.[81] Ions with increased charges transit the cell faster since they experience greater separation field strengths.[82] The time taken for ions to travel through the IM cell is called the drift time (DT). Measurement of the DT facilitates calculation of a unique molecular descriptor called the collision cross-section (CCS), which is related to the two-dimensional area of an ion's gas-phase conformation and is measured in units of square Angströms ($Å^2$).[83] CCS has been described as "a normalized measure of gas phase size".[84]

IMS separations occur on the millisecond time scale. As a result, IMS is easily coupled to chromatographic and MS instruments, which perform separations on the minute and microsecond range, respectively.[80] IM-MS measurements can be particularly useful in structural investigations such as isomer separation and protein conformational studies.

CCS is beneficial in the analysis of complex matrices since it facilitates DT alignment. This is where signals are grouped according to their DT and background interferences from co-eluting compounds in the mass spectra with different DT can be removed.[85] Together with retention time, exact mass, isotope ratio and fragmentation patterns, CCS values serve as a valuable additional parameter to aid in compound identification and improve confidence in non-target feature annotation.[84, 86] They are unaffected by matrix effects[79, 86] and independent of the chromatographic separation process.[81] Furthermore, CCS values are largely reproducible across different laboratories[86] and instrument platforms[81] although variations can occur based on experimental conditions and drift gas. The utility of IMS hyphenated to MS and LC/GC in the analysis of POPs and other contaminants of emerging concern has been illustrated by many publications within the past decade.[52, 79, 83, 85-90]

There are many existing variations of IM-MS designs with common ones including drift tube IMS (DTIMS), traveling-wave IMS (TWIMS) and trapped IMS (TIMS).[84, 91] However, in combination with other factors, the separation path length limits the resolving power of these conventional IM-MS devices.[92] Recent advancements in commercial IM-MS instrumentation have led to the emergence of a cyclic system from Waters Corporation based on TWIMS.[77] This cyclic ion mobility-mass spectrometer (cIM-MS) delivers improved resolving power via a multi-pass approach. It achieved a resolving power of 750 with 100 passes around the cyclic ion mobility device for two isomeric pentapeptides. The instrument also offers multifunction capabilities such as IM isolation where species outside a specified mobility range can be ejected out of the cIM while the remaining ones continue separating, and IMS^n, analogous to MS^n separation. With this

feature, precursor ions that have already been cIM separated, undergo selective activation followed by further cIM separation of product ions.

Ions exiting the quadrupole of the instrument enter the trap region (Figure 1.4) where they are accumulated and released as packets of ions into the cIM for mobility separation one after the next. In other words, one packet collects in the trap while a second undergoes separation in the cIM cell. When the first packet exits the cIM cell, the second enters and so on. This allows a high duty cycle (close to 100%) to be achieved since minimal ions are lost while separation occurs.[77] Prior to entry into the cIM, ions pass through a cell filled with helium gas (He) that offers two benefits: 1) it reduces ion scattering under the elevated pressure of the cIM device thereby providing high ion transmission and maintaining the sensitivity of the Q-TOF 2) it minimizes activation or fragmentation of ions.[93]

The cIM cell is filled with buffer gas (typically N_2) at a pressure of approximately 2 mbar. It consists of two main parts as shown in Figure 1.4: 1) the main body of the separator, which is located orthogonally to the primary beam path of the spectrometer and 2) the ion entry/exit section, which intersects the main ion optical axis. The main body of the separator contains a series of electrodes in which adjacent plates are subjected to opposite phases of RF voltage. Superimposed on the RF of a pair of adjacent electrodes is a DC voltage that is switched to an adjacent plate pair after a given time resulting in "traveling waves"[94] (TWs) being propagated along the separator. Ions "surf" on a wave through the buffer gas for a period of time and then the wave overtakes. This process is repeated with waves that follow. The mobility of ions dictate how often they are overtaken

by waves such that ions with low mobility get overtaken more frequently than those with high mobility and thus take more time to traverse the IM cell.[77] The ion entry/exit region of the cIM device consists of a planar array of electrodes that control the TW direction thereby facilitating entry of ions into the separator, mobility separation and ion ejection. The combined length of these two regions gives the cIM device a path length of 98 cm for mobility separation. After separation, ions move into the transfer region, which uses axial fields to maintain the reliability of mobility separation and then into the TOF for *m/z* separation. If standard Q-TOF operation of the mass spectrometer is desired, the TWs in the array electrodes are set to allow ions to "bypass" the cIM separator. In this mode, there is continuous transmission of ions to the TOF without accumulation in the trap region.

During multipass experiments a separation time is set to determine how many passes ions will make around the cIM separator before being ejected. If a relatively short separation time is used (2-5 ms), ions undertake a single pass giving a resolution of about 80. For higher mobility resolution, a separation time of several seconds can be used to lengthen the path that ions can travel. Resolution was shown to increase with the square root of the number of passes around the device.[77] When ions undergo multiple passes, it is possible that high-mobility ions catch up to low mobility ones resulting in a phenomenon called "wrap-around" where separation is obscured. Breen et al.[95] recently presented a method for "unwrapping" cIM data to take advantage of the comprehensive two-dimensional nature of the technique when performing multipass experiments. This was achieved by measuring and comparing the DTs of ions during single and multipass separations and then calculating how many passes each ion had made.

With classical DTIMS, CCS values (Ω) can be determined from first principles using the Mason-Schamp equation[88] (Equation 1.2) since the electric field is uniform. This requires experimental conditions such as temperature (T) and pressure (P) in the drift tube to be accurately known.[80] Equation variables are as follows: z is the ion charge state, e is the elementary charge, N_0 is the buffer gas density, m_B and m_A are the masses of the drift gas molecule and analyte ion respectively, L is the length of the drift tube, t_d is the drift time and E is the electric field strength.[88] Equation 1.2 assumes that T and P are in units of Kelvin and Torr, respectively.

$$\Omega = \frac{3ze}{16N_0} \bullet \sqrt{\frac{2\pi}{k_b T}} \sqrt{\frac{1}{m_B} + \frac{1}{m_A}} \frac{t_d E}{L} \frac{760}{p} \frac{T}{273.2} \qquad \text{(Equation 1.2)}$$

This approach cannot be used for instruments based on TWs where the electric field varies. Therefore, like other TWIMS devices, CCS determination with the cIM is achieved through calibration using standards with well-characterized CCS values previously obtained on DTIMS instruments.[77] Comparison between CCS values obtained from DTIMS ($^{DT}CCS_{N2}$) versus TWIMS ($^{TW}CCS_{N2}$) usually give uncertainties of <2%.[81, 96] A study by Gelb et al.[97] on the influence of calibrant ions during CCS determination using TWIMS recommended that molecular class and charge state be matched to ensure more accurate and reproducible CCS values are obtained.

1.3. Data acquisition and processing strategies

Analytical investigations into POPs can be performed utilizing three different data processing strategies: target, suspect and non-target analysis.[54, 60, 85, 98] Target analysis involves the identification and quantification of known substances using reference

standards. With suspect screening, reference standards are unavailable but lists containing compound-specific information are used to search the acquired data for known substances likely to be present. Finally, in non-target screening (NTS) there are no standards, lists or prior information available, only unknown ions whose identities must be determined from the first-principles interpretation of their mass spectra.[71, 99] The HRMS/MS spectrometer used in this research allows a combination of all three strategies to be utilized in an all-in-one approach.[100] Figure 1.5 demonstrates a typical workflow.

There are two major types of data acquisition methods employed in environmental analysis: data-dependent acquisition (DDA) and data-independent acquisition (DIA).[72, 79, 98, 101] Both methods allow quantitative (obtained from the MS full scan) and structural (obtained from the MS^2 spectra) information to be acquired in the same sample run. In DDA mode, the MS instrument performs full-scan and then MS^2 scans are automatically triggered if certain predefined criteria are met (e.g., signal intensity threshold, presence of a compound on a target list, isotope patterns).[102] This method produces high quality MS^2 spectra since there are less interferences. However, it is unable to screen for novel or unknown contaminants and excludes low abundance compounds that may be of interest.[102] With DIA, all precursor ions in the full *m/z* range are fragmented thus permitting the unrestricted and unbiased generation of fragment ion spectra. A disadvantage of DIA is that fragmentation occurs for analytes of interest as well as co-eluting compounds resulting in a complicated MS^2 spectrum that is difficult to deconvolve and interpret.[72] This has led to a preference for DDA versus DIA (60% vs 19%) in the NTS process.[103] Nevertheless, DIA remains an attractive option for wide scope screening of unknown contaminants and

retrospective analysis.[102] One way of performing DIA is using an MS^E method where all precursor ions are fragmented simultaneously by alternating low and high collision energies producing full precursor and product spectra. Data for this thesis was collected using DIA in the MS^E mode.

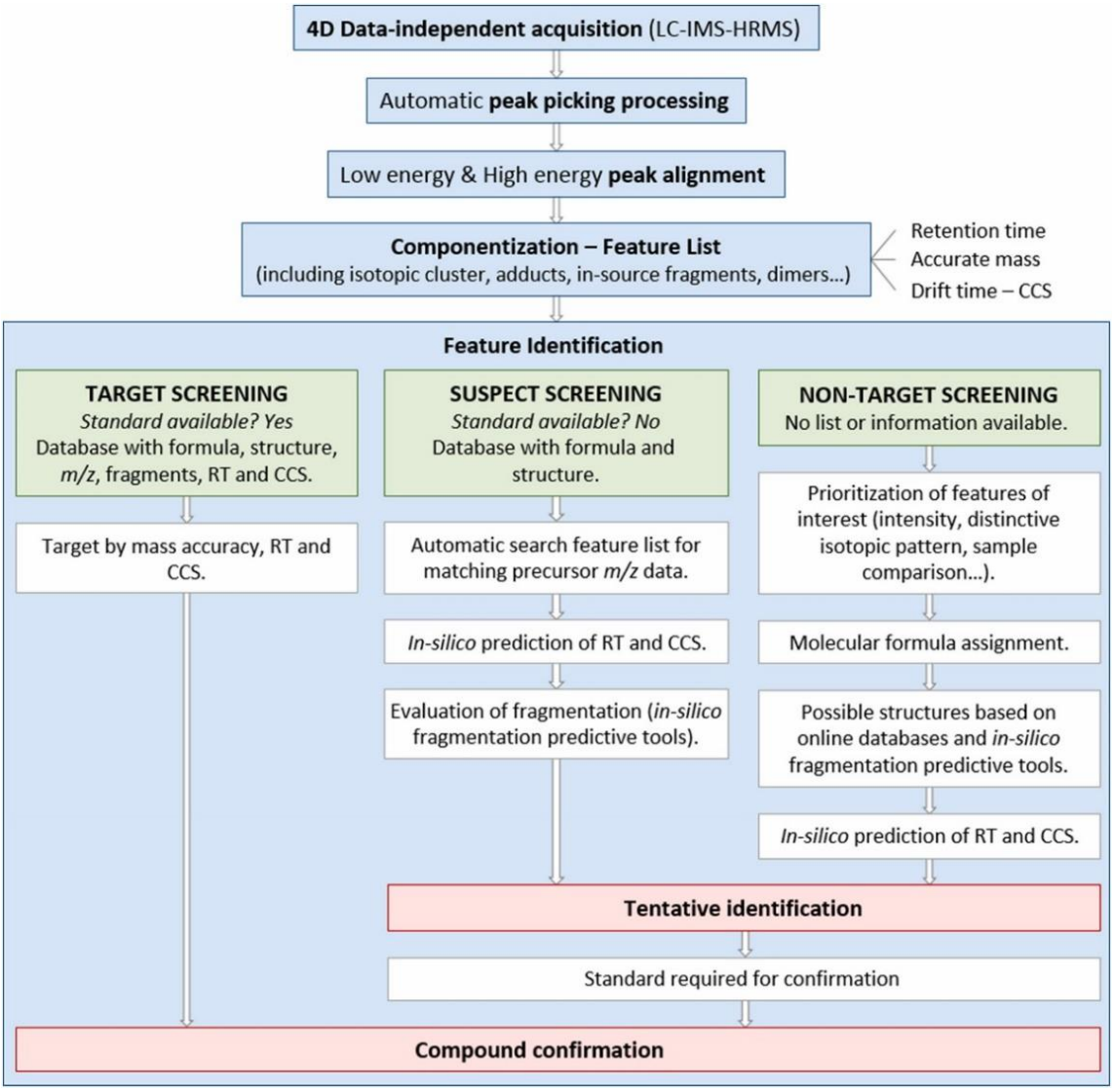

Figure 1.5. An example LC-IMS-HRMS workflow illustrating the all-in-one approach to target, suspect and non-target screening. Reprinted with permission from Celma et al.[79] Copyright © 2021, Elsevier Ltd.

Once acquired, steps must be taken to reduce the quantity and complexity of the data.[71] While most workflows include similar steps, differences may exist in the execution.[104] The first step involves peak picking or feature detection (Figure 1.5), which can be achieved using vendor specific software or other open access tools. The peak picking algorithm creates features (peaks) by combining *m/z*, RT and intensity/area.[103] At this stage noise removal can be performed, the simplest form of which removes datapoints below an intensity threshold set by the user. For instance, an intensity threshold of 100 counts per second was used by Bader et al.[105] to differentiate instrumental noise from real peaks. Subtraction of compounds present in blanks (procedural, solvent or field blanks) may also be done. Next up is componentization where all signals belonging to a single compound (e.g., isotopic peaks, adducts, in-source fragments, etc.) are grouped together based on RT, accurate mass and CCS (when available). Components/peaks can also be aligned across several samples to facilitate further processing by statistical methods such as principal component analysis, clustering and regression analysis.[71] For NTS, prioritization strategies need to be implemented to isolate compounds of interest from the wealth of HRMS data generated.[104] Attempts at feature identification can then be made through molecular formula assignment, spectral library matching, *in silico* fragmentation, etc.[103] Feature prioritization and identification will be discussed further in subsequent sections.

1.3.1. Target analysis

Current analytical methods for targeted analysis of POPs typically employ GC or LC coupled to low resolution mass spectrometry (LRMS) instruments with a triple

quadrupole (QqQ).[54, 56, 57, 106-108] These techniques are characterized by high sensitivity (low femtogram detection) and selectivity since interfering ions from complex matrices can be filtered out.[50] However, they focus on a limited number of analytes and can be difficult to set up as compound-specific MS conditions such as product ion masses, ion-source parameters, and collision energies need to be optimized for each analyte.[66] Target analysis using HRMS in full-scan mode overcomes these limitations because an unlimited number of analytes can be detected simultaneously without pre-selecting precursor or product ions. In addition, sensitivity and selectivity comparable to QqQ-LRMS can be achieved in full scan mode.[67] HRMS is also beneficial in target analysis at the analyte confirmation stage where the acquisition of accurate mass product ion spectra facilitates comparison of fragmentation patterns between standards and analytes. A disadvantage of the QTOF-HRMS in quantification is the limited linear dynamic range (2-3 orders of magnitude), which is ten times lower than QqQ-LRMS.

To obtain reliable identification and confirmation of target compounds, certain guidelines should be followed to establish confidence. For this purpose, a five-level system proposed by Schymanski et al.[109] was utilized in this thesis. The reference standard should be measured under the same analytical conditions as the sample containing the analyte to enable proper comparisons. Then, MS (exact mass, isotope, adduct), MS/MS (i.e., fragmentation) and RT matching allow target compounds to achieve Level 1 assignments or *confirmed structure* status. Additional evidence can be supplied by orthogonal methods (e.g., CCS) when possible.

Literature reports of QTOF use for quantification of analytes in environmental analysis are few.[110, 111] Nevertheless, when HRMS instruments are used for targeted analyses, method validation similar to LRMS should be performed.[66] Parameters to be evaluated include linearity, precision, recovery, matrix effects, and limits of detection (LOD) and quantification (LOQ). Method validation ensures that an analytical method is fit for its intended purpose and generates reliable results.[112] A calibration curve must be constructed to determine the relationship between known amounts of analyte and the response of the instrument. IUPAC guidelines recommend six or more calibration standards measured in at least duplicate. The calibration range should extend between 50-150% of the expected sample concentrations and standards should be evenly spaced over this range.[113] The use of isotope dilution is common to correct for potential recovery losses or minimize matrix effects.[62, 114, 115] Assessing recovery is one way of demonstrating the trueness of the method.[112] The goal is to determine how well repeated measured values agree with the true value. To determine recovery, known amounts of analyte are spiked into the sample matrix and the percentage of the quantity measured to the true value is calculated. Another way of ascertaining recovery is to use certified reference materials if available. Although close to 100% is desirable, lower recoveries are acceptable if the sensitivity of the method is adequate. The precision of the method, which seeks to characterize how close replicate measurements are to each other, can also be found from these spike/recovery experiments. It is usually expressed as absolute standard deviation (s or SD), relative standard deviation (RSD), coefficient of variation (CV) or variance (s^2).[112] LOD sometimes referred to as method detection limit (MDL) represents the lowest

amount of analyte that can be reliably distinguished from zero.[113] One approach of determining MDL is to analyze at least seven replicate samples free from or containing low level of the target analyte and then multiply the standard deviation by the student's t-value at a 99% percentile for n−1 degrees of freedom.[116] Evaluation of the parameters described previously was deemed sufficient for the scope of work in this thesis.

1.3.2. Suspect screening

Suspect screening lists generally contain molecular formulae, accurate masses and structures of compounds that are likely constituents of a sample. Compounds on these lists can be transformation products (TPs), pesticides, pharmaceuticals, potentially persistent and bioaccumulative organic chemicals in commerce, etc.[99] Larger compound databases such as the United States Environmental Protection Agency (U.S. EPA) CompTox Chemistry Dashboard can also serve as suspect lists and may prove useful for obtaining literature references or patent information.[71] The suspect screen is performed by comparing the list of experimental features to the suspect list under constraints such as mass accuracy <5 ppm. Hits obtained at this stage are not enough for identification alone.[109] Observed isotopic ratios should be checked for close agreement with that predicted for the molecular formula of the suspect, and fragmentation data should be evaluated. Spectral library searches can be performed using literature, publicly available databases such as ChemSpider, NIST, PubChem and Massbank, or with commercial ones like Agilent Water Contaminant LC/MS Personal Compound Database and Library. Care must be exercised when matching MS/MS spectra since the number and abundance of fragments may vary depending on the collision energy used.[117] Difficulties may also be encountered at this stage

if experimental mass spectra contain only one or a few fragments that are common to most candidates.[118] Although MS/MS libraries continue to expand, coverage is currently limited to several thousand chemicals.[71] As such, not all suspect hits will yield spectral library matches. In these cases, *in silico* fragmentation tools (e.g., MetFrag) can be employed.[119] This approach uses algorithms to propose a list of potential candidates from large compound databases (e.g., PubChem) based on the assigned molecular formulae or exact mass. These candidates are then fragmented and the resulting theoretical MS/MS spectra are compared to the experimental one generating match scores that require expert knowledge for consideration and final selection.[103] Additional evidence to support identifications can be obtained by predicting chromatographic retention times[120, 121] and using experimental or predicted CCS. [79, 85, 86, 88, 122] Suspect screening is advantageous in cases where standards are not yet commercially available (e.g., TPs or by-products). It also makes it possible to survey which compounds are present before spending exorbitant amounts of cash on standards for target analysis.

1.3.3. Non-target screening (NTS)

NTS is essential in the detection and identification of compounds that have not yet been reported in the environment. In this quest, feature prioritization is necessary to isolate relevant sample components such as those possessing toxicity, exhibiting persistence, or undergoing transformations. Strategies for prioritization in NTS have been comprehensively summarized in the literature.[71, 103, 117] Intensity-based[98, 101] and statistical approaches[83, 123] are common. With the former, high intensity features are hypothesized to correspond to higher sample concentrations and therefore greater environmental

significance. However, this assumption may not always hold true as features with lower intensities can display high toxicity.[103, 117] Statistical prioritization techniques are useful for handling sample sets where sampling locations, sampling periods and/or treatments vary.[71] The disadvantage with this approach is that many replicates are required to ensure sufficient statistical power when comparing differences between groups.[103]

Prioritization strategies for the NTS discovery of PFAS have largely focused on mass defect filtering, homologous series searching and CF_2-normalized mass defect plots.[16] Mass defect (MD) is defined as the difference between the nominal and exact mass of an atom or molecule. Due to the substitution of multiple hydrogen atoms (each with $\Delta m/z = +0.0079$) with numerous fluorine atoms (each with $\Delta m/z = -0.0016$), PFAS typically display low or negative mass defects, unlike hydrocarbons. To identify novel fluorochemicals in aqueous film forming foams, Place and Field[124] screened their initial chromatograms using MDs from -0.100 to +0.150, which encompass a large number of PFAS. It should be noted that other compounds containing elements such as chlorine, bromine, sulfur, etc., also possess low to negative MD and so, mass defect filtering has generally been used in combination with other PFAS recognition strategies.[24, 60] Homologous series searching is based on the fact that PFAS manufacturing processes usually result in mixtures containing homologues that differ in *m/z* spacing units.[16] For instance, those produced by electrochemical fluorination and telomerization differ by CF_2 and CF_2-CF_2 units, respectively.[125, 126] CF_2-normalized mass defect plots is a widely used PFAS discovery tool that combines the previous two approaches. Application of this method resulted in detection of fifty congener classes of mixed halogenated

(chlorine/fluorine) thermal decomposition products of polychlorotrifluoroethylene.[127] The prioritization strategy applied in this thesis uses CCS and mass to reveal the presence of PFAS without previous knowledge of their occurrence.[52] In contrast to nonhalogenated molecules of similar mass, PFAS and other polyhalogenated compounds contain relatively fewer atoms leading to low molecular volume and smaller CCS values. As such, when CCS is plotted against *m/z*, 48%, 27% and 59% of compounds comprising >5 fluorine, >3 chlorine, and >2 bromine atoms respectively, are expected to exist in the region of chemical space defined by CCS < 0.2•*m/z* + 100 Å^2. This NTS prioritization approach has led to the discovery of unknown chlorofluoro n-alkanes in indoor dust[52] and fluorotelomer ethoxylates (FTEO) in indoor dust and industrial wastewater effluents.[128]

Once chemical features have been prioritized, efforts can be made to identify them. Molecular formula assignment is first done using the exact mass (5-10 ppm) and isotopic ratios to assign a probable molecular formula.[117] Plausible structures are then obtained by searching the molecular formula in large compound databases such as PubChem and ChemSpider. This will likely result in numerous matches that will require further ranking using MS/MS data.[110] As with suspect screening, spectral library searches can be performed and if that fails, *in silico* fragmentation techniques may prove useful. Features lacking sufficient information to assign a molecular formula are classed as *exact masses* of interest (Level 5) using the identification levels proposed by Schymanski et al.[109] Such features should only be annotated if they are useful to the investigation, for instance, features displaying multiple detections or trends. If an unambiguous molecular formula is determined but insufficient evidence exists to propose a structure, features are deemed

Level 4 (*unequivocal molecular formula*). This may occur if MS^2 spectra are absent, vague, or complicated by interferences. *Tentative candidates* (Level 3) are those possessing molecular formulae and some structural evidence but not enough to suggest one exact structure (e.g., positional isomers). Another example of a Level 3 identification would be a top-ranked structure from *in silico* fragmentation of candidates acquired from searching compound databases. Features classified as Level 2 or *probable structures* must either be matched to library/literature spectra or have adequate diagnostic evidence such as MS^2 fragments and/or experimental information (e.g., retention behavior) to rule out all other structures.[109] Features identified through NTS start at Level 5 while those obtained through suspect screens begin at Level 3.[99] As more MS (exact mass, isotope, adduct), MS/MS and experimental information becomes available, suspect and non-target components can increase in confidence to higher levels. As previously mentioned in Section 1.3.1, Level 1 status can only be achieved when a feature/component is confirmed with an authentic reference standard.

1.4. Objectives

It has been almost 40 years since the Government of Ontario introduced the Municipal Industrial Strategy for Abatement (MISA) – a policy for controlling municipal and industrial discharges into surface waters. During this time there may have been a shift in the types of chemicals being used in manufacturing and processing sectors. As such, the goal of this thesis is to acquire a better understanding of the current state of chemical pollution due to industrial discharges in the Ontario environment, with an emphasis on PFAS. Wastewater samples from over 10 industrial sectors will be extracted using different

techniques to encompass a wide range of polar, mid-polar and non-polar compounds. Extracts will then be analyzed via GC-APCI-cIM-MS (Chapter 2) and LC-ESI-cIM-MS (Chapter 3) to determine the identities and quantities of pollutants present. The performance of the developed analytical methods will be evaluated. A novel NTS strategy that prioritizes data based on CCS and *m/z* will be applied to find halogenated compounds of interest in the complex datasets. Distribution of pollutants across industrial sectors and possible applications will be investigated. This study will lay the groundwork for identifying problematic chemicals and provide information for source specific reduction efforts.

1.5. References

1. UNEP, 2009. The nine new pops: An Introduction to the Nine Chemicals Added to the Stockholm Convention by the Conference of the Parties at its Fourth Meeting. Geneva, Switzerland. http://chm.pops.int/Programmes/NewPOPs/Publications/tabid/695/language/en-US/Default.aspx
2. Xu, W.; Wang, X.; Cai, Z., Analytical chemistry of the persistent organic pollutants identified in the Stockholm Convention: A review. *Analytica Chimica Acta* **2013,** *790*, 1-13.
3. Secretariat of the Stockholm Convention. Stockholm Convention on persistent organic pollutants (POPs): Text and Annexes. 2020. Geneva, Switzerland. https://chm.pops.int/theconvention/overview/textoftheconvention/tabid/2232/default.aspx
4. Persistent Organic Pollutants. Donyinah, S. K., Ed. IntechOpen: London, United Kingdom, 2019.
5. Sinkkonen, S.; Paasivirta, J., Degradation half-life times of PCDDs, PCDFs and PCBs for environmental fate modeling. *Chemosphere* **2000,** *40* (9), 943-949.
6. Ashraf, M. A., Persistent organic pollutants (POPs): a global issue, a global challenge. *Environmental Science and Pollution Research* **2017,** *24* (5), 4223-4227.
7. El-Shahawi, M. S.; Hamza, A.; Bashammakh, A. S.; Al-Saggaf, W. T., An overview on the accumulation, distribution, transformations, toxicity and analytical methods for the monitoring of persistent organic pollutants. *Talanta* **2010,** *80* (5), 1587-1597.
8. Armitage, J. M.; MacLeod, M.; Cousins, I. T., Modeling the Global Fate and Transport of Perfluorooctanoic Acid (PFOA) and Perfluorooctanoate (PFO) Emitted from Direct Sources Using a Multispecies Mass Balance Model. *Environmental Science & Technology* **2009,** *43* (4), 1134-1140.
9. Armitage, J. M.; Schenker, U.; Scheringer, M.; Martin, J. W.; MacLeod, M.; Cousins, I. T., Modeling the Global Fate and Transport of Perfluorooctane Sulfonate (PFOS) and Precursor Compounds in Relation to Temporal Trends in Wildlife Exposure. *Environmental Science & Technology* **2009,** *43* (24), 9274-9280.
10. Hao, Y.; Li, Y.; Han, X.; Wang, T.; Yang, R.; Wang, P.; Xiao, K.; Li, W.; Lu, H.; Fu, J.; Wang, Y.; Shi, J.; Zhang, Q.; Jiang, G., Air monitoring of polychlorinated biphenyls, polybrominated diphenyl ethers and organochlorine pesticides in West Antarctica during 2011-2017: Concentrations, temporal trends and potential sources. *Environmental Pollution* **2019,** *249*, 381-389.
11. Hung, H.; Kallenborn, R.; Breivik, K.; Su, Y.; Brorström-Lundén, E.; Olafsdottir, K.; Thorlacius, J. M.; Leppänen, S.; Bossi, R.; Skov, H.; Manø, S.; Patton, G. W.; Stern, G.; Sverko, E.; Fellin, P., Atmospheric monitoring of organic pollutants in the Arctic under the Arctic Monitoring and Assessment Programme (AMAP): 1993-2006. *Science of The Total Environment* **2010,** *408* (15), 2854-2873.
12. Wania, F.; Mackay, D., Tracking the Distribution of Persistent Organic Pollutants. *Environmental Science & Technology* **1996,** *30* (9), 390A-396A.

13. Bonefeld-Jørgensen, E. C.; Ghisari, M.; Wielsøe, M.; Bjerregaard-Olesen, C.; Kjeldsen, L. S.; Long, M., Biomonitoring and hormone-disrupting effect biomarkers of persistent organic pollutants in vitro and ex vivo. *Basic and Clinical Pharmacology and Toxicology* **2014,** *115* (1), 118-28.
14. Kong, D.; MacLeod, M.; Hung, H.; Cousins, I. T., Statistical Analysis of Long-Term Monitoring Data for Persistent Organic Pollutants in the Atmosphere at 20 Monitoring Stations Broadly Indicates Declining Concentrations. *Environmental Science & Technology* **2014,** *48* (21), 12492-12499.
15. Muir, D.; Zhang, X.; de Wit, C. A.; Vorkamp, K.; Wilson, S., Identifying further chemicals of emerging arctic concern based on 'in silico' screening of chemical inventories. *Emerging Contaminants* **2019,** *5*, 201-210.
16. Liu, Y.; D'Agostino, L. A.; Qu, G.; Jiang, G.; Martin, J. W., High-resolution mass spectrometry (HRMS) methods for nontarget discovery and characterization of poly- and per-fluoroalkyl substances (PFASs) in environmental and human samples. *TrAC Trends in Analytical Chemistry* **2019,** *121*, 115420.
17. Rahman, M. F.; Peldszus, S.; Anderson, W. B., Behaviour and fate of perfluoroalkyl and polyfluoroalkyl substances (PFASs) in drinking water treatment: A review. *Water Research* **2014,** *50*, 318-340.
18. Wang, Z.; DeWitt, J. C.; Higgins, C. P.; Cousins, I. T., A Never-Ending Story of Per- and Polyfluoroalkyl Substances (PFASs)? *Environmental Science & Technology* **2017,** *51* (5), 2508-2518.
19. Koch, A.; Aro, R.; Wang, T.; Yeung, L. W. Y., Towards a comprehensive analytical workflow for the chemical characterisation of organofluorine in consumer products and environmental samples. *TrAC Trends in Analytical Chemistry* **2020,** *123*, 115423.
20. Buck, R. C.; Franklin, J.; Berger, U.; Conder, J. M.; Cousins, I. T.; de Voogt, P.; Jensen, A. A.; Kannan, K.; Mabury, S. A.; van Leeuwen, S. P. J., Perfluoroalkyl and polyfluoroalkyl substances in the environment: Terminology, classification, and origins. *Integrated Environmental Assessment and Management* **2011,** *7* (4), 513-541.
21. Guy, W. S.; Taves, D. R.; Brey, W. S. J., Organic Fluorocompounds in Human Plasma: Prevalence and Characterization. In *Biochemistry Involving Carbon-Fluorine Bonds*, AMERICAN CHEMICAL SOCIETY: 1976; Vol. 28, pp 117-134.
22. Giesy, J. P.; Kannan, K., Global distribution of perfluorooctane sulfonate in wildlife. *Environmental Science & Technology* **2001,** *35* (7), 1339-42.
23. Land, M.; de Wit, C. A.; Bignert, A.; Cousins, I. T.; Herzke, D.; Johansson, J. H.; Martin, J. W., What is the effect of phasing out long-chain per- and polyfluoroalkyl substances on the concentrations of perfluoroalkyl acids and their precursors in the environment? A systematic review. *Environmental Evidence* **2018,** *7* (1), 4.
24. Liu, Y.; Qian, M.; Ma, X.; Zhu, L.; Martin, J. W., Nontarget Mass Spectrometry Reveals New Perfluoroalkyl Substances in Fish from the Yangtze River and Tangxun Lake, China. *Environmental Science & Technology* **2018,** *52* (10), 5830-5840.
25. Secretariat of the Stockholm Convention. Stockholm Convention on persistent organic pollutants (POPs): PFASs listed under the Stockholm Convention.

https://chm.pops.int/Implementation/IndustrialPOPs/PFAS/Overview/tabid/5221/Default.aspx
26. Prevedouros, K.; Cousins, I. T.; Buck, R. C.; Korzeniowski, S. H., Sources, Fate and Transport of Perfluorocarboxylates. *Environmental Science & Technology* **2006,** *40* (1), 32-44.
27. Wania, F., A Global Mass Balance Analysis of the Source of Perfluorocarboxylic Acids in the Arctic Ocean. *Environmental Science & Technology* **2007,** *41* (13), 4529-4535.
28. Ahrens, L.; Shoeib, M.; Del Vento, S.; Codling, G.; Halsall, C., Polyfluoroalkyl compounds in the Canadian Arctic atmosphere. *Environmental Chemistry* **2011,** *8* (4), 399-406.
29. Wong, F.; Shoeib, M.; Katsoyiannis, A.; Eckhardt, S.; Stohl, A.; Bohlin-Nizzetto, P.; Li, H.; Fellin, P.; Su, Y.; Hung, H., Assessing temporal trends and source regions of per- and polyfluoroalkyl substances (PFASs) in air under the Arctic Monitoring and Assessment Programme (AMAP). *Atmospheric Environment* **2018,** *172*, 65-73.
30. Ahrens, L.; Siebert, U.; Ebinghaus, R., Total body burden and tissue distribution of polyfluorinated compounds in harbor seals (Phoca vitulina) from the German Bight. *Marine Pollution Bulletin* **2009,** *58* (4), 520-5.
31. Shi, Y.; Wang, J.; Pan, Y.; Cai, Y., Tissue distribution of perfluorinated compounds in farmed freshwater fish and human exposure by consumption. *Environmental Toxicology and Chemistry* **2012,** *31* (4), 717-23.
32. Taniyasu, S.; Kannan, K.; Horii, Y.; Hanari, N.; Yamashita, N., A survey of perfluorooctane sulfonate and related perfluorinated organic compounds in water, fish, birds, and humans from Japan. *Environmental Science & Technology* **2003,** *37* (12), 2634-9.
33. Ng, C. A.; Hungerbühler, K., Bioaccumulation of Perfluorinated Alkyl Acids: Observations and Models. *Environmental Science & Technology* **2014,** *48* (9), 4637-4648.
34. DeWitt, J. C., *Toxicological Effects of Perfluoroalkyl and Polyfluoroalkyl Substances*. Springer International Publishing: Cham, 2015.
35. Kim, M.; Li, L. Y.; Grace, J. R.; Yue, C., Selecting reliable physicochemical properties of perfluoroalkyl and polyfluoroalkyl substances (PFASs) based on molecular descriptors. *Environmental Pollution* **2015,** *196*, 462-472.
36. USEPA, 2016a. Drinking Water Health Advisory for Perfluorooctane Sulfonate (PFOS). EPA 822-R-16-004. https://www.epa.gov/sites/production/files/2016-05/documents/pfos_health_advisory_final_508.pdf
37. UNEP, 2006. Report of the Persistent Organic Pollutants Review Committee on the Work of its Second Meeting. Addendum: Risk profile on perfluorooctane sulfonate. http://chm.pops.int/Default.aspx?tabid=2301
38. Butt, C. M.; Berger, U.; Bossi, R.; Tomy, G. T., Levels and trends of poly- and perfluorinated compounds in the arctic environment. *Science of The Total Environment* **2010,** *408* (15), 2936-2965.
39. Conder, J. M.; Hoke, R. A.; Wolf, W. d.; Russell, M. H.; Buck, R. C., Are PFCAs Bioaccumulative? A Critical Review and Comparison with Regulatory Criteria and

Persistent Lipophilic Compounds. *Environmental Science & Technology* **2008,** *42* (4), 995-1003.
40. Cui, Q.; Pan, Y.; Zhang, H.; Sheng, N.; Wang, J.; Guo, Y.; Dai, J., Occurrence and Tissue Distribution of Novel Perfluoroether Carboxylic and Sulfonic Acids and Legacy Per/Polyfluoroalkyl Substances in Black-Spotted Frog (Pelophylax nigromaculatus). *Environmental Science & Technology* **2018,** *52* (3), 982-990.
41. Shi, Y.; Vestergren, R.; Zhou, Z.; Song, X.; Xu, L.; Liang, Y.; Cai, Y., Tissue Distribution and Whole Body Burden of the Chlorinated Polyfluoroalkyl Ether Sulfonic Acid F-53B in Crucian Carp (Carassius carassius): Evidence for a Highly Bioaccumulative Contaminant of Emerging Concern. *Environmental Science & Technology* **2015,** *49* (24), 14156-65.
42. De Silva, A. O.; Armitage, J. M.; Bruton, T. A.; Dassuncao, C.; Heiger-Bernays, W.; Hu, X. C.; Kärrman, A.; Kelly, B.; Ng, C.; Robuck, A.; Sun, M.; Webster, T. F.; Sunderland, E. M., PFAS Exposure Pathways for Humans and Wildlife: A Synthesis of Current Knowledge and Key Gaps in Understanding. *Environmental Toxicology and Chemistry* **2021,** *40* (3), 631-657.
43. USEPA, 2021a. Human Health Toxicity Values for Perfluorobutane Sulfonic Acid and Related Compound Potassium Perfluorobutane Sulfonate. EPA/600/R-20/345F. Washington, DC. https://cfpub.epa.gov/ncea/risk/recordisplay.cfm?deid=350888
44. USEPA, 2021b. Human Health Toxicity Values for Hexafluoropropylene Oxide (HFPO) Dimer Acid and Its Ammonium Salt (CASRN 13252-13-6 and CASRN 62037-80-3). 822R-21-010. Washington, D.C. https://www.epa.gov/system/files/documents/2021-10/genx-chemicals-toxicity-assessment_tech-edited_oct-21-508.pdf
45. CONCAWE, 2016. Environmental Fate and Effects of Poly- and Perfluoroalkyl Substances (PFAS). Auderghem, Belgium. https://www.concawe.eu/publication/environmental-fate-and-effects-of-poly-and-perfluoroalkyl-substances-pfas-report-no-816/
46. USEPA, 2016b. Drinking Water Health Advisory for Perfluorooctanoic Acid (PFOA). EPA 822-R-16-005. Washington, DC: U.S. Environmental Protection Agency. https://www.epa.gov/sites/production/files/2016-05/documents/pfoa_health_advisory_final_508.pdf
47. ITRC (Interstate Technology & Regulatory Council), 2022. PFAS Technical and Regulatory Guidance Document and Fact Sheets PFAS-1. https://pfas-1.itrcweb.org/wp-content/uploads/2022/09/PFAS-Guidance-Document-9-2022.pdf
48. Arp, H. P. H.; Aurich, D.; Schymanski, E. L.; Sims, K.; Hale, S. E., Avoiding the Next Silent Spring: Our Chemical Past, Present, and Future. *Environmental Science & Technology* **2023,** *57* (16), 6355-6359.
49. Tang, H. P.-o., Recent development in analysis of persistent organic pollutants under the Stockholm Convention. *TrAC Trends in Analytical Chemistry* **2013,** *45*, 48-66.
50. Reiner, E. J.; Jobst, K. J.; Megson, D.; Dorman, F. L.; Focant, J.-F., Analytical methodology of POPs. In *Environmental forensics for persistent organic pollutants*, Elsevier: 2014; pp 59-139.

51. Megson, D.; Reiner, E. J.; Jobst, K. J.; Dorman, F. L.; Robson, M.; Focant, J.-F., A review of the determination of persistent organic pollutants for environmental forensics investigations. *Analytica Chimica Acta* **2016,** *941*, 10-25.
52. MacNeil, A.; Li, X.; Amiri, R.; Muir, D. C. G.; Simpson, A.; Simpson, M. J.; Dorman, F. L.; Jobst, K. J., Gas Chromatography-(Cyclic) Ion Mobility Mass Spectrometry: A Novel Platform for the Discovery of Unknown Per-/Polyfluoroalkyl Substances. *Analytical Chemistry* **2022,** *94* (31), 11096-11103.
53. Nakayama, S. F.; Yoshikane, M.; Onoda, Y.; Nishihama, Y.; Iwai-Shimada, M.; Takagi, M.; Kobayashi, Y.; Isobe, T., Worldwide trends in tracing poly- and perfluoroalkyl substances (PFAS) in the environment. *TrAC Trends in Analytical Chemistry* **2019,** *121*, 115410.
54. Coggan, T. L.; Anumol, T.; Pyke, J.; Shimeta, J.; Clarke, B. O., A single analytical method for the determination of 53 legacy and emerging per- and polyfluoroalkyl substances (PFAS) in aqueous matrices. *Analytical and Bioanalytical Chemistry* **2019,** *411* (16), 3507-3520.
55. D'Agostino, L. A.; Mabury, S. A., Identification of Novel Fluorinated Surfactants in Aqueous Film Forming Foams and Commercial Surfactant Concentrates. *Environmental Science & Technology* **2014,** *48* (1), 121-129.
56. Gremmel, C.; Frömel, T.; Knepper, T. P., HPLC–MS/MS methods for the determination of 52 perfluoroalkyl and polyfluoroalkyl substances in aqueous samples. *Analytical and Bioanalytical Chemistry* **2017,** *409* (6), 1643-1655.
57. Guo, R.; Reiner, E. J.; Bhavsar, S. P.; Helm, P. A.; Mabury, S. A.; Braekevelt, E.; Tittlemier, S. A., Determination of polyfluoroalkyl phosphoric acid diesters, perfluoroalkyl phosphonic acids, perfluoroalkyl phosphinic acids, perfluoroalkyl carboxylic acids, and perfluoroalkane sulfonic acids in lake trout from the Great Lakes region. *Analytical and Bioanalytical Chemistry* **2012,** *404* (9), 2699-2709.
58. Joerss, H.; Apel, C.; Ebinghaus, R., Emerging per- and polyfluoroalkyl substances (PFASs) in surface water and sediment of the North and Baltic Seas. *Science of The Total Environment* **2019,** *686*, 360-369.
59. Kim, K. Y.; Ndabambi, M.; Choi, S.; Oh, J.-E., Legacy and novel perfluoroalkyl and polyfluoroalkyl substances in industrial wastewater and the receiving river water: Temporal changes in relative abundances of regulated compounds and alternatives. *Water Research* **2021,** *191*, 116830.
60. Bugsel, B.; Zwiener, C., LC-MS screening of poly- and perfluoroalkyl substances in contaminated soil by Kendrick mass analysis. *Analytical and Bioanalytical Chemistry* **2020,** *412* (20), 4797-4805.
61. Kaboré, H. A.; Vo Duy, S.; Munoz, G.; Méité, L.; Desrosiers, M.; Liu, J.; Sory, T. K.; Sauvé, S., Worldwide drinking water occurrence and levels of newly-identified perfluoroalkyl and polyfluoroalkyl substances. *Science of The Total Environment* **2018,** *616-617*, 1089-1100.
62. Concha-Graña, E.; Fernández-Martínez, G.; López-Mahía, P.; Prada-Rodríguez, D.; Muniategui-Lorenzo, S., Fast and sensitive determination of per- and polyfluoroalkyl substances in seawater. *Journal of Chromatography A* **2018,** *1555*, 62-73.

63. Amiri, R. Structure-diagnostic ion molecule reactions with environmental pollutants studied by theory and experiment. Memorial University, St. Johns, NL, 2023.
64. Skoog, D. A.; West, D. M.; Holler, F. J.; Crouch, S. R., *Fundamentals of Analytical Chemistry*. 9th ed.; Brooks/Cole Cengage Learning: CA, USA, 2014.
65. Guo, Y.; Kannan, K., Chapter 1 - Analytical Methods for the Measurement of Legacy and Emerging Persistent Organic Pollutants in Complex Sample Matrices. In *Comprehensive Analytical Chemistry*, Zeng, E. Y., Ed. Elsevier: 2015; Vol. 67, pp 1-56.
66. Aceña, J.; Stampachiacchiere, S.; Pérez, S.; Barceló, D., Advances in liquid chromatography–high-resolution mass spectrometry for quantitative and qualitative environmental analysis. *Analytical and Bioanalytical Chemistry* **2015,** *407* (21), 6289-6299.
67. Farré, M.; Kantiani, L.; Petrovic, M.; Pérez, S.; Barceló, D., Achievements and future trends in the analysis of emerging organic contaminants in environmental samples by mass spectrometry and bioanalytical techniques. *Journal of Chromatography A* **2012,** *1259*, 86-99.
68. Skoog, D. A.; Holler, F. J.; Crouch, S. R., *Principles of Instrumental Analysis*. 6th ed.; Thomson Brooks/Cole: CA, USA, 2007.
69. Li, X.; Dorman, F. L.; Helm, P. A.; Kleywegt, S.; Simpson, A.; Simpson, M. J.; Jobst, K. J., Nontargeted Screening Using Gas Chromatography–Atmospheric Pressure Ionization Mass Spectrometry: Recent Trends and Emerging Potential. *Molecules* **2021,** *26* (22).
70. Lai, S.; Jones, R.; Douce, D.; Dunstan, J.; Stevens, D., Characteristics of charge exchange chemical ionization (CI) in an atmospheric pressure gas chromatography (APGC) source and applied uses. Waters Corporation: 2013.
71. Hollender, J.; Schymanski, E. L.; Singer, H. P.; Ferguson, P. L., Nontarget Screening with High Resolution Mass Spectrometry in the Environment: Ready to Go? *Environmental Science & Technology* **2017,** *51* (20), 11505-11512.
72. Schreckenbach, S. A.; Simmons, D.; Ladak, A.; Mullin, L.; Muir, D. C. G.; Simpson, M. J.; Jobst, K. J., Data-Independent Identification of Suspected Organic Pollutants Using Gas Chromatography–Atmospheric Pressure Chemical Ionization–Mass Spectrometry. *Analytical Chemistry* **2021,** *93* (3), 1498-1506.
73. Amiri, R.; Bissram, M. J.; Hashemihedeshi, M.; Dorman, F. L.; Megson, D.; Jobst, K. J., Differentiating Toxic and Nontoxic Tricresyl Phosphate Isomers Using Ion–Molecule Reactions with Oxygen. *Journal of the American Society for Mass Spectrometry* **2023,** *34* (4), 640-648.
74. Ho, C. S.; Lam, C. W.; Chan, M. H.; Cheung, R. C.; Law, L. K.; Lit, L. C.; Ng, K. F.; Suen, M. W.; Tai, H. L., Electrospray ionisation mass spectrometry: principles and clinical applications. *The Clinical Biochemist Reviews* **2003,** *24* (1), 3-12.
75. Cech, N. B.; Enke, C. G., Practical implications of some recent studies in electrospray ionization fundamentals. *Mass Spectrometry Reviews* **2001,** *20* (6), 362-387.
76. Waters Corporation. StepWave. https://www.waters.com/waters/en_US/StepWave/nav.htm?cid=134673601&locale=en_US

77. Giles, K.; Ujma, J.; Wildgoose, J.; Pringle, S.; Richardson, K.; Langridge, D.; Green, M., A Cyclic Ion Mobility-Mass Spectrometry System. *Analytical Chemistry* **2019,** *91* (13), 8564-8573.
78. Allen, D. R.; McWhinney, B. C., Quadrupole Time-of-Flight Mass Spectrometry: A Paradigm Shift in Toxicology Screening Applications. *The Clinical Biochemist Reviews* **2019,** *40* (3), 135-146.
79. Celma, A.; Ahrens, L.; Gago-Ferrero, P.; Hernández, F.; López, F.; Lundqvist, J.; Pitarch, E.; Sancho, J. V.; Wiberg, K.; Bijlsma, L., The relevant role of ion mobility separation in LC-HRMS based screening strategies for contaminants of emerging concern in the aquatic environment. *Chemosphere* **2021,** *280*, 130799.
80. D'Atri, V.; Causon, T.; Hernandez-Alba, O.; Mutabazi, A.; Veuthey, J.-L.; Cianferani, S.; Guillarme, D., Adding a new separation dimension to MS and LC–MS: What is the utility of ion mobility spectrometry? *Journal of Separation Science* **2018,** *41* (1), 20-67.
81. Hinnenkamp, V.; Klein, J.; Meckelmann, S. W.; Balsaa, P.; Schmidt, T. C.; Schmitz, O. J., Comparison of CCS Values Determined by Traveling Wave Ion Mobility Mass Spectrometry and Drift Tube Ion Mobility Mass Spectrometry. *Analytical Chemistry* **2018,** *90* (20), 12042-12050.
82. Ruotolo, B. T.; Benesch, J. L. P.; Sandercock, A. M.; Hyung, S.-J.; Robinson, C. V., Ion mobility–mass spectrometry analysis of large protein complexes. *Nature Protocols* **2008,** *3* (7), 1139-1152.
83. Mullin, L.; Jobst, K.; DiLorenzo, R. A.; Plumb, R.; Reiner, E. J.; Yeung, L. W. Y.; Jogsten, I. E., Liquid chromatography-ion mobility-high resolution mass spectrometry for analysis of pollutants in indoor dust: Identification and predictive capabilities. *Analytica Chimica Acta* **2020,** *1125*, 29-40.
84. Dodds, J. N.; Baker, E. S., Ion Mobility Spectrometry: Fundamental Concepts, Instrumentation, Applications, and the Road Ahead. *Journal of the American Society for Mass Spectrometry* **2019,** *30* (11), 2185-2195.
85. Celma, A.; Sancho, J. V.; Schymanski, E. L.; Fabregat-Safont, D.; Ibáñez, M.; Goshawk, J.; Barknowitz, G.; Hernández, F.; Bijlsma, L., Improving Target and Suspect Screening High-Resolution Mass Spectrometry Workflows in Environmental Analysis by Ion Mobility Separation. *Environmental Science & Technology* **2020,** *54* (23), 15120-15131.
86. Belova, L.; Caballero-Casero, N.; van Nuijs, A. L. N.; Covaci, A., Ion Mobility-High-Resolution Mass Spectrometry (IM-HRMS) for the Analysis of Contaminants of Emerging Concern (CECs): Database Compilation and Application to Urine Samples. *Analytical Chemistry* **2021,** *93* (16), 6428-6436.
87. Dodds, J. N.; Hopkins, Z. R.; Knappe, D. R. U.; Baker, E. S., Rapid Characterization of Per- and Polyfluoroalkyl Substances (PFAS) by Ion Mobility Spectrometry–Mass Spectrometry (IMS-MS). *Analytical Chemistry* **2020,** *92* (6), 4427-4435.
88. Stephan, S.; Hippler, J.; Köhler, T.; Deeb, A. A.; Schmidt, T. C.; Schmitz, O. J., Contaminant screening of wastewater with HPLC-IM-qTOF-MS and LC+LC-IM-qTOF-

MS using a CCS database. *Analytical and Bioanalytical Chemistry* **2016,** *408* (24), 6545-6555.
89. Zheng, X.; Dupuis, K. T.; Aly, N. A.; Zhou, Y.; Smith, F. B.; Tang, K.; Smith, R. D.; Baker, E. S., Utilizing ion mobility spectrometry and mass spectrometry for the analysis of polycyclic aromatic hydrocarbons, polychlorinated biphenyls, polybrominated diphenyl ethers and their metabolites. *Analytica Chimica Acta* **2018,** *1037*, 265-273.
90. Aly, N. A.; Dodds, J. N.; Luo, Y.-S.; Grimm, F. A.; Foster, M.; Rusyn, I.; Baker, E. S., Utilizing ion mobility spectrometry-mass spectrometry for the characterization and detection of persistent organic pollutants and their metabolites. *Analytical and Bioanalytical Chemistry* **2022,** *414* (3), 1245-1258.
91. Cumeras, R.; Figueras, E.; Davis, C. E.; Baumbach, J. I.; Gràcia, I., Review on Ion Mobility Spectrometry. Part 1: current instrumentation. *Analyst* **2015,** *140* (5), 1376-1390.
92. Cho, E.; Riches, E.; Palmer, M.; Giles, K.; Ujma, J.; Kim, S., Isolation of Crude Oil Peaks Differing by m/z ~0.1 via Tandem Mass Spectrometry Using a Cyclic Ion Mobility-Mass Spectrometer. *Analytical Chemistry* **2019,** *91* (22), 14268-14274.
93. Giles, K.; Williams, J. P.; Campuzano, I., Enhancements in travelling wave ion mobility resolution. *Rapid Communications in Mass Spectrometry* **2011,** *25* (11), 1559-1566.
94. Giles, K.; Pringle, S. D.; Worthington, K. R.; Little, D.; Wildgoose, J. L.; Bateman, R. H., Applications of a travelling wave-based radio-frequency-only stacked ring ion guide. *Rapid Communications in Mass Spectrometry* **2004,** *18* (20), 2401-14.
95. Breen, J.; Hashemihedeshi, M.; Amiri, R.; Dorman, F. L.; Jobst, K. J., Unwrapping Wrap-around in Gas (or Liquid) Chromatographic Cyclic Ion Mobility–Mass Spectrometry. *Analytical Chemistry* **2022,** *94* (32), 11113-11117.
96. Hines, K. M.; May, J. C.; McLean, J. A.; Xu, L., Evaluation of Collision Cross Section Calibrants for Structural Analysis of Lipids by Traveling Wave Ion Mobility-Mass Spectrometry. *Analytical Chemistry* **2016,** *88* (14), 7329-7336.
97. Gelb, A. S.; Jarratt, R. E.; Huang, Y.; Dodds, E. D., A Study of Calibrant Selection in Measurement of Carbohydrate and Peptide Ion-Neutral Collision Cross Sections by Traveling Wave Ion Mobility Spectrometry. *Analytical Chemistry* **2014,** *86* (22), 11396-11402.
98. Schymanski, E. L.; Singer, H. P.; Longrée, P.; Loos, M.; Ruff, M.; Stravs, M. A.; Ripollés Vidal, C.; Hollender, J., Strategies to Characterize Polar Organic Contamination in Wastewater: Exploring the Capability of High Resolution Mass Spectrometry. *Environmental Science & Technology* **2014,** *48* (3), 1811-1818.
99. Schymanski, E. L.; Singer, H. P.; Slobodnik, J.; Ipolyi, I. M.; Oswald, P.; Krauss, M.; Schulze, T.; Haglund, P.; Letzel, T.; Grosse, S.; Thomaidis, N. S.; Bletsou, A.; Zwiener, C.; Ibáñez, M.; Portolés, T.; de Boer, R.; Reid, M. J.; Onghena, M.; Kunkel, U.; Schulz, W.; Guillon, A.; Noyon, N.; Leroy, G.; Bados, P.; Bogialli, S.; Stipaničev, D.; Rostkowski, P.; Hollender, J., Non-target screening with high-resolution mass spectrometry: critical review using a collaborative trial on water analysis. *Analytical and Bioanalytical Chemistry* **2015,** *407* (21), 6237-6255.

100. Escher, B. I.; Stapleton, H. M.; Schymanski, E. L., Tracking complex mixtures of chemicals in our changing environment. *Science* **2020,** *367* (6476), 388-392.
101. Chiaia-Hernandez, A. C.; Schymanski, E. L.; Kumar, P.; Singer, H. P.; Hollender, J., Suspect and nontarget screening approaches to identify organic contaminant records in lake sediments. *Analytical and Bioanalytical Chemistry* **2014,** *406* (28), 7323-7335.
102. Yang, Y.; Yang, L.; Zheng, M.; Cao, D.; Liu, G., Data acquisition methods for non-targeted screening in environmental analysis. *TrAC Trends in Analytical Chemistry* **2023,** *160*, 116966.
103. Schulze, B.; Jeon, Y.; Kaserzon, S.; Heffernan, A. L.; Dewapriya, P.; O'Brien, J.; Gomez Ramos, M. J.; Ghorbani Gorji, S.; Mueller, J. F.; Thomas, K. V.; Samanipour, S., An assessment of quality assurance/quality control efforts in high resolution mass spectrometry non-target workflows for analysis of environmental samples. *TrAC Trends in Analytical Chemistry* **2020,** *133*, 116063.
104. Hohrenk, L. L.; Itzel, F.; Baetz, N.; Tuerk, J.; Vosough, M.; Schmidt, T. C., Comparison of Software Tools for Liquid Chromatography–High-Resolution Mass Spectrometry Data Processing in Nontarget Screening of Environmental Samples. *Analytical Chemistry* **2020,** *92* (2), 1898-1907.
105. Bader, T.; Schulz, W.; Kümmerer, K.; Winzenbacher, R., General strategies to increase the repeatability in non-target screening by liquid chromatography-high resolution mass spectrometry. *Analytica Chimica Acta* **2016,** *935*, 173-186.
106. Camino-Sánchez, F. J.; Zafra-Gómez, A.; Pérez-Trujillo, J. P.; Conde-González, J. E.; Marques, J. C.; Vílchez, J. L., Validation of a GC–MS/MS method for simultaneous determination of 86 persistent organic pollutants in marine sediments by pressurized liquid extraction followed by stir bar sorptive extraction. *Chemosphere* **2011,** *84* (7), 869-881.
107. Lin, Y.-p.; Pessah, I. N.; Puschner, B., Simultaneous determination of polybrominated diphenyl ethers and polychlorinated biphenyls by gas chromatography–tandem mass spectrometry in human serum and plasma. *Talanta* **2013,** *113*, 41-48.
108. Geng, D.; Jogsten, I. E.; Dunstan, J.; Hagberg, J.; Wang, T.; Ruzzin, J.; Rabasa-Lhoret, R.; van Bavel, B., Gas chromatography/atmospheric pressure chemical ionization/mass spectrometry for the analysis of organochlorine pesticides and polychlorinated biphenyls in human serum. *Journal of Chromatography A* **2016,** *1453*, 88-98.
109. Schymanski, E. L.; Jeon, J.; Gulde, R.; Fenner, K.; Ruff, M.; Singer, H. P.; Hollender, J., Identifying Small Molecules via High Resolution Mass Spectrometry: Communicating Confidence. *Environmental Science & Technology* **2014,** *48* (4), 2097-2098.
110. Krauss, M.; Singer, H.; Hollender, J., LC–high resolution MS in environmental analysis: from target screening to the identification of unknowns. *Analytical and Bioanalytical Chemistry* **2010,** *397* (3), 943-951.
111. Hernández, F.; Sancho, J. V.; Ibáñez, M.; Abad, E.; Portolés, T.; Mattioli, L., Current use of high-resolution mass spectrometry in the environmental sciences. *Analytical and Bioanalytical Chemistry* **2012,** *403* (5), 1251-1264.

112. Raposo, F.; Ibelli-Bianco, C., Performance parameters for analytical method validation: Controversies and discrepancies among numerous guidelines. *TrAC Trends in Analytical Chemistry* **2020,** *129*, 115913.
113. Thompson, M.; Ellison, S. L. R.; Wood, R., Harmonized guidelines for single-laboratory validation of methods of analysis (IUPAC Technical Report). **2002,** *74* (5), 835-855.
114. Munoz, G.; Duy, S. V.; Labadie, P.; Botta, F.; Budzinski, H.; Lestremau, F.; Liu, J.; Sauvé, S., Analysis of zwitterionic, cationic, and anionic poly- and perfluoroalkyl surfactants in sediments by liquid chromatography polarity-switching electrospray ionization coupled to high resolution mass spectrometry. *Talanta* **2016,** *152*, 447-456.
115. Frederiksen, M.; Thomsen, C.; Frøshaug, M.; Vorkamp, K.; Thomsen, M.; Becher, G.; Knudsen, L. E., Polybrominated diphenyl ethers in paired samples of maternal and umbilical cord blood plasma and associations with house dust in a Danish cohort. *International Journal of Hygiene and Environmental Health* **2010,** *213* (4), 233-242.
116. Muir, D.; Sverko, E., Analytical methods for PCBs and organochlorine pesticides in environmental monitoring and surveillance: a critical appraisal. *Analytical and Bioanalytical Chemistry* **2006,** *386* (4), 769-789.
117. González-Gaya, B.; Lopez-Herguedas, N.; Bilbao, D.; Mijangos, L.; Iker, A. M.; Etxebarria, N.; Irazola, M.; Prieto, A.; Olivares, M.; Zuloaga, O., Suspect and non-target screening: the last frontier in environmental analysis. *Analytical Methods* **2021,** *13* (16), 1876-1904.
118. Ruttkies, C.; Schymanski, E. L.; Wolf, S.; Hollender, J.; Neumann, S., MetFrag relaunched: incorporating strategies beyond in silico fragmentation. *Journal of Cheminformatics* **2016,** *8* (1), 3.
119. Wolf, S.; Schmidt, S.; Müller-Hannemann, M.; Neumann, S., In silico fragmentation for computer assisted identification of metabolite mass spectra. *BMC Bioinformatics* **2010,** *11* (1), 148.
120. Celma, A.; Bijlsma, L.; López, F. J.; Sancho, J. V., Development of a Retention Time Interpolation scale (RTi) for liquid chromatography coupled to mass spectrometry in both positive and negative ionization modes. *Journal of Chromatography A* **2018,** *1568*, 101-107.
121. Hu, M.; Müller, E.; Schymanski, E. L.; Ruttkies, C.; Schulze, T.; Brack, W.; Krauss, M., Performance of combined fragmentation and retention prediction for the identification of organic micropollutants by LC-HRMS. *Analytical and Bioanalytical Chemistry* **2018,** *410* (7), 1931-1941.
122. Bijlsma, L.; Bade, R.; Celma, A.; Mullin, L.; Cleland, G.; Stead, S.; Hernandez, F.; Sancho, J. V., Prediction of Collision Cross-Section Values for Small Molecules: Application to Pesticide Residue Analysis. *Analytical Chemistry* **2017,** *89* (12), 6583-6589.
123. Gago-Ferrero, P.; Schymanski, E. L.; Bletsou, A. A.; Aalizadeh, R.; Hollender, J.; Thomaidis, N. S., Extended Suspect and Non-Target Strategies to Characterize Emerging Polar Organic Contaminants in Raw Wastewater with LC-HRMS/MS. *Environmental Science & Technology* **2015,** *49* (20), 12333-12341.

124. Place, B. J.; Field, J. A., Identification of Novel Fluorochemicals in Aqueous Film-Forming Foams Used by the US Military. *Environmental Science & Technology* **2012,** *46* (13), 7120-7127.
125. Luo, Y.-S.; Aly, N. A.; McCord, J.; Strynar, M. J.; Chiu, W. A.; Dodds, J. N.; Baker, E. S.; Rusyn, I., Rapid Characterization of Emerging Per- and Polyfluoroalkyl Substances in Aqueous Film-Forming Foams Using Ion Mobility Spectrometry–Mass Spectrometry. *Environmental Science & Technology* **2020,** *54* (23), 15024-15034.
126. Trier, X.; Granby, K.; Christensen, J. H., Tools to discover anionic and nonionic polyfluorinated alkyl surfactants by liquid chromatography electrospray ionisation mass spectrometry. *Journal of Chromatography A* **2011,** *1218* (40), 7094-7104.
127. Myers, A. L.; Jobst, K. J.; Mabury, S. A.; Reiner, E. J., Using mass defect plots as a discovery tool to identify novel fluoropolymer thermal decomposition products. *Journal of Mass Spectrometry* **2014,** *49* (4), 291-296.
128. Steeves, K. L.; Bissram, M. J.; Kleywegt, S.; Stevens, D.; Dorman, F. L.; Simpson, A. J.; Simpson, M. J.; Cahill, L. S.; Jobst, K. J., Nontargeted screening reveals fluorotelomer ethoxylates in indoor dust and industrial wastewater. *Environment International* **2023,** *171*, 107634.

Chapter 2. Target, suspect and non-target screening of unknown persistent organic pollutants in industrial wastewater of Ontario, Canada

2.1. Introduction

Globally, there are over 350,000 chemicals in production and use.[1] Recent screening of the industrial chemical inventories of Europe, Canada, and the USA has yielded a list of 3421 substances that have the potential to be persistent organic pollutants (POPs).[2] These chemicals are of particular interest since they persist in the environment for extended periods, bioaccumulate in humans and animals, undergo long-range transport and are toxic to humans and wildlife.[3] Despite widespread concern, only 31 classes of POPs are currently monitored under international agreements such as the Stockholm Convention (SC).[4] The disparity in number between the chemicals being restricted and those exhibiting POPs characteristics suggests the existence of many more unregulated POPs.[5] In the 1980s, the government of Ontario introduced the Municipal Industrial Strategy for Abatement (MISA),[6] which was a collaborative program where government and industry worked together via a monitoring, consideration of "best available technologies economically achievable" and regulatory phase-in approach to reduce the environmental impacts of industrial emissions. Through chemical analysis and toxicity testing of directly discharged industrial effluents, Effluent Monitoring Effluent Limits regulations and toxicity testing requirements were introduced for industries that directly discharge to the aquatic environment. On the other hand, wastewaters discharged to the sewer system in the province of Ontario, Canada is regulated at the municipal (city) level. Each municipality

can set their own sewer-use bylaw for industrial facilities, which generally have concentration limits on conventional parameters like metals, nutrients, some organics, and pH. Typically, these limits apply to all businesses in the municipality and are not specific to different types of industrial or commercial facilities. In addition, most receiving wastewater treatment plants (WWTPs) are owned and operated at the municipal level of government. Almost 4 decades later and with the significant increase in chemical numbers and diversity on the global market, a better understanding of the types of chemicals used in manufacturing and processing sectors that discharge their effluents to municipal sewers and/or the environment is needed.

Since wastewater effluents are major point sources of organic contaminants to the environment,[7] they are appropriate sample choices when searching for unknown pollutants. Over the past 2 decades, several papers have been published characterizing the vast number of polar and non-polar organic pollutants present in wastewater effluents.[7-14] A wide range of contaminants are detected at ng/L to µg/L concentrations ranging from pharmaceuticals and personal care products to industrial chemicals to pesticides. Commonly detected pollutants in wastewaters influenced by industries include corrosion inhibitors (e.g., benzotriazole), organophosphate flame retardants (OPFRs) and plasticizers (e.g., tributyl phosphate; TBP, tris(2-chloroisopropyl)phosphate; TCPP), and per- and polyfluoroalkyl substances (PFAS) (e.g., perfluorooctanoic acid; PFOA, perfluorohexane sulfonic acid; PFHxS).[12, 13, 15] Although overwhelming evidence suggests that many OPFRs[16, 17] and PFAS[18, 19] exhibit POP characteristics, most continue to evade control measures and some are yet to be identified.

Whether the goal is discovering unknown pollutants in the environment or demonstrating the occurrence of known ones to inform risk assessment and pollution regulations, the first step involves being able to isolate compounds of interest from other sample components. For wastewater analysis, combinations of targeted, suspect and/or non-targeted approaches are common based on gas or liquid chromatography (GC or LC) coupled to tandem mass spectrometry (MS/MS) or high-resolution mass spectrometry (HRMS).[7-12] The high mass accuracy and resolution afforded by HRMS instruments, together with its increased availability in recent times has contributed to a renewed interest in non-target screening (NTS) strategies.[20] The utility and potential of HRMS in NTS for unknown chemical discovery in the environment has been discussed[21] and reviewed[22] elsewhere. Nevertheless, challenges remain in identifying important sample components from HRMS experiments due to the vast quantity of data generated[20] and the complex nature of environmental samples.[21] Several prioritization strategies continue to be employed including mass defect plots, ranking by frequency and signal intensity of masses, neutral loss filtering and using characteristic isotope pattern.[21] For identifying PFAS and other halogenated compounds, a novel NTS method using collision cross section (CCS) values derived from ion mobility spectrometry (IMS) has recently been developed by MacNeil et al.[20] CCS values are representative of an ion's mobility, which depends on its size, shape and charge. Polyhalogenated compounds with >5 Fluorine (F), >3 Chlorine (Cl) and >2 Bromine (Br) atoms have relatively small CCSs compared to other compounds with similar masses. As a result, they occupy a unique region of chemical space defined by *m/z* and CCS. According to the model,[20] 48%, 27% and 59% of compounds with >5 F, >3 Cl

and >2 Br atoms, respectively, will exist below a line described by CCS = 0.2•*m/z* + 100 where 150 < CCS < 250 Å.

The goal of this study is to use the above NTS model in combination with a suspect screening list of approximately 3000 suspected POPs to characterize industrial wastewater samples collected from 11 sectors in Ontario, Canada. Distribution, levels and possible sources of unknown halogenated chemicals will be examined, and comparisons made across different industrial sectors and regions.

2.2. Experimental Methods

2.2.1. Chemical Standards

Native and isotopically labeled standards of known and suspected POPs were purchased from Wellington Laboratories (Guelph, ON, Canada) and Cambridge Isotope Laboratories (CIL, Tewksbury, MA, USA). Lists of these standards can be found in Tables A.1 and A.2 of Appendix A. Mixed standards of native (6.67-33.33 pg/µL) and isotopically labelled compounds (20-40 pg/µL) were prepared in acetone for spiking as a means of evaluating method recovery and accuracy. *N*-cyclohexyl-2,2,3,3,4,4,5,5,6,6,7,7,7-tridecafluoroheptanamide was obtained from Sigma Aldrich (St. Louis, MO, USA) to confirm the identity one unknown PFAS. The identities of two other unknown PFAS were confirmed using standards synthesized in-house according to procedures described by Afzal et al.[23] (*N*-diethoxylated perfluorooctanamide) and Jackson and Mabury[24] (*N*-methylperfluoroheptanamide). Chemicals used for these syntheses were obtained from Sigma Aldrich (Oakville, ON, Canada) [2-(2-aminoethoxy) ethanol, zinc oxide, methyl

perfluorooctanoate, methyl amine] and Synquest Laboratories (Alachua, FL, USA) [perfluoroheptanoyl chloride]. The standard used for confirmation of 6:2 fluorotelomer ethoxylate (6:2 FTEO) was previously described.[25]

2.2.2. Sample collection

In collaboration with 4 Municipalities in Ontario, 5 L of wastewater samples were collected in 1L jars between September 13th and December 1st, 2021, from 33 industrial facilities and 1 municipal WWTP (Table A.3). Samples were kept at ~4 °C during transport and filtered by gravity using either Whatman grade 202 filter paper or 20 µm cellulose fiber filters into 500 mL polyethylene terephthalate bottles. Both wastewater samples and filters were frozen at -18 °C (to minimize analyte degradation) until shipping and analysis.

2.2.3. Liquid-liquid extraction

Wastewater samples were extracted using a modified version of an MECP method (E3186), similar to USEPA method 3510C separatory funnel liquid-liquid extraction (LLE).[26] A 100 mL aliquot of each sample was measured into a 250 mL separatory funnel and 100 µL of the mixed isotopically labeled standard was spiked in yielding a final extract concentration of 10-20 pg/µL. After thorough mixing, the pH of the samples was adjusted to approximately 12 using 50% NaOH. Each sample was then serially extracted 3 times with 10 mL portions of DCM. This was repeated under acidic conditions (~pH 2 using concentrated HCl). The combined extracts were reduced in volume via nitrogen blowdown and then concentrated further in a CentriVap concentrator system (Fisher Scientific, ON, Canada). The solvent was exchanged to toluene (final volume 200 uL) and extracts were stored at 5 °C until analysis.

2.2.4. Accelerated solvent extraction (ASE)

Filter papers were spiked with 2-4 ng of mixed isotopically labeled standard and extracted using a pressurized liquid extraction system (ASE 350, Accelerated Solvent Extraction System from Dionex Corporation, Sunnyvale, CA, USA). Extractions were performed using hexane/acetone (3/1, v/v; 2 cycles) at 100 °C, 5 min static cycle with a 50% flush and 200 s purge. Extracts were subjected to the same procedure as mentioned previously for the LLE extracts in Section 2.2.3.

2.2.5. Instrumental analysis

Gas chromatography-cyclic ion mobility mass spectrometry (GC-cIMS) experiments were performed using a Waters Cyclic ion mobility mass spectrometer (Wilmslow, UK) coupled to an Agilent 8890 Gas chromatograph using atmospheric pressure chemical ionization (APCI). Analyte separation was performed with an Rtx-5 column (15 m × 0.25 mm × 0.1 µm). The initial temperature was 90 °C, held for 1 min; the oven was then ramped at 95 °C/min to 115 °C, at 65 °C/min to 150 °C, at 45 °C/min to 210 °C, at 35 °C/min to 280 °C, at 30 °C/min to 310 °C, and finally at 25 °C/min to 330 °C for a 10 min run time. Sample extracts and standard solutions (1 µL) were injected in the split-less mode. The inlet and transfer line temperatures were set to 280 °C and 330 °C, respectively. A helium (~99.99% purity) carrier gas flow of 10 mL/min was used with nitrogen (~99.99% purity) make-up gas added to the APCI source at a rate of 350 mL/min. APCI was initiated by a corona discharge (2 µA) in both the positive and negative ion modes. The source conditions were as follows: source temperature, 150 °C; sampling cone, 30 V; extraction cone, 10 V; cone gas, 175 L/hour; auxiliary gas, 100 L/hour. Column bleed

($C_9H_{27}O_5Si_5^+$ - *m/z* 355.0699) and background ions ($C_{16}H_{31}O_2^-$ - *m/z* 255.2324 and $C_{18}H_{35}O_2^-$ - 283.2637) were used to internally correct the measured *m/z* in the positive and negative ion modes, respectively. Mass spectra were collected for *m/z* 50-1200 using data independent acquisition (DIA). The collision energy was ramped from 10 to 40 eV for the high-energy channel and held at 4 eV for the low-energy channel. Nitrogen gas was used as the buffer gas in the cyclic ion mobility cell, which was operated in the single pass mode with the separation time set to 2 ms and a traveling wave height of 22 V. Calibration of the instrument to measure CCS was performed according to standard procedure using a mixture of 22 compounds (aka, "major mix") supplied by Waters Corp.

2.2.6. Suspect Database and CCS Prediction

A list of 3421 organic compounds compiled by Muir et al.[2] through *in silico* screening for POPs was used as the basis for the suspect screening database. CCS values for most of the suspects in the database were predicted using AllCCS. AllCCS is a machine-learning based program,[27] which predicts CCS values from SMILES (simplified molecular input line entry system) structures. Chemicals from the original list whose CCSs could not be predicted, were removed and POPs already regulated under SC were added back in. GC-APCI typically yields $M^{\bullet+}$ and $[M+H]^+$ ions, but only ions of the latter form were computed because predictive models do not yet exist for radical cations. To account for the error introduced by this assumption, a relatively large CCS deviation of 10% was used during screening.

2.2.7. Data Processing

Raw samples and blanks were imported into Progenesis QI software (Waters Corp). Lock mass correction, alignment, peak picking and deconvolution were done automatically in the software. Two separate excel spreadsheets, one containing the compounds with accurate masses and the other with corresponding predicted CCS values were imported into Progenesis QI. Progenesis Metascope was used to perform the suspect screening with search parameters of 5 ppm and 10% for mass tolerance and CCS percent deviation, respectively. The results were exported in an excel spreadsheet for further processing. Normalized ion abundances were first blank subtracted (10-fold). Remaining ions were then subjected to the filtering criteria $CCS < 0.2 \bullet m/z + 100$ where $150 < CCS < 250$ Å. A script tool (R code) described in Zhang et al.[28] was used to filter out chlorinated and brominated ions. Finally, manual investigation of those ions furthest to the right of the CCS to *m/z* line revealed potential halogenated ions.

2.2.8. Quality Assurance and Quality Control

Table 2.1 summarizes the proposed assignments for the compounds matched by suspect and non-target screening. The accurate mass and CCSs of the (quasi)molecular ions of all proposed identifications fall within 5 ppm and ± 15% of the theoretical values. Confidence in these assignments is characterized using the 5-level scale proposed by Schymanski et al.[29] All compounds reported herein are present at levels that exceed their estimated method detection limits (MDL). Experiments to estimate MDLs were done using 18.2 MΩ•cm water samples (n=3 or 6). For non-target compounds, the mean peak area in the blanks was summed to the standard deviation times 3.365 (n=6). For targeted

compounds, the average concentration in the blanks was summed to the standard deviation times 6.965 (n=3). Method performance data for analyte quantification in wastewater and filter samples is given in Tables A.4 and A.5 of the supporting information.

2.2.9. Statistical Analysis

Two-dimensional hierarchical cluster analysis (2D-HCA) was performed using Metaboanalyst 5.0.[30] Peak areas for the compounds tentatively identified by target, suspect and non-target screening were obtained using TargetLynx V4.2 (Waters Corp). 2D-HCA was applied to the peak areas that exceeded estimated MDLs. Non-detects were replaced with one-fifth of the minimum positive values of their corresponding variables. The data set was subjected to log transformation prior to 2D-HCA**.**

2.3. Results and Discussion

2.3.1. Screening data for halogenated pollutants based on *m/z* and CCS

Data processing by Progenesis yielded approximately 27,000 ions after blank subtraction with 1100 suspects. Finding compounds of interest in this wealth of data poses significant challenges to analytical chemists. To reduce this massive data set, we chose to use a novel filtering criterion for polyhalogenated compounds based on *m/z* and CCS.[20] After plotting experimental CCS vs *m/z* for the blank subtracted dataset and imposing a boundary line defined by CCS < 0.2•*m/z* + 100 Å^2, 755 ions remained, of which 50 were matched by suspect screening. To minimize the false positive discovery of halogenated compounds,[20] an additional constraint of 150 < CCS < 250 Å^2 was employed resulting in another decrease to 344 ions with 27 suspects (Figure 2.1a). These remaining 344 ions are likely to be from compounds containing >5 F, >3 Cl and >2 Br atoms and represent a

worst-case scenario since false positives could still be present. In addition, some ions will be fragments and/or isotopic peaks of the same compounds. Thus, the actual number of halogenated species is anticipated to be much less than 344.

Suspect screening accounted for 16 chlorinated/brominated (Cl/Br) ions belonging to 6 compounds that are known pollutants (**22-25** in Table 2.1) and 4 fluorinated ions originating from a popular PFAS, *N*-EtFOSE (6% of filtered ions). Two of the known Cl/Br suspects were present at levels below estimated MDLs and were therefore omitted from Table 2.1. Twenty other ions were matched by suspect screening, but further investigation of the raw data suggested that they were false positives arising from compounds in the suspect database with coincidentally the same masses. With the use of a script tool,[28] 52 more Cl/Br ions were clustered into 15 groups based on retention times (RTs), isotopic specific mass differences and isotope ratios. Manual interrogation of the peak list and raw spectra yielded a further 12 groups (32 ions) and 17 ungrouped ions. Unfortunately, these ions could not be grouped together due to non-detection of isotopic peaks by Progenesis. Additionally, the process of associating fragments with molecular ions was hindered by overlapping chromatographic peaks. Nevertheless, by filtering the data in this way we were able to isolate 101 (29%) Cl/Br ions stemming from roughly 30-40 compounds that evaded suspect screening attempts. This highlights the importance of complementing suspect screening with non-target methods.

Once Cl/Br ions below the CCS-*m/z* line were tagged (Figure 2.1b), attention shifted to PFAS discovery. As noted by MacNeil at al.,[20] distinguishing per- and polyfluorinated ions is more difficult than Cl/Br ions because ^{19}F exists as a single stable

isotope whereas the latter displays characteristic isotope patterns. The search began by reviewing the spectra of those untagged Cl/Br ions furthest below the CCS-*m/z* line. Compounds presenting with a simple isotopic pattern consisting of a weak M+1 peak resulting from ^{13}C and a negative or small, slightly positive mass defect (MD) were readily identified as PFAS. Others with greater positive MDs were more difficult to confirm and are thus categorized as level 5 on the scale proposed by Schymanski et al.[29] in Table 2.1. In this way, 19 PFAS (30 ions, 9%) were tentatively identified (Figure 2.1b). Worth noting is that *N*-EtFOSE, FOSE and other potentially related sulfur containing PFAS are concentrated in the top right portion of plot. The remaining unassigned 193 ions (56%) could be siloxanes that were not background subtracted, false positives or even halogenated compounds with <5 F, <3 Cl, and <2 Br atoms.[20] Figure 2.2 displays the final distribution of the 344 ions isolated based on CCS and *m/z*. Collectively, 35 (ion intensity) to 44% (number of ions) of filtered ions are likely halogenated. Of this proportion, only 9-14% of the halogenated intensities and ions can be explained by suspect compounds. This means

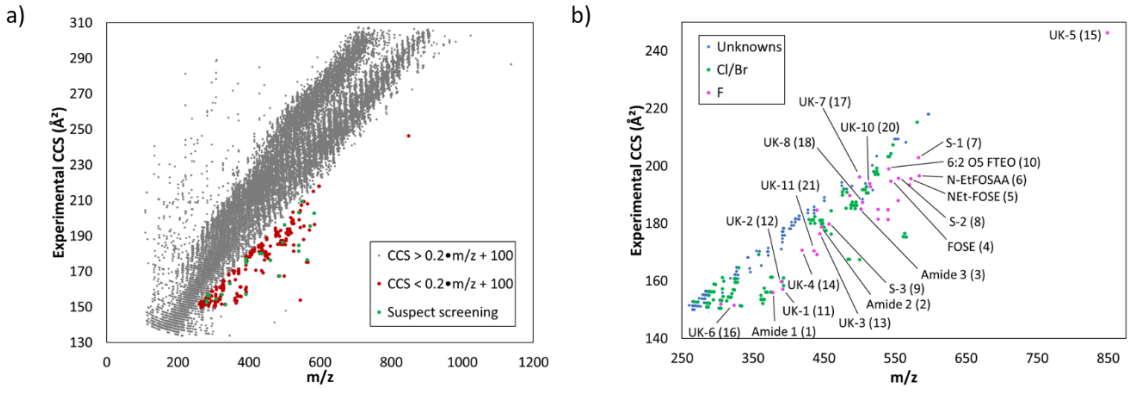

Figure 2.1. Experimental CCS_{N_2} vs *m/z* and for **(a)** approximately 27,000 ions present in industrial wastewater samples after blank subtraction (10-fold) and **(b)** only ions characterized by CCS values that are less than the sum of 100 $Å^2$ and one fifth of their mass.

that approximately 86-91% of the halogenated chemicals being used, produced or discharged as degradation or by-products in Ontario, Canada are truly unknown.

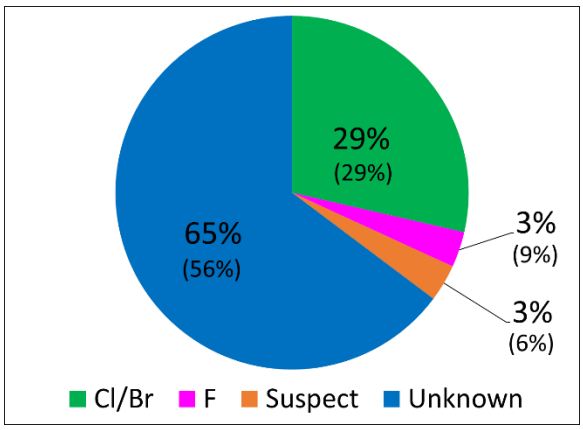

Figure 2.2. Distribution of ions isolated by filtering criteria CCS < 0.2•*m/z* + 100 using ion intensities. Values in parentheses show distribution using the number of ions.

Table 2.1 summarizes the compounds identified and tentatively identified through target, suspect and non-target screening. These include common halogenated pollutants such as BDE-47, BDE-99 and TDCPP as well as the frequently detected PFAS, *N*-EtFOSE. Compounds assigned with Level 1 confidence were confirmed with commercial or synthetic standards based on mass accuracy <5 ppm, RT ±0.01 min, CCS percent deviation <1.5% and agreements between the isotopic ratios of suspects and proposed compounds (±10%). Identification and confirmation of 6:2 fluorotelomer ethoxylate (6:2 FTEO) was previously described in Steeves el al.[25] A confidence Level of 3 was allocated to FOSE and *N*-EtFOSAA since the analytical data supported the proposal but a standard was unavailable to confirm. Most other compounds were assigned a confidence Level 4 where plausible elemental compositions were suggested but there was insufficient fragmentation

data for structural proposals. PCB-52 was not detected by Progenesis but was included after being found through target analysis.

Table 2.1. Summary of compounds tentatively identified by target, suspect and non-target screening of GC-APCI-cIM-MS data. CCS (Exp.) and CCS (Std.) are experimentally derived values for ions in the wastewater samples and authentic standards, respectively while CCS (Calc.) represents predicted values from AllCCS.[27] The CCS deviation (%) is calculated between CCS (Exp.) and CCS (Std.) in most cases or between CCS (Exp.) and CCS (Calc.) where CCS (Std.) is unavailable. The detection frequency (DF) of compounds across samples (n=37) is shown in the last column.

Compound ID	Class	Structure	Elemental composition	ID Lvl [29]	ID Mtd	Ion(s)	m/z	Mass error (ppm)	RT (min)	CCS (Exp.)	CCS (Std.)	CCS (Calc.)	CCS dev (%)	DF
Amide 1 **(1)**	Perfluoroalkyl amides (PFAAs)	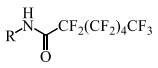 R=CH_3, C_6H_{11}	$C_8H_4F_{13}NO$	1	NTS	$[M+H]^+$	378.0171	1.9	0.33	156.0	154.0	169.5	1.3	6
Amide 2 **(2)**			$C_{13}H_{12}F_{13}NO$	1	NTS	$[M+H]^+$	446.0795	1.1	1.17	182.9	182.9	183.3	0.0	1
Amide 3 **(3)**	Alcohol PFAAs	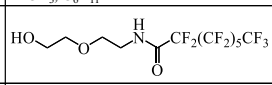	$C_{12}H_{10}F_{15}NO_3$	1	NTS	$[M+H]^+$	502.0497	-0.4	1.53	193.6	192.2	188.2	0.7	8
FOSE **(4)**	Alcohol perfluoroalkyl-sulfonamides (PFSMs)	C_8F_{17}-S(=O)$_2$NHCH$_2$CH$_2$OH	$C_{10}H_6F_{17}NO_3S$	3	NTS	$[M+H]^+$	543.9869	-1.8	1.60	194.7	-	190.2	2.4	5
N-EtFOSE **(5)**		C_8F_{17}-S(=O)$_2$N(CH$_2$CH$_3$)CH$_2$CH$_2$OH	$C_{12}H_{10}F_{17}NO_3S$	1	S	$[M+H]^+$	572.0178	-1.7	1.63	206.2	203.6	198.2	1.3	7
N-EtFOSAA **(6)**	Carboxylic acid-PFSMs	C_8F_{17}-S(=O)$_2$N(CH$_2$CH$_3$)CH$_2$CO$_2$H	$C_{12}H_8F_{17}NO_4S$	3	NTS	$[M-H]^+$	583.9819	-0.9	1.89	196.5	-	192.0	2.4	7
S-1 **(7)**	Unknown Sulphur containing PFAS		$C_{13}H_{11}F_{17}N_2O_2S$	4	NTS	$[M+H]^+$	583.0343	-0.9	2.19	202.9				8
S-2 **(8)**			$C_{11}H_7F_{17}N_2O_2S$	4	NTS	$[M+H]^+$	555.0029	-1.1	2.07	195.7				5
S-3 **(9)**			$C_{10}H_9F_{13}O_3S$	4	NTS	$[M+H]^+$	457.0135	-1.8	1.65	179.8				5
6:2-O5 FTEO **(10)**	Fluorotelomer ethoxylates (FTEOs)	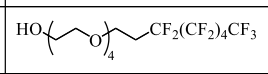	$C_{16}H_{21}F_{13}O_5$	1	NTS	$[M+H]^+$	541.1258	-0.4	2.21	207.8	207.8	197.2	0.0	10
UK-1 **(11)**	Unknown Level 4 & 5 PFAS		$C_9H_6F_{13}NO$	4	NTS	$[M+H]^+$	392.0302	-4.6	0.35	157.2				2
UK-2 **(12)**			$C_{13}H_{14}F_{13}NO_2$	4	NTS	$[M+H]^+$	464.0897	0.4	1.22	-				1
UK-3 **(13)**			$C_{11}H_6F_{13}N_3O$	4	NTS	$[M+H]^+$	444.0393	2.7	1.39	176.5				1
UK-4 **(14)**			$C_{10}H_7F_{13}N_2O$	4	NTS	$[M+H]^+$	419.0440	2.6	1.44	170.7				1
UK-5 **(15)**			$C_{20}H_{15}F_{27}O_5$	4	NTS	$[M+H]^+$	849.0574	0.9	2.21	246.3				2
UK-6 **(16)**				5	NTS	$[M+H]^+$	322.9778		3.08	151.6				4
UK-7 **(17)**				5	NTS	$[M+H]^+$	500.1515		4.74	196.2				7
UK-8 **(18)**				5	NTS	$[M+H]^+$	505.2005		6.16	187.4				1
UK-9 **(19)**				5	NTS	$[M+H]^+$	486.1840		6.25	189.8				1
UK-10 **(20)**				5	NTS	$[M+H]^+$	515.2339		6.64	192.8				2
UK-11 **(21)**				5	NTS	$[M+H]^+$	435.9991		1.27	170.5				10
TDCPP **(22)**	OPFRs		$C_9H_{15}Cl_6O_4P$	1	S, T	$[M+H]^+$	430.8890	0.5	3.21	180.1	179.0	175.3	0.7	28
BDE-47 **(23)**	PBDEs		$C_{12}H_6Br_4O$	1	S, T	M^{-+}	485.7102	-1.9	3.54	167.6	167.6	162.7	0.0	3
BDE-99 **(24)**			$C_{12}H_5Br_5O$	1	S, T	M^{-+}	563.6221	0.9	4.02	176.5	176.5	190.2	0.0	2
PCB-101 **(25)**	PCBs		$C_{12}H_5Cl_5$	1	S, T	M^{-+}	325.8817	4.0	2.84	160.9	159.5	156.3	0.8	1
PCB-52 **(26)**			$C_{12}H_6Cl_4$	1	T	M^{-+}	291.9202	2.7	2.51					2

2.3.2. Identification of 2 new classes of perfluoroalkylamides in wastewater samples

The quest to elucidate the structures of unknown PFAS ions tentatively identified in Figure 2.1b began with obtaining the extracted ion chromatograms (XICs) of masses

provided by Progenesis and examining the corresponding MS spectra in both positive and negative ion modes. For compound **1**, the MS spectrum in positive ion mode revealed a ^{13}C monoisotopic peak with an abundance of 9.1%, implying a molecule with approximately 8 carbon atoms. Absence of an $[M+2]^+$ peak ruled out the presence of sulfur (or chlorine or bromine) atoms. Guided by the fact that previous PFAS analysis[20, 25] on our instrument demonstrated their preference for the formation of $[M+H]^+$ adducts (behavior also displayed by *N*-EtFOSE in this study), an even-electron ion of elemental composition $C_8H_5NOF_{13}^+$ was considered (*m/z* = 378.0171, Δm = 1.9 ppm). A simple search on PubChem for $C_8H_4NOF_{13}$ produced 6 possible isomers, only one of which contained a C6 perfluorinated side chain. Upon examination of the negative mode MS spectrum shown in Figure 2.3a, there were 2 prominent peaks at *m/z* 318.9796 and 315.9819 in addition to a smaller molecular ion peak $[M-H]^-$ at *m/z* 376.0007 (Δm = 0 ppm). *m/z* 318.9796 was consistent with $C_6F_{13}^-$ (Δm = 1.3 ppm) pointing towards *N*-methylperfluoroheptanamide as a tentative candidate. The ion with *m/z* 315.9819 could be explained by the formation of $C_8F_{10}NO^-$ (Δm = 0.3 ppm) via the consecutive losses of 3 molecules of hydrogen fluoride (HF) from the molecular ion. This structure proposal is likely the result of gas-phase rearrangements that occur during mass spectrometry experiments.[31] The MS^2 spectrum for compound **1** in the positive mode (Figure 2.3d) also displays a fragment at 330.0150 ($C_7H_4F_{12}N^+$ Δm = -0.6 ppm) formed through similar means. With this structural support for the candidate in hand, we then decided to synthesize a standard to increase the confidence in the assignment of our tentative candidate. Figure 2.3g displays the positive mode MS/MS spectrum of the synthetic product with mass 378 selected in the quadrupole.

The mass accuracies of the molecular ion 378.0157 and main fragment 330.0155 were -1.9 ppm and 0.9 ppm, respectively. Although the main fragment is non-diagnostic, accurate masses in 2 ionization modes and a match between the two positive mode MS^2 spectra as well as agreements between RTs and drift times (DTs) (Figures 2.4a and 2.4d) provide sufficient evidence to suggest that compound **1** is *N*-methylperfluoroheptanamide.

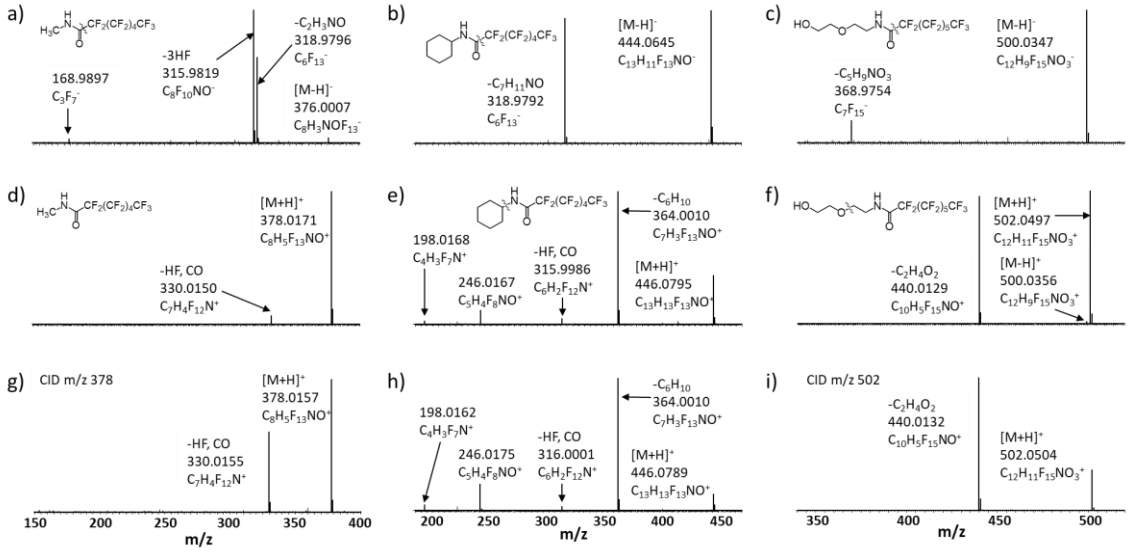

Figure 2.3. Mass spectra of compounds **1-3** under **(a-c)** negative ion mode conditions, **(d-f)** positive ion mode conditions and **(g-i)** commercial/synthetic standards of each in positive ion mode. Unless otherwise noted, all spectra were obtained from either the high or low energy channels of DIA experiments.

Next, the MS^2 spectrum of compound **2** in positive mode (Figure 2.3e) gave a ^{13}C isotope ratio of 14.3% for $[M+H+1]^+/[M+H]^+$ indicating a molecule with roughly 13 carbons. The $[M+H+2]^+$ peak had a low relative abundance, once again eliminating sulfur from the elemental composition. $C_{13}H_{13}NOF_{13}^+$ ($\Delta m = 1.1$ ppm) was investigated as a possibility for $[M+H]^+$ 446.0795. The major fragment in Figure 2.3e, 364.0010 corresponding to an elemental composition of $C_7H_3NOF_{13}^+$ (0.8 ppm) implied loss of

C_6H_{10}, which was hypothesized to be cyclohexene. Successive losses of CO and HF from this fragment could then explain the ion at 315.9986 ($C_6H_2F_{12}N^+$, Δm = -3.2 ppm). This fragmentation pathway resembled that observed with compound **1** and so, compound **2** was also thought to be a perfluoroalkyl amide. The negative ion mode spectrum (Figure 2.3b) was dominated by 319.9792 alluding to the presence of $C_6F_{13}^-$ (Δm = 0 ppm) as seen previously. A mass accuracy of 2.7 ppm (*m/z* = 444.0645) for the $[M-H]^-$ (quasi)molecular ion provided additional evidence to support the chosen elemental composition. Since the MS^2 fragments appeared to fit the structure of *N*-cyclohexyl-2,2,3,3,4,4,5,5,6,6,7,7,7-tridecafluoroheptanamide, an authentic standard was acquired to confirm. With DTs and RTs coinciding (Figures 2.4b and 2.4e) and fragments in the MS^2 spectra aligning (Figures 2.3e and 2.3h), the compounds were considered a match.

For compound **3**, a molecule with approximately 10 carbons and no sulfur was inferred using the ^{13}C isotope ratios. This led to an elemental composition of $C_{12}H_{11}F_{15}NO_3^+$ ($[M+H]^+$ = 502.0497, Δm = -0.4 ppm) being selected for further investigation. The MS^2 spectrum in Figure 2.3f features an intense peak at *m/z* 440.0129 possibly signifying loss of $C_2H_4O_2$ from the protonated molecular ion to give $C_{10}H_7F_{15}NO^+$ (Δm = -0.7 ppm). This loss was thought to be that of ethylene glycol due to recent collision induced experiments performed with fluorotelomer ethoxylates.[25] Present in the negative ion mode spectrum (Figure 2.3c) was a fragment at *m/z* 368.9754 most likely due to $C_7F_{15}^-$ (Δm = -1.6 ppm) and a $[M-H]^-$ ion exhibiting a mass accuracy of 0.8 ppm (*m/z* = 500.0347). The structure shown in Table 2.1 for Amide **3** seemed plausible based on findings thus far, so attempts were made to synthesize a standard. Collision induced dissociation (CID) of

m/z 502 following GC separation of the synthetic products generated the MS/MS spectrum in Figure 2.3i. The observed matches in *m/z*, fragmentation, RT and DT (Figures 2.4c and 2.4f) between compound **3** and the synthetic standard provided strong evidence that *N*-diethoxylated perfluorooctanamide was present.

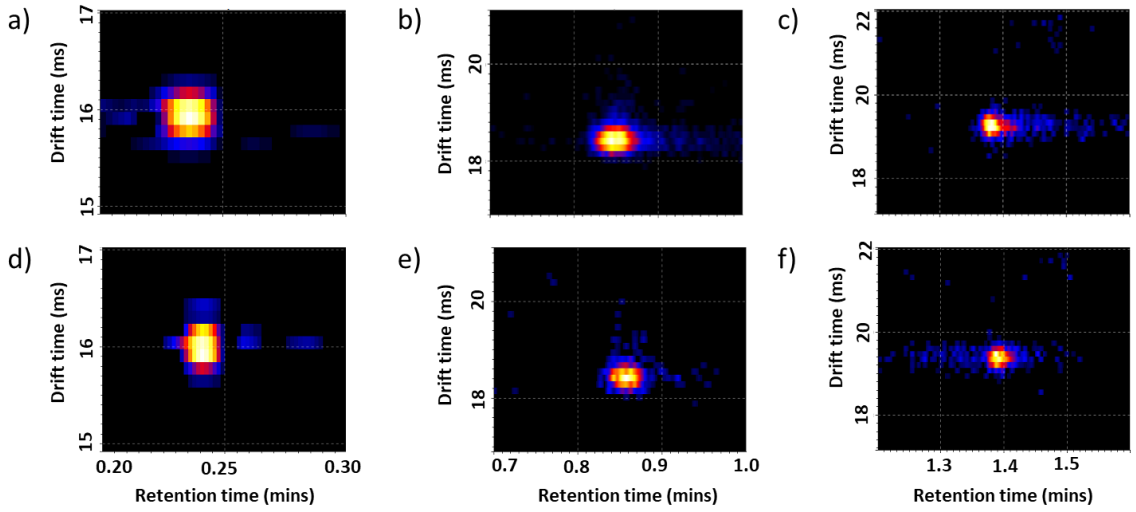

Figure 2.4. DT vs RT contour plots of the (quasi)molecular ions $[M+H]^+$ of compounds **1-3** in **(a-c)** synthetic/commercial standards and **(d-f)** wastewater samples. RTs differ slightly from those reported in Table 2.1 due to column maintenance being performed after initial sample runs.

2.3.3. Distribution of chemicals in wastewater samples

Figure 2.5 depicts the distribution of ions satisfying the criteria CCS < 0.2•*m/z* + 100 using summed ion intensities per site. Immediately evident is the fact that more than three quarters of the total fluorinated content is present in a treated wastewater effluent site. This is not surprising as studies around the world have noted high concentrations of PFAS in effluent wastewater.[32-34] This is because wastewater treatment processes only partially remove the more water soluble PFAS.[33] Most of the fluorinated content in this site was due to a single sulfur containing PFAS suspected to be *N*-EtFOSAA.

Evidence to support this tentative identification was provided by a significantly tailing peak in the XIC, the presence of $[M-H]^-$ in negative mode and $[M-H]^+$ in positive mode and fragmentation via the loss of CO_2 in positive mode leading to the formation of $C_{11}H_7F_{17}NO_2S^+$ (Δm = -0.75 ppm), which is also common to *N*-EtFOSE. LC-HRMS data (negative mode) of this sample showed high levels of this compound. The RT and isotope ratios of the $[M-H]^-$ ion for an authentic *N*-EtFOSAA standard closely matched that of the compound providing further support of its identity. *N*-EtFOSAA is the major biodegradation product of *N*-EtFOSE[35] and since *N*-EtFOSE was also detected at this site, it's likely some of it underwent conversion to *N*-EtFOSAA.

Approximately 7% of the fluorinated ion intensity was contributed by 3 electroplating sites. This is expected since PFAS usage in electroplating industries is well-known.[25, 36, 37] One of the newly identified compounds (Amide **2**) was an important contributor to the PFAS levels at the electroplating 5 site. Synthesis of this perfluorinated acid derivative was previously reported under a German patent with potential use as a surfactant[38] but no current uses could be found in the literature. Next, a site that cleans linen for healthcare workers was found to have appreciable quantities of suspected PFAS. Figure 2.6 shows that these contributors include newly identified Amide **1** and 6:2-O5 FTEO as well as UK-5. As a thorough study of FTEOs has recently been published,[25] it will not be repeated here. A SciFinder search for Amide **1** produced 2 hits from the 1980s once again implying no current applications available in the public domain. Jackson and Mabury[24] also noted a scarcity of published information on polyfluorinated amides (PFAMs). Their study demonstrated that products based on perfluorooctane sulfonyl

fluoride (POSF) contained PFAMs as byproducts of the electrochemical fluorination (ECF) process. Additionally, Wang et al.[39] noted the presence of non-C8 homologues as low-level impurities in POSF-based products. Thus, with many POSF-based compounds having applications in the textiles industry,[40] it's possible that Amide **1** was released as an impurity. Such impurities when released during the life cycle of POSF-based products, can degrade into perfluoroalkyl carboxylic acids (PFCAs) in the environment and biota.[24] Another

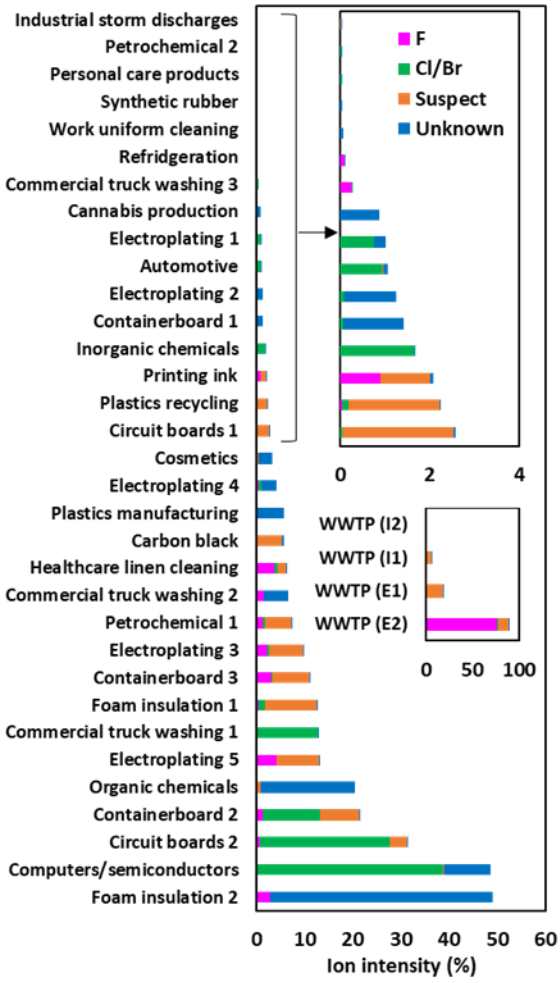

Figure 2.5. Distribution of suspected halogenated ions based on their intensities across individual industrial facilities and sectors. Also shown is the distribution of these ions in two effluent (E1 & E2) and influent samples (I1 and I2) from a municipal WWTP.

possibility is that Amide **1** (as well as Amide **2**) is a degradation product of a side-chain fluorinated polymer (SCFP) or part of the monomer used in the synthesis of one. A 2022 report by the Organization for Economic Co-operation and Development (OECD)[41] listed a perfluorohexanoic acid (PFHxA)-derivative [CASRN 154380-34-4; $CF_3(CF_2)_4CONH(CH_2)_3Si(OCH_3)_3$] as a monomer used to make silicone based SCFPs. Although there were no findings in the literature for perfluoroheptanoic acid derivatives (as in the cases of Amides **1** and **2**), the report also notes that many silicone SCFPs and monomers are not made public due to confidentiality claims. Besides the healthcare linen cleaning site, Figure 2.6 illustrates that Amide **1** was also present in sites such as cosmetics and petrochemical 1. Since silicone SCFPs have been applied as surface treatment products for textiles, oil and water repellents in cosmetics and antifoaming agents in the petroleum industry,[41] it is possible that these amides are indeed degradation products of a confidential silicone SCFP or monomer.

Relatively high levels of fluorinated compounds were also detected in 2 containerboard sites and a petrochemical site. *N*-EtFOSE, FOSE, S-1, S-2, and S-3 were the culprits in these cases. There seems to be a relationship between these compounds as they are clustered together in the top left-hand region of Figure 2.6. Their isotopic ratios indicate that they are all sulfur-containing PFAS. A plausible explanation for their association may be their co-existence in an industrial formulation with wide ranging applications in electroplating, containerboard, and petrochemical industries. Interestingly, this formulation appears to be utilized in only one municipality (R2). Similarly, Amide **3** has a higher DF in region R3 compared to other regions. Amide **3** has been reported in the

literature as a nonionic fluorocarbon surfactant with applications as a foaming agent,[42, 43] emulsifier[44, 45] and wetting agent.[46] Glüdge et al.[36] has noted that PFAS are used in the oil and gas industry as foaming agents in drilling fluids and in the production of plastic and rubber as foam blowing agents. This offers a possible explanation for the presence of Amide **3** in sites such as petrochemical 2, synthetic rubber and plastics recycling.

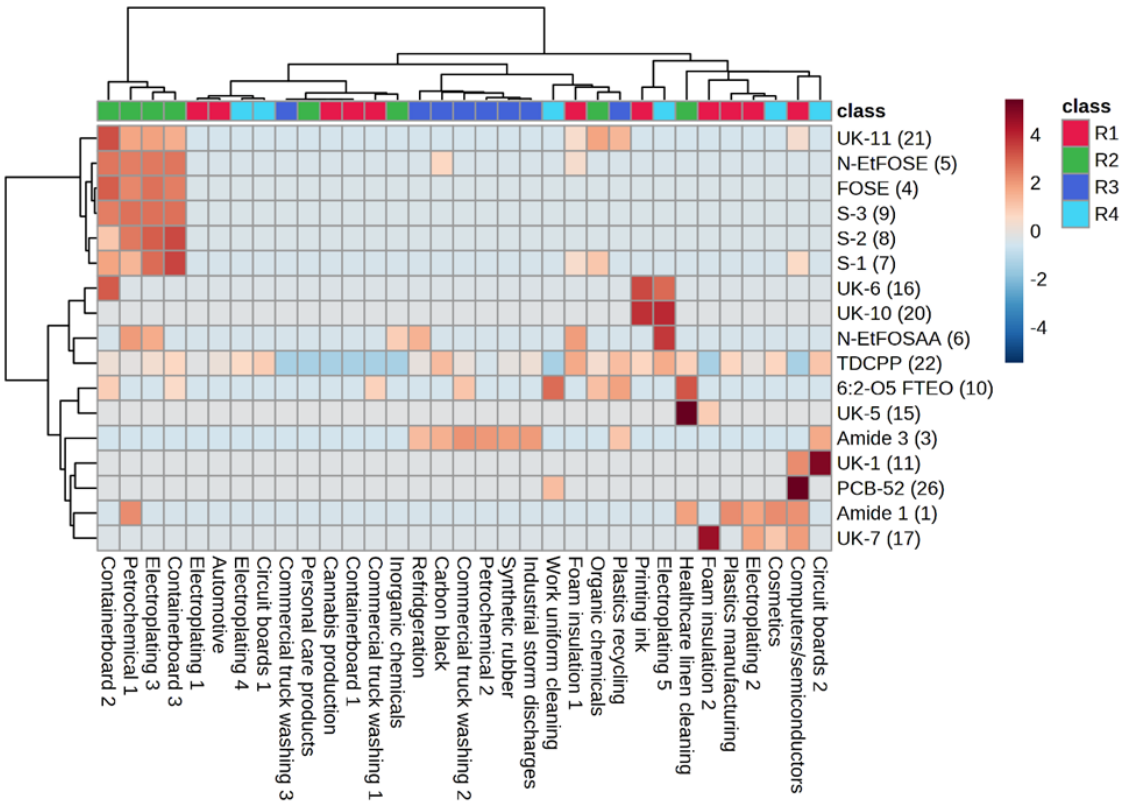

Figure 2.6. 2D-HCA with heat map plot showing compounds tentatively identified by target, suspect and non-target screening of industrial effluent samples collected in Ontario, Canada. Red and blue colors represent the most intense and least intense relative abundance values (log scale), respectively. Compounds with a constant or single value across samples were removed by the software.

Figure 2.6 demonstrates that the most widely distributed contaminant was TDCPP with a DF of 76%. Its presence is seen in several industrial sectors such as electroplating, computers and semiconductors, plastic and rubber and foam insulation. This is not

surprising as Environment and Climate Change Canada notes that hundreds of thousands of kilograms of TDCPP are imported for use as additive flame retardant in flexible foam products (e.g., mattresses, furniture), building and construction materials and in plastics and rubbers.[47] A recent review by Wang et al.[48] describes TDCPP as the most popular flame retardant applied in the polyurethane foam of all product categories. Target analysis showed that TDCPP concentrations in industrial wastewater effluents were 1.4-74.4 ng/L (Table A.6). Similar values were obtained in Spanish rivers that are close to industrial areas (5.3-39 ng/L).[49] However, the values from this study are 1-2 orders of magnitude lower than rivers[50] and seawaters[51] in China that are influenced by industrial activity. The TDCPP concentrations in 2 effluent samples collected from a municipal WWTP were 85 and 202 ng/L. This result compares well with two previous Canadian wastewater studies where TDCPP effluent concentrations ranged from 210-400 ng/L.[52, 53] In addition, a European-wide survey on the occurrence of emerging polar organic contaminants in 90 WWTP effluents (both industrial and domestic), reported maximum and average concentrations of 860 ng/L and 176 ng/L, respectively for TDCPP.[13]

Concentrations of legacy pollutants BDE-47 and BDE-99 ranged from 2-4.3 ng/L (Table A.6) in WWTP influent samples. These values are an order of magnitude lower than the minimum influent value measured by a previous study on Canadian WWTPs.[54] No PBDEs were detected in the WWTP effluent suggesting efficient removal by wastewater treatment processes and agreeing with the aforementioned study where much lower effluent concentrations were observed.[54] The peak areas for 6:2 O5 FTEO in Figure 2.6 range from 1-3 orders of magnitude corresponding to 1-3 orders of magnitude

concentrations (ng/L) as previously reported by Steeves et al.[25] The other PFAS in Figure 2.6 also have peak areas in that range suggesting that their concentrations would be similar to that measured for 6:2 O5 FTEO. Since these levels are comparable to that of known toxic and regulated PFAS such as PFOA and PFOS,[25] further studies are warranted to determine if these compounds or their degradation products could have any harmful ecological or human health effects. Detection of these PFAS across multiple industrial sectors and regions provides further evidence to support this conclusion.

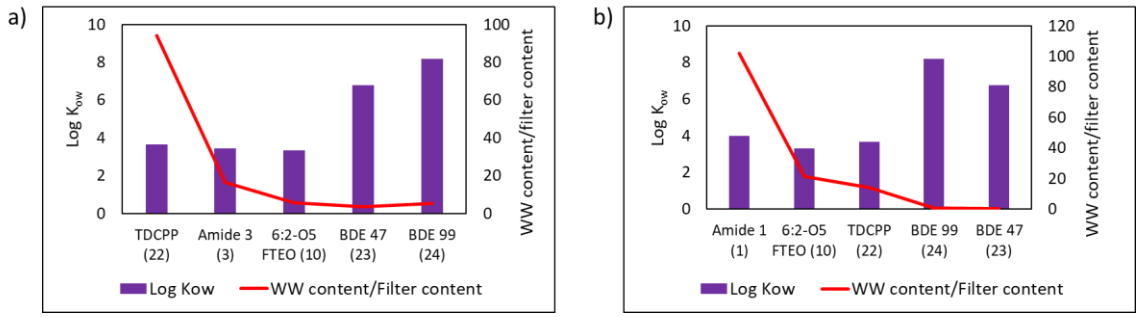

Figure 2.7. Distribution of known pollutants and recently identified PFAS in wastewater samples vs sediments collected on filter papers for **(a)** a plastics recycling facility and **(b)** Healthcare linen cleaning service. Non-detects in either the wastewater or filter were replaced by estimated MDLs. Log K_{ow} values for Amide **1**, Amide **3** and 6:2 O5 FTEO were predicted using US EPA EPI Suite[55] while others were retrieved from ChemSpider.

Figure 2.7 provides a simplistic overview of how the newly identified PFAS were found to partition between aqueous and solid matrices compared to known pollutants. The higher ratio for compounds such as Amide **1**, Amide **3**, 6:2 O5 FTEO and TDCPP suggest a higher presence in the wastewater versus the sediments while the opposite is true for BDE 47 and 99. This observation correlated well with what is predicted using the octanol-water partitioning coefficient (K_{ow}). With $2.5 < \log K_{ow} < 4$ for Amide **1**, Amide **3**, 6:2 O5 FTEO and TDCPP, they are expected to have medium mobility while a $\log K_{ow} > 4$ for BDE 47

and 99 indicates low mobility/high retention in solid matrix.[56] The implication for this is higher bioavailability for the PFAS and a greater likelihood of human consumption through ingestion of drinking water.

2.4. Conclusion

A novel prioritization strategy based on *m/z* and CCS was successfully applied to a set of 33 industrial and 4 municipal wastewater samples resulting in the tentative identification of 19 suspected PFAS and several other halogenated pollutants not matched by a suspect screening database. The identities of 3 of these PFAS were elucidated and subsequently confirmed using synthetic and commercial standards. To the best of our knowledge, this study represents the first detection of these 2 classes of perfluoroalkyl amides in the environment. While most studies focus on LC-HRMS methods for characterizing PFAS, this study highlights the importance of having complementary GC-HRMS methods for detecting neutral compounds that may not ionize well by ESI and thus evade detection. Contaminant distribution across different industrial sectors were investigated leading to possible sources being hypothesized. Although the identities of most PFAS remain unknown, this study demonstrates the presence of thousands of unknown and possible new pollutants in the wastewaters of Ontario, Canada.

2.5. References

1. Wang, Z.; Walker, G. W.; Muir, D. C. G.; Nagatani-Yoshida, K., Toward a Global Understanding of Chemical Pollution: A First Comprehensive Analysis of National and Regional Chemical Inventories. *Environmental Science & Technology* **2020,** *54* (5), 2575-2584.
2. Muir, D.; Zhang, X.; de Wit, C. A.; Vorkamp, K.; Wilson, S., Identifying further chemicals of emerging arctic concern based on 'in silico' screening of chemical inventories. *Emerging Contaminants* **2019,** *5*, 201-210.
3. UNEP, 2009. The nine new pops: An Introduction to the Nine Chemicals Added to the Stockholm Convention by the Conference of the Parties at its Fourth Meeting. Geneva, Switzerland. http://chm.pops.int/Programmes/NewPOPs/Publications/tabid/695/language/en-US/D-efault.aspx
4. Secretariat of the Stockholm Convention. Stockholm Convention on Persistent Organic Pollutants. http://chm.pops.int/TheConvention/ThePOPs/ListingofPOPs/tabid/2509/Default.aspx
5. Li, X.; Dorman, F. L.; Helm, P. A.; Kleywegt, S.; Simpson, A.; Simpson, M. J.; Jobst, K. J., Nontargeted Screening Using Gas Chromatography–Atmospheric Pressure Ionization Mass Spectrometry: Recent Trends and Emerging Potential. *Molecules* **2021,** *26* (22).
6. Municipal-Industrial Strategy for Abatement (MISA), 1986. A policy and program statement of the Government of Ontario on controlling municipal and industrial discharges into surface waters. https://archive.org/details/municipalindustr00ontauoft
7. Schymanski, E. L.; Singer, H. P.; Longrée, P.; Loos, M.; Ruff, M.; Stravs, M. A.; Ripollés Vidal, C.; Hollender, J., Strategies to Characterize Polar Organic Contamination in Wastewater: Exploring the Capability of High Resolution Mass Spectrometry. *Environmental Science & Technology* **2014,** *48* (3), 1811-1818.
8. Murrell, K. A.; Dorman, F. L., A suspect screening analysis for contaminants of emerging concern in municipal wastewater and surface water using liquid–liquid extraction and stir bar sorptive extraction. *Analytical Methods* **2020,** *12* (36), 4487-4495.
9. Sánchez-Avila, J.; Bonet, J.; Velasco, G.; Lacorte, S., Determination and occurrence of phthalates, alkylphenols, bisphenol A, PBDEs, PCBs and PAHs in an industrial sewage grid discharging to a Municipal Wastewater Treatment Plant. *Science of The Total Environment* **2009,** *407* (13), 4157-4167.
10. Barco-Bonilla, N.; Romero-González, R.; Plaza-Bolaños, P.; Garrido Frenich, A.; Martínez Vidal, J. L., Analysis and study of the distribution of polar and non-polar pesticides in wastewater effluents from modern and conventional treatments. *Journal of Chromatography A* **2010,** *1217* (50), 7817-7825.
11. Deeb, A. A.; Schmidt, T. C., Tandem anion and cation exchange solid phase extraction for the enrichment of micropollutants and their transformation products from ozonation in a wastewater treatment plant. *Analytical and Bioanalytical Chemistry* **2016,** *408* (16), 4219-4232.

12. Choi, Y.; Lee, J.-H.; Kim, K.; Mun, H.; Park, N.; Jeon, J., Identification, quantification, and prioritization of new emerging pollutants in domestic and industrial effluents, Korea: Application of LC-HRMS based suspect and non-target screening. *Journal of Hazardous Materials* **2021,** *402*, 123706.
13. Loos, R.; Carvalho, R.; António, D. C.; Comero, S.; Locoro, G.; Tavazzi, S.; Paracchini, B.; Ghiani, M.; Lettieri, T.; Blaha, L.; Jarosova, B.; Voorspoels, S.; Servaes, K.; Haglund, P.; Fick, J.; Lindberg, R. H.; Schwesig, D.; Gawlik, B. M., EU-wide monitoring survey on emerging polar organic contaminants in wastewater treatment plant effluents. *Water Research* **2013,** *47* (17), 6475-6487.
14. Campos-Mañas, M. C.; Plaza-Bolaños, P.; Sánchez-Pérez, J. A.; Malato, S.; Agüera, A., Fast determination of pesticides and other contaminants of emerging concern in treated wastewater using direct injection coupled to highly sensitive ultra-high performance liquid chromatography-tandem mass spectrometry. *Journal of Chromatography A* **2017,** *1507*, 84-94.
15. Xu, C.; Zhu, J.; Li, Y.; Yu, Y.; Duan, G., Fluorous solid-phase extraction (F-SPE) as a pilot tool for quantitative determination of perfluorochemicals in water samples coupled with liquid chromatography-tandem mass spectrometry. *RSC Advances* **2015,** *5* (17), 13192-13199.
16. Blum, A.; Behl, M.; Birnbaum, L. S.; Diamond, M. L.; Phillips, A.; Singla, V.; Sipes, N. S.; Stapleton, H. M.; Venier, M., Organophosphate Ester Flame Retardants: Are They a Regrettable Substitution for Polybrominated Diphenyl Ethers? *Environmental Science & Technology Letters* **2019,** *6* (11), 638-649.
17. Du, J.; Li, H.; Xu, S.; Zhou, Q.; Jin, M.; Tang, J., A review of organophosphorus flame retardants (OPFRs): occurrence, bioaccumulation, toxicity, and organism exposure. *Environmental Science and Pollution Research* **2019,** *26* (22), 22126-22136.
18. DeWitt, J. C., *Toxicological Effects of Perfluoroalkyl and Polyfluoroalkyl Substances*. Springer International Publishing: Cham, 2015.
19. Land, M.; de Wit, C. A.; Bignert, A.; Cousins, I. T.; Herzke, D.; Johansson, J. H.; Martin, J. W., What is the effect of phasing out long-chain per- and polyfluoroalkyl substances on the concentrations of perfluoroalkyl acids and their precursors in the environment? A systematic review. *Environmental Evidence* **2018,** *7* (1), 4.
20. MacNeil, A.; Li, X.; Amiri, R.; Muir, D. C. G.; Simpson, A.; Simpson, M. J.; Dorman, F. L.; Jobst, K. J., Gas Chromatography-(Cyclic) Ion Mobility Mass Spectrometry: A Novel Platform for the Discovery of Unknown Per-/Polyfluoroalkyl Substances. *Analytical Chemistry* **2022,** *94* (31), 11096-11103.
21. Hollender, J.; Schymanski, E. L.; Singer, H. P.; Ferguson, P. L., Nontarget Screening with High Resolution Mass Spectrometry in the Environment: Ready to Go? *Environmental Science & Technology* **2017,** *51* (20), 11505-11512.
22. Schymanski, E. L.; Singer, H. P.; Slobodnik, J.; Ipolyi, I. M.; Oswald, P.; Krauss, M.; Schulze, T.; Haglund, P.; Letzel, T.; Grosse, S.; Thomaidis, N. S.; Bletsou, A.; Zwiener, C.; Ibáñez, M.; Portolés, T.; de Boer, R.; Reid, M. J.; Onghena, M.; Kunkel, U.; Schulz, W.; Guillon, A.; Noyon, N.; Leroy, G.; Bados, P.; Bogialli, S.; Stipaničev, D.; Rostkowski, P.; Hollender, J., Non-target screening with high-resolution mass

spectrometry: critical review using a collaborative trial on water analysis. *Analytical and Bioanalytical Chemistry* **2015,** *407* (21), 6237-55.
23. Afzal, J.; Fung, B. M.; O'Rear, E. A., Syntheses of perfluoroalkyl N-polyethoxylated amides. *Journal of Fluorine Chemistry* **1987,** *34* (3), 385-393.
24. Jackson, D. A.; Mabury, S. A., Polyfluorinated Amides as a Historical PFCA Source by Electrochemical Fluorination of Alkyl Sulfonyl Fluorides. *Environmental Science & Technology* **2013,** *47* (1), 382-389.
25. Steeves, K. L.; Bissram, M. J.; Kleywegt, S.; Stevens, D.; Dorman, F. L.; Simpson, A. J.; Simpson, M. J.; Cahill, L. S.; Jobst, K. J., Nontargeted screening reveals fluorotelomer ethoxylates in indoor dust and industrial wastewater. *Environment International* **2023,** *171*, 107634.
26. USEPA, 1996. Method 3510C: separatory funnel liquid-liquid extraction. https://www.epa.gov/sites/default/files/2015-12/documents/3510c.pdf
27. Zhou, Z.; Luo, M.; Chen, X.; Yin, Y.; Xiong, X.; Wang, R.; Zhu, Z.-J., Ion mobility collision cross-section atlas for known and unknown metabolite annotation in untargeted metabolomics. *Nature Communications* **2020,** *11* (1), 4334.
28. Zhang, X.; Di Lorenzo, R. A.; Helm, P. A.; Reiner, E. J.; Howard, P. H.; Muir, D. C. G.; Sled, J. G.; Jobst, K. J., Compositional space: A guide for environmental chemists on the identification of persistent and bioaccumulative organics using mass spectrometry. *Environment International* **2019,** *132*, 104808.
29. Schymanski, E. L.; Jeon, J.; Gulde, R.; Fenner, K.; Ruff, M.; Singer, H. P.; Hollender, J., Identifying Small Molecules via High Resolution Mass Spectrometry: Communicating Confidence. *Environmental Science & Technology* **2014,** *48* (4), 2097-2098.
30. Pang, Z.; Zhou, G.; Ewald, J.; Chang, L.; Hacariz, O.; Basu, N.; Xia, J., Using MetaboAnalyst 5.0 for LC–HRMS spectra processing, multi-omics integration and covariate adjustment of global metabolomics data. *Nature Protocols* **2022,** *17* (8), 1735-1761.
31. Jacob, P.; Barzen-Hanson, K. A.; Helbling, D. E., Target and Nontarget Analysis of Per- and Polyfluoralkyl Substances in Wastewater from Electronics Fabrication Facilities. *Environmental Science & Technology* **2021,** *55* (4), 2346-2356.
32. Houtz, E. F.; Sutton, R.; Park, J.-S.; Sedlak, M., Poly- and perfluoroalkyl substances in wastewater: Significance of unknown precursors, manufacturing shifts, and likely AFFF impacts. *Water Research* **2016,** *95*, 142-149.
33. Gallen, C.; Eaglesham, G.; Drage, D.; Nguyen, T. H.; Mueller, J. F., A mass estimate of perfluoroalkyl substance (PFAS) release from Australian wastewater treatment plants. *Chemosphere* **2018,** *208*, 975-983.
34. Lenka, S. P.; Kah, M.; Padhye, L. P., A review of the occurrence, transformation, and removal of poly- and perfluoroalkyl substances (PFAS) in wastewater treatment plants. *Water Research* **2021,** *199*, 117187.
35. Liu, J.; Mejia Avendaño, S., Microbial degradation of polyfluoroalkyl chemicals in the environment: A review. *Environment International* **2013,** *61*, 98-114.
36. Glüge, J.; Scheringer, M.; Cousins, I. T.; DeWitt, J. C.; Goldenman, G.; Herzke, D.; Lohmann, R.; Ng, C. A.; Trier, X.; Wang, Z., An overview of the uses of per- and

polyfluoroalkyl substances (PFAS). *Environmental Science: Processes & Impacts* **2020,** *22* (12), 2345-2373.
37. Järnberg, U.; Holmström, K.; van Bavel, B.; Kärrman, A., Perfluoroalkylated acids and related compounds (PFAS) in the Swedish environment. Stockholms universitet, institutionen för tillämpad miljövetenskap (ITM): 2007.
38. Wakselman, C.; Tordeux, M. Perfluorinated compounds. European Patent Office DE2922881A1. 1979.
39. Wang, Z.; Boucher, J. M.; Scheringer, M.; Cousins, I. T.; Hungerbühler, K., Toward a Comprehensive Global Emission Inventory of C4–C10 Perfluoroalkanesulfonic Acids (PFSAs) and Related Precursors: Focus on the Life Cycle of C8-Based Products and Ongoing Industrial Transition. *Environmental Science & Technology* **2017,** *51* (8), 4482-4493.
40. Smith, J. W. N.; Beuthe, B.; Dunk, M.; Demeure, S.; Carmona, J. M. M.; Medve, A.; Spence, M. J.; Pancras, T.; Schrauwen, G.; Held, T., Environmental fate and effects of polyand perfluoroalkyl substances (PFAS). *CONCAWE Reports* **2016,** *8*, 1-107.
41. OECD, 2022. Synthesis Report on Understanding Side-Chain Fluorinated Polymers and Their Life Cycle, OECD Series on Risk Management, No. 73, Environment, Health and Safety, Environment Directorate, OECD. https://www.oecd.org/chemicalsafety/portal-perfluorinated-chemicals/synthesis-report-on-understanding-side-chain-fluorinated-polymers-and-their-life-cycle.pdf
42. Dai, C.; Ding, Q.; Zhao, M.; Zhao, J.; Fang, J.; Li, H., Construction and performance evaluation of a highly efficient mixed foaming system. *RSC Advances* **2015,** *5* (35), 27978-27985.
43. You, Q.; Li, Z.; Ding, Q.; Liu, Y.; Zhao, M.; Dai, C., Investigation of micelle formation by N-(diethyleneglycol) perfluorooctane amide fluorocarbon surfactant as a foaming agent in aqueous solution. *RSC Advances* **2014,** *4* (96), 53899-53906.
44. Fung, B. M.; Mamrosh, D. L.; O'Rear, E. A.; Frech, C. B.; Afzal, J., Unusual micellar properties of a new class of fluorinated nonionic surfactants. *The Journal of Physical Chemistry* **1988,** *92* (15), 4405-4411.
45. Fung, B. M.; O'Rear, E. A.; Afzal, J.; Freeh, C. B.; Mamrosh, D. L.; Gangoda, M., Perfluorochemical Emulsions with Fluorinated Surfactants and Anticancer Drugs. *Biomaterials, Artificial Cells and Artificial Organs* **1988,** *16* (1-3), 439-440.
46. Dai, C.; Fang, J.; Ding, Q.; Wang, T.; Zhao, M.; Wu, Y., Study on adsorption characteristic of novel nonionic fluorocarbon surfactant (4-hydroxyethyl ether) (pentadecafluoro-alkyl) amide at coal-water interface. *Colloid & Polymer Science* **2018,** *296* (1), 21-30.
47. Environment and Climate change Canada. Updated risk management scope for TCPP and TDCPP. https://www.canada.ca/en/environment-climate-change/services/evaluating-existing-substances/updated-risk-management-scope-tcpp-tdcpp.html
48. Wang, C.; Chen, H.; Li, H.; Yu, J.; Wang, X.; Liu, Y., Review of emerging contaminant tris(1,3-dichloro-2-propyl)phosphate: Environmental occurrence, exposure, and risks to organisms and human health. *Environment International* **2020,** *143*, 105946.

49. Cristale, J.; García Vázquez, A.; Barata, C.; Lacorte, S., Priority and emerging flame retardants in rivers: Occurrence in water and sediment, Daphnia magna toxicity and risk assessment. *Environment International* **2013,** *59*, 232-243.
50. Liu, Y.; Xie, Z.; Zhu, T.; Deng, C.; Qi, X.; Hu, R.; Wang, J.; Chen, J., Occurrence, distribution, and ecological risk of organophosphorus flame retardants and their degradation products in water and upper sediment of two urban rivers in Shenzhen, China. *Environmental Science and Pollution Research* **2023,** *30* (6), 14932-14942.
51. Hu, M.; Li, J.; Zhang, B.; Cui, Q.; Wei, S.; Yu, H., Regional distribution of halogenated organophosphate flame retardants in seawater samples from three coastal cities in China. *Marine Pollution Bulletin* **2014,** *86* (1), 569-574.
52. Hao, C.; Helm, P. A.; Morse, D.; Reiner, E. J., Liquid chromatography-tandem mass spectrometry direct injection analysis of organophosphorus flame retardants in Ontario surface water and wastewater effluent. *Chemosphere* **2018,** *191*, 288-295.
53. Woudneh, M. B.; Benskin, J. P.; Wang, G.; Grace, R.; Hamilton, M. C.; Cosgrove, J. R., Quantitative determination of 13 organophosphorous flame retardants and plasticizers in a wastewater treatment system by high performance liquid chromatography tandem mass spectrometry. *Journal of Chromatography A* **2015,** *1400*, 149-155.
54. Kim, M.; Guerra, P.; Theocharides, M.; Barclay, K.; Smyth, S. A.; Alaee, M., Parameters affecting the occurrence and removal of polybrominated diphenyl ethers in twenty Canadian wastewater treatment plants. *Water Research* **2013,** *47* (7), 2213-2221.
55. USEPA, 2012. Estimation Program Interface Suite™ for Microsoft® Windows, v 4.11. https://www.epa.gov/tsca-screening-tools/epi-suitetm-estimation-program-interface
56. Rout, P. R.; Zhang, T. C.; Bhunia, P.; Surampalli, R. Y., Treatment technologies for emerging contaminants in wastewater treatment plants: A review. *Science of The Total Environment* **2021,** *753*, 141990.

Chapter 3. Application of collision cross section and mass for the non-targeted discovery of unknown per- and polyfluoroalkyl substances by liquid chromatography-cyclic ion mobility-mass spectrometry

3.1. Introduction

Twenty-two years have elapsed since per- and polyfluoroalkyl substances (PFAS) were first identified as global contaminants.[1] They have been widely detected in wildlife,[2-5] human samples,[6-10] drinking water,[11-14] wastewater[15-17] and in the distant regions of the Arctic[18, 19] and Antarctic.[20, 21] This has led to the inclusion of a few members of the class under international agreements such as the Stockholm Convention (SC).[22] Due to the restrictions imposed on conventional PFAS chemicals and public concern, PFAS production has shifted toward novel replacement molecules in recent years.[23] Arp et al.[24] have suggested that millions of PFAS exist today. However, targeted methods for PFAS analysis focus on only a few dozen compounds.[25] The implication for the huge gap between the number of PFAS manufactured and those analyzed is a gross underestimation of anthropogenic PFAS releases.[26, 27] In fact, mass balance analyses from several studies have demonstrated that >90% of the total organic fluorine comes from unknown compounds. These unknowns could be legacy PFASs that were previously unidentified, new alternatives, transformation products[28] or even PFAS unintentionally created as byproducts.[29] The development of analytical methods capable of identifying and characterizing such unknown PFAS is necessary to understand the scope of PFAS

contamination and serves as the starting point for generating knowledge to inform risk assessment.[30]

Non-targeted screening (NTS) or workflows designed for unknown compound identification[31] has been pivotal in unknown PFAS discovery. Specifically, NTS strategies based on high resolution mass spectrometry (HRMS) are increasingly common for the discovery and identification of PFAS in environmental and biological samples.[32] The utility of these methods is mainly due to the high-mass spectral resolving power of modern HRMS instruments, which reduce interferences, and their high mass accuracy, which facilitates accurate elemental composition determinations.[28] NTS-HRMS analytical approaches have resulted in the discovery of over 750 PFAS, classified into more than 130 different sub-categories, in carefully chosen environmental samples, biofluids, or commercial products.[30] A challenge with HRMS experiments is finding compounds of interest in the extensive amounts of data generated.[31] To this end, several PFAS recognition strategies have been employed including mass defect filtering,[33, 34] homologous series searching,[35] CF_2 normalized mass defect plots,[29, 36] study design[37, 38] and use of diagnostic fluorine-containing fragment ions (e.g., $C_3F_7^-$, SO_3F^-, $C_2F_5O^-$) and/or neutral losses (e.g., HF).[38, 39]

Recently, a novel NTS method for revealing the presence of unknown PFAS was developed by combining HRMS with ion mobility spectrometry (IMS).[40] IMS enables the determination of a parameter called the collision cross section (CCS), which depends on the size, shape and charge of the analyzed ions.[41] When CCS is plotted against *m/z*, PFAS tend to occupy a region of chemical space defined by $CCS < 0.2 \bullet m/z + 100$.[40] The ability

of this NTS method to discover PFAS in complex real-world samples such as dust and industrial wastewater has been achieved using gas chromatography (GC).[42] Workflows incorporating liquid chromatography (LC) with IMS-HRMS analysis have been gaining popularity in environmental analysis.[43-48] However, most focus on targeted screening and using CCS values as an additional parameter to support compound identification together with chromatographic retention time and accurate masses.

The goal of this study is to demonstrate the applicability of the novel filtering criteria based on CCS and *m/z* to discover unknown PFAS in industrial wastewater samples analyzed by LC-cIM-HRMS with electrospray ionization (ESI). Once multiply charged ions do not complicate the region of chemical space occupied by PFAS, this novel NTS strategy will be useful in aiding complex mixture analysis by LC-cIM-HRMS. Since the wastewater samples were previously characterized by GC-cIM-HRMS, comparisons will also be made to determine which method is better suited to unknown PFAS discovery. Finally, the performance of the analytical method will be evaluated to demonstrate the reliability of results obtained from it.

3.2. Experimental methods

3.2.1. Chemical standards

Methanol was purchased from Fisher Scientific and was HPLC grade. Ultrapure water (UP water, 18.2 MΩ•cm) was from an in-house MilliQ supply. Formic acid (96%) and ammonium acetate (98%) were purchased from Sigma Aldrich (Oakville, ON, Canada). Ammonium hydroxide (28%) and ethyl acetate (ACS grade) were acquired from ACP chemicals (Montreal, QC, Canada). “Major Mix” calibration solution was purchased

from Waters Corporation (Milford, MA, USA). The 18-component PFAS mixture and perfluorooctane sulfonamide (FOSA) used for spike-recovery experiments were obtained from Chromatographic Specialties Inc. (Brockville, ON, Canada) and Toronto Research Chemicals (Toronto, ON, Canada), respectively. Three isotopically labeled analogues were purchased from Wellington Laboratories (Guelph, ON, Canada). These compounds are listed in Table B.1 of Appendix B. Stock solutions of 100 pg/µL for native and surrogate PFAS were prepared in methanol for spiking. A 100 pg/µL methanolic solution of $^{13}C_3$ PFHxS was also prepared for use as an injection standard. Calibration standards were prepared at 5 levels from 0.1 to 25 pg/µL. Standards with purity >96% were used as is while concentrations were corrected for those with purities between 94 and 96%. Each calibration standard had surrogate and injection standard concentrations of 2 pg/µL to match the expected concentrations of 2 pg/µL in the final extracts.

3.2.2. Sample collection and preparation

Sampling details for the examined wastewater samples can be found in Section 2.2.2 and Table A.3. The extraction protocol used to extract the approximately 250 mL wastewater samples was based on a combination of existing methods employing solid phase extraction (SPE).[34, 49-51] Oasis weak anion exchange (WAX) and Oasis weak cation exchange (WCX) cartridges (6 mL, 150 mg, 30 µm; Waters, Milford, MA) were used in a tandem configuration. Samples were first vacuum filtered through glass microfiber filters (GF/F, 0.7 µm average pore size, 47 mm diameter). The filter funnel was rinsed with 5 mL UP water followed by 5 mL 50:50 mixture of methanol/ethyl acetate. This served as an organic modifier (~2%, v/v) to avoid possible analyte adsorptions in the glass

filtration apparatus.[52] Samples were then spiked with 20 µL of the mixed isotopically labeled solution consisting of $^{13}C_4$ PFOA and $^{13}C_4$ PFOS. After swirling for ~1 min, the pH was adjusted to 6.4 ± 0.2 with 5% formic acid or 1.4 M ammonium hydroxide to ensure both ion exchange materials were present in the desired charge state.[53] Prior to extraction, SPE WAX cartridges were conditioned sequentially with 4 mL 0.1% (v/v) ammonium hydroxide in a 50:50 mixture of methanol/ethyl acetate followed by 4 mL 50:50 mixture of methanol/ethyl acetate and 4 mL UP water. Conditioning for the WCX cartridges involved the same procedure as for the WAX cartridges except that the 4 mL 0.1% ammonium hydroxide was replaced with 4 mL 0.1% (v/v) formic acid in a 50:50 mixture of methanol/ethyl acetate. Care was taken to avoid the cartridges dying out at any stage. The two cartridges were then connected together in a tandem mode where the Oasis WAX cartridge was connected directly to the sample reservoir and Oasis WCX was attached to the SPE manifold.

Wastewater samples were passed through the cartridge under vacuum at a rate of 1 drop per second. Once loading was complete, cartridges were separated and each washed with 4 mL UP water followed by 4 mL 25 mM ammonium acetate buffer (pH 4 for WAX, pH 7.5 for WCX). They were then dried under vacuum for 10 min. WAX cartridges were subsequently eluted with 2 × 4 mL of 0.1% (v/v) ammonium hydroxide in 50:50 methanol/ethyl acetate, one portion of which was previously used to rinse the sample bottle. 4 mL 0.1% (v/v) formic acid in 50:50 mixture of methanol/ethyl acetate was used to elute the WCX cartridges into the same polypropylene tube as the WAX fraction. Extracts were reduced to <1 mL via nitrogen gas blowdown and then filtered through

0.2 µm regenerated cellulose syringe filters into 2 mL polypropylene vials. Polypropylene tubes were rinsed with 2 × 0.5 mL methanol and these washings were also filtered into the 2 mL vials to remove any residual analytes from the filter. Extracts were once again reduced to ~0.5 mL with a gentle stream of nitrogen gas. 20 µL of $^{13}C_3$ PFHxS injection standard was added, and the final volume was brought to 1 mL with UP water. Extracts were capped with polyethylene covers and stored at 5 °C until analysis.

3.2.3. Instrumental analysis

Standards and wastewater extracts were analyzed on an Acquity H-Class UPLC (Waters Corporation) coupled to a cyclic IMS-QTOF mass spectrometer (Waters Corporation) using an electrospray ionization interface operated in the negative ionization mode. Chromatographic separation was performed on a Bridged Ethylene Hybrid (BEH) C_{18} analytical column (2.1 × 50 mm, 1.7 µm, Waters Corporation) held at 40 °C during the analysis. The gradient[50] (water:methanol, both with 0.1% formic acid) was 90:10 at 0 min, to 50:50 at 4 min, to 5:95 at 17 min, held until 25 min then 90:10 at 25.1 to 30 min at a flow rate of 200 µL/min. A BEH C_{18} isolator column (50 × 2.1 mm, 3.5 µm) was inserted between the pumps and injector to trap system PFASs. An injection volume of 10 µL was used. The source conditions were as follows: source temperature, 150 °C; desolvation temperature, 250 °C; cone gas, 150 L/hour; desolvation gas, 300 L/hour; cone voltage, 40 V and capillary voltage, 2.0 kV. MS data were acquired over the range *m/z* 50-1200 using data independent acquisition (DIA) mode. An MS^E acquisition method was used with the collision energy set to 4 eV for precursor ion transmission and a ramp of 10 to 40 eV used for the high-energy channel to obtain fragmentation data. Leucine enkephalin

(*m/z* 554.26202) was used for mass correction. With a short separation time of 2 ms, the cyclic ion mobility cell (nitrogen drift gas) was operated in single pass mode. A traveling wave height of 22 V and wave velocity of 375 m/s was employed to effect separation. Instrument calibration to measure CCS was performed according to standard procedure using the 22-component "Major Mix" solution from Waters Corp.

3.2.4. Data processing

Raw data files for method blanks and samples were uploaded into the Progenesis QI software created by Waters Corporation. The software automatically performed several processes, including lock mass correction, peak picking, alignment, and deconvolution. A consolidated list of PFAS substances designated "PFASMaster" was downloaded from the EPA's dashboard[54] for use in suspect screening. It contained 12034 PFAS chemicals (when accessed in July 2022) of potential interest based on environmental occurrence, manufacturing process data and research programs within the EPA. A mass tolerance of 5 ppm was used in Progenesis Metascope to execute the suspect screen. Peaks with tentative identifications were tagged and the entire list exported in .csv format. Microsoft Excel was then used to perform a 10-fold blank subtraction. Ions that remained were subjected to the filtering criteria $CCS < 0.2 \bullet m/z + 100$ where $150 < CCS < 250$ Å. Finally, a script tool (R code) described in Zhang et al.[55] was used to filter out chlorinated and brominated ions, leaving behind potentially fluorinated ones.

3.2.5. Quality Assurance and Quality Control

19 targeted analytes were used to assess method performance characteristics. Calibration curves were created in TargetLynx (Waters Corporation) by plotting the ratio

of the area of the analyte to the area of the $^{13}C_4$-PFOS surrogate on the y-axis and the ratio of the concentration of the analyte to the concentration of $^{13}C_4$-PFOS on the x-axis. $^{13}C_3$ PFHxS injection standard was used to correct variations in instrument response due to ion suppression/enhancement during ESI. Calibration curves ranged between 0.1 to 25 pg/μL (3-5 levels). Method detection limits (MDLs) were estimated from procedural blanks and were defined as the average concentration of the analytes in the blanks plus the standard deviation times 6.965 (n=3). For compounds not detected in the blank, MDLs were estimated as the concentration of chemical generating a signal-to-noise of ~5. Concentrations were normalized to 0.25 L of UP water. To evaluate the absolute recovery, accuracy and precision, target PFASs were spiked (2 ng each) in triplicate into 18.2 MΩ•cm UP water samples. Absolute recoveries were calculated based on a one-point external standard calibration while concentration values for use in accuracy and precision determination were obtained from the calibration curves. Confidence in the assignments for the compounds matched by suspect and non-target screening in Table 3.1, is characterized using the 5-level scale proposed by Schymanski et al.[56]

3.3. Results and Discussion

3.3.1. Screening LC-ESI-cIM-MS data for halogenated pollutants based on *m/z* and CCS

Figure 3.1a displays the approximately 50,000 ions (4046 suspects) detected by Progenesis across all samples following a 10-fold blank subtraction. The complex nature of these samples is obvious, highlighting the need for efficient PFAS recognition strategies.

The filtering criterion applied here is based on the fact that PFAS and other polyhalogenated substances contain fewer atoms than their nonhalogenated counterparts with similar mass and are therefore relatively compact, leading to small CCS values and high molecular density.[40] As such, the region of chemical space defined by CCS < 0.2•m/z + 100 Å^2 is expected to be rich in fluorinated, chlorinated and brominated compounds. When this filter was applied to the blank subtracted dataset, 2046 ions and 473 PFAS suspects remained. A further restriction of 150 < CCS < 250 Å^2 was then imposed to minimize the false positive discovery of halogenated compounds.[40] However, it is worth mentioning that shorter chain PFAS[47] (≤ 6 carbons) can have CCS values less than 150 Å^2

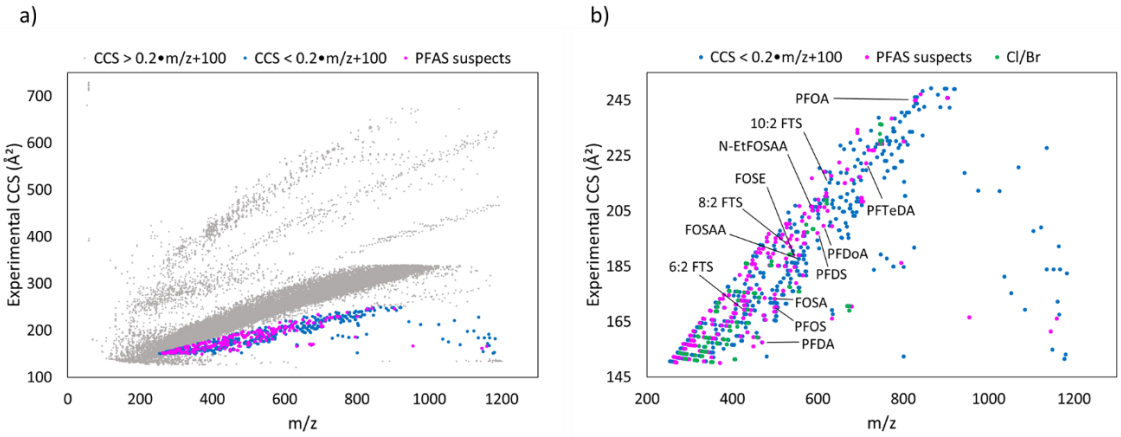

Figure 3.1. Experimental CCS_{N_2} vs *m/z* and for **(a)** approximately 50,000 ions present in industrial wastewater samples after blank subtraction (10-fold) and **(b)** only ions characterized by CCS values that are less than the sum of 100 Å^2 and one fifth of their mass.

and may be excluded from the analysis. Figure 3.1b illustrates the filtered dataset containing 937 ions and 278 suspects. Application of the CCS-*m/z* filter resulted in a fifty- and fifteen-fold reduction in ions and PFAS suspects, respectively. One hundred chlorinated/brominated ions were then removed using a previously developed script tool

that clusters ions based on retention times, isotopic specific mass differences and isotope ratios.[55] The final dataset was comprised of 837 ions that were potentially fluorinated, 245 of which were matched by suspect screening. Even after these extensive filtering steps it is unlikely that all these compounds are fluorinated. Nevertheless, an in-depth look at this smaller, more manageable dataset is now possible.

Table 3.1 is a compilation of PFAS tentatively identified through manual interrogation of the mass spectra of potential PFAS ions in Figure 3.1b. The presence of several well-known subclasses of PFAS including homologues of perfluorocarboxylic acids (PFCAs), perfluorosulfonic acids (PFSAs) and fluorotelomer sulfonic acids (FTSAs) validate the applicability of the CCS-*m/z* filtering criterion for PFAS discovery in LC-ESI-cIM-HRMS data. Since members of a homologous series are known to fall on a diagonal line in DT vs RT plots[40] or CCS vs *m/z* plots,[47] the identification of 1 homologue facilitated the discovery of others. Seven compounds were assigned with Level 1 confidence using several points of comparison with authentic standards: mass accuracy <5 ppm, retention time ±0.2 min, CCS percent deviation <1.5% (except PFOA) and agreements between the isotopic ratios of suspects and proposed compounds (±10%). Level 3 identifications were allocated to candidates that had a homologue identified with Level 1 confidence and the candidate's retention time was consistent with the homologous series. Members of the FTSA homologous series were only recognized as Level 4 since no member was confirmed with an authentic standard. Their tentative structures (and FOSE's) were based on their presence on the PFAS suspect screening list and CCS percent deviations of less than 5% from published values.[57] Finally, several exact masses of interest

were assigned a Level 5 status until further resources could be allocated toward their elemental composition determination and spectral interpretation.

Table 3.1. Summary of compounds tentatively identified by suspect and non-target screening of LC-ESI-cIM-MS data. CCS (Exp.) and CCS (Std.) are experimentally derived values for ions in the wastewater samples and authentic standards, respectively while CCS (Lit.) are literature values from PubChem[57] (underlined values were predicted by AllCCS[58]). The CCS deviation (%) is calculated between CCS (Exp.) and CCS (Std.) in most cases or between CCS (Exp.) and CCS (Lit.) where CCS (Std.) is unavailable. The detection frequency (DF) of compounds across samples (n=37) is shown in the last column.

Compound ID	Class	Structure	Elemental composition	ID Lvl [56]	ID Mtd	Ion(s)	m/z	Mass error (ppm)	RT (min)	CCS (Exp.)	CCS (Std.)	CCS (Lit.)	CCS dev (%)	DF
PFOA **(1)**	Perfluoro-carboxylic acids (PFCAs)	C_7F_{15}-COOH	$C_8HF_{15}O_2$	1	S	$[2M-H]^-$	826.9419	2.1	14.89	245.0	-	226.6	8.1	2
PFDA **(2)**		C_9F_{19}-COOH	$C_{10}HF_{19}O_2$	1	NTS	$[M-H-CO_2]^-$	468.9710	0.6	16.94	157.6	157.6	155.6	0.0	1
PFDoA **(3)**		$C_{11}F_{23}$-COOH	$C_{12}HF_{23}O_2$	1	S	$[M-H]^-$	612.9549	2.1	19.49	199.7	199.7	192.2	0.0	7
PFTeDA **(4)**		$C_{13}F_{27}$-COOH	$C_{14}HF_{27}O_2$	1	S	$[M-H]^-$	712.9480	1.0	21.93	222.2	222.2	209.9	0.0	1
PFOS **(5)**	Perfluorosulfonic acids (PFSAs)	C_8F_{17}-S(=O)$_2$OH	$C_8HF_{17}SO_3$	1	NTS	$[M-H]^-$	498.9313	3.2	15.32	170.2	170.2	168.9	0.0	10
PFDS **(6)**		$C_{10}F_{21}$-S(=O)$_2$OH	$C_{10}HF_{21}SO_3$	3	S	$[M-H]^-$	598.9244	1.0	17.91	194.4	-	186.9	4.0	3
FOSA **(7)**	Perfluoroalkyl-sulfonamides (PFSMs)	C_8F_{17}-S(=O)$_2$NH$_2$	$C_8H_2F_{17}NO_2S$	1	S	$[M-H]^-$	497.9471	1.8	15.11	173.3	173.3	163.2	0.0	6
FOSE **(8)**	Alcohol-PFSMs	C_8F_{17}-S(=O)$_2$NHCH$_2$CH$_2$OH	$C_{10}H_6F_{17}NO_3S$	4	S	$[M-H]^-$	541.9730	1.0	15.61	189.2	-	180.5	4.8	9
FOSAA **(9)**	Carboxylic acid-PFSMs	C_8F_{17}-S(=O)$_2$NHCH$_2$COOH	$C_{10}H_4F_{17}NO_4S$	3	S	$[M-H]^-$	555.9517	0.0	15.43	187.6	-	181.7	3.3	7
N-EtFOSAA **(10)**		C_8F_{17}-S(=O)$_2$N(CH$_2$CH$_3$)CH$_2$CO$_2$H	$C_{12}H_8F_{17}NO_4S$	1	S	$[M-H]^-$	583.9832	0.4	16.94	206.6	204.0	196.8	1.3	2
10:2 FTS **(11)**	Fluorotelomer sulfonic acid (FTSAs)	$C_{10}F_{21}$-CH$_2$CH$_2$-S(=O)$_2$OH	$C_{12}H_5F_{21}O_3S$	4	S	$[M-H]^-$	626.9557	0.9	19.53	215.3	-	204.2	5.4	6
8:2 FTS **(12)**		C_8F_{17}-CH$_2$CH$_2$-S(=O)$_2$OH	$C_{10}H_5F_{17}O_3S$	4	S	$[M-H]^-$	526.9622	1.2	16.79	193.6	-	186.4	3.8	8
6-2 FTS **(13)**		C_6F_{13}-CH$_2$CH$_2$-S(=O)$_2$OH	$C_8H_5F_{13}O_3S$	4	NTS	$[M-H]^-$	426.9678	0.9	13.67	169.4	-	168.5	0.6	5
S-1 **(14)**	Unknown sulfur containing PFAS			5	NTS	$[M-H]^-$	386.9561		13.60	163.5				2
S-2 **(15)**				5	NTS	$[M-H]^-$	376.9716		11.90	158.7				1
S-3 **(16)**				5	NTS	$[M-H]^-$	534.9566		10.83	194.9				1
S-4 **(17)**				5	NTS	$[M-H]^-$	518.9617		13.38	192.2				3
S-5 **(18)**				5	NTS	$[M-H]^-$	494.9556		13.67	189.6				5
S-6 **(19)**				5	NTS	$[M-H]^-$	455.0017		14.78	184.3				1
S-7 **(20)**				5	NTS	$[M-H]^-$	480.0044		3.21	195.4				35
S-8 **(21)**				5	NTS	$[M-H]^-$	566.9179		15.25	193.2				10
S-9 **(22)**				5	NTS	$[M-H]^-$	568.9479		15.43	193.2				5
S-10 **(23)**				5	NTS	$[M-H]^-$	535.9523		13.17	192.1				1
S-11 **(24)**				5	NTS	$[M-H]^-$	524.9467		16.79	187.9				9
S-12 **(25)**				5	NTS	$[M-H]^-$	440.9476		13.63	167.7				13
UK-1 **(26)**				5	NTS	$[M-H]^-$	564.9224		16.65	181.8				5
UK-2 **(27)**				5	NTS	$[M-H]^-$	548.9274		15.97	179.0				11
UK-3 **(28)**				5	NTS	$[M-H]^-$	469.9740		16.72	157.6				2
UK-4 **(29)**				5	NTS	$[M-H]^-$	498.9404		27.12	173.3				4
UK-5 **(30)**				5	NTS	$[M-H]^-$	700.9240		19.42	208.4				1

3.3.2. GC-APCI-cIM-MS vs LC-ESI-cIM-MS

The results of data filtering based on CCS and *m/z* for the analysis of wastewater samples by GC-APCI-cIM-MS and LC-ESI-cIM-MS are summarized in Figure 3.2. Initial

data reduction strategies previously discussed led to the number of potential PFAS being 2 to 3 times higher for LC than GC, depending on whether the number of potential PFAS were identified by suspect screening with the "PFASMaster" list or through the NTS filter CCS < 0.2•m/z + 100 with 150 < CCS < 250 Å. Closer examination of both datasets showed that many background ions had evaded blank subtraction. For instance, with GC, there were 66 ions with RT > 7 min that were likely due to column bleed as the oven temperature was ramped higher toward the end of the analysis. With LC, 371 ions with RT <0.8 min were suspected to be from the solvent peak. Two example chromatograms of such ions are shown in Figures B.1 and B.2. To allow for a more meaningful comparison of the data, these ions were removed. Datasets were then subjected to mass defect analysis. Mass defect is defined as the difference between the nominal and exact mass of a molecule. PFAS usually have low or negative mass defects since many hydrogen atoms (each with $\Delta m/z = 0.0079$) are substituted with many fluorine atoms (each with $\Delta m/z = 0.0016$).[30] Bugsel and Zwiener[36] used a PFAS list of 3213 compounds from the EPA dashboard to show that 92.8% of PFAS in the database had a mass defect between -0.25 and +0.1. When this filter was applied to the remaining ions, the ratio of the number of potential PFAS by LC vs GC remained almost the same for NTS but increased slightly for suspect screening. To conclude, although three times more PFAS were detected by LC, the difference was not huge.

	GC	LC	LC/GC
Ions filtered by NTS (-Cl/Br)	243	837	3.4
PFAS suspects	121	245	2.0

Further removal of background ions

Mass defect filtering 0.1 to -0.25

	GC	LC	LC/GC
Ions filtered by NTS (-Cl/Br)	112	340	3.0
PFAS suspects	58	154	2.7

Figure 3.2. Comparison of the results of suspect and non-target screening of wastewater samples from GC-APCI-cIM-MS and LC-ESI-cIM-MS.

3.3.3. Effect of multiply charged ions on CCS-mass filtering criterion

Unlike atmospheric pressure chemical ionization (APCI) which primarily generates singly charged species,[59] electrospray ionization (ESI) can produce a mixture of singly and multiply charged ions resulting in increased spectral complexity.[60] A simple comparison between Figures 2.1a and 3.3a demonstrates this. Besides the 2 bands of singly charged halogenated and non-halogenated ions in Figure 2.1a, there are now 3 additional bands of doubly charged ions in Figure 3.3a. There appears to be no overlap between the doubly charged ions and the polyhalogenated ones in blue filtered by the model. What about higher charged ions? Figure 3.3b displays the appearance of the CCS vs mass plot when triply charged ions are present. The only difference between Figures 3.3a and 3.3b is that an $[M-3H]^{3-}$ adduct was selected in addition to the $[M-H]^{-}$ and $[M-2H]^{2-}$ adducts during the initial import of raw data files into Progenesis QI. Like Progenesis QI, most other commercial and open access software would be able to recognize multiply charged ions by their isotope spacing. As a result, any potential interferences by these ions when using this NTS workflow can be easily removed. Figures 3.3c and 3.3d reproduced from Sproß et al.[61] and Vakhrushev et al.[62] respectively, illustrate the appearance of data when *m/z* is plotted versus DT using software such as Driftscope (Waters Corp). Once again, there appears to be no overlap between multiply charged ions and singly charged ones. However, these plots are for non-halogenated molecules such as peptides. It's possible that PFAS will have short enough drift times that they will occur in the region of *m/z* vs DT space occupied by doubly charged ions. Consequently, unknown PFAS discovery in LC-ESI-cIM-MS data processed

using Driftscope or similar software using DT instead of CCS could be problematic. Further investigation is required to determine the extent of overlap.

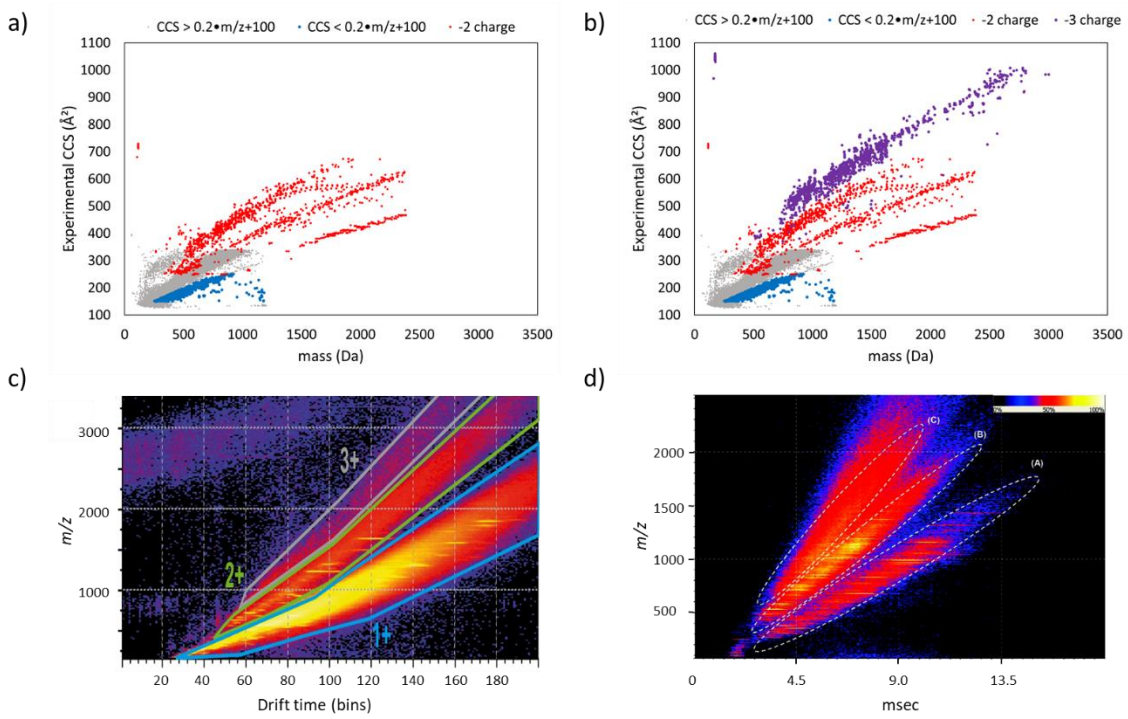

Figure 3.3. Plots of **(a)** CCS vs mass for singly (grey and blue) and doubly (red) charged ions in wastewater samples **(b)** CCS vs mass for singly (grey and blue), doubly (red) and triply (purple) charged ions in wastewater samples **(c)** *m/z* vs DT for singly, doubly and triply charged peptide ions **(d)** *m/z* vs DT for singly (A), doubly (B), and triply (C) charged ionic species of a glycoconjugate mixture. **(c)** and **(d)** were adapted from Sproß et al.[61] Copyright © 2019, Springer-Verlag GmbH Germany, part of Springer Nature and Vakhrushev et al.[62] © Copyright 2008, American Chemical Society, respectively.

3.3.4. Evaluation of method performance

Method validation ensures that an analytical procedure is appropriate for its intended use and generates high quality data.[63] To validate the method used in the present study, several method performance parameters including linearity, absolute recovery, corrected recovery/accuracy, precision, and MDLs were assessed. Results are summarized

in Table 3.2. Linearities for all analytes were >0.99. However, due to a high chromatographic baseline from system contamination for some analytes, the lowest or lowest 2 calibration standards were excluded resulting in 4- or 3-point calibrations, respectively. In addition, the highest standard was not included in the calibration for 4 analytes due to signal saturation. Figure B.3 illustrates a sample calibration curve for the emerging and replacement PFAS 8:2 Cl-PFESA (8:2 chlorinated perfluoroether sulfonic acid). MDLs ranged from 0.1 to 3.1 ng/L for 14 of 19 compounds and were comparable to MDLs reported in Coggan et al.[15] (0.28-1.5 ng/L). Higher MDLs (4-17 ng/L) were obtained for PFHxA, PFHpA, HFPO-DA and PFHxS while PFOA was present at extremely high levels in the method blanks. Although the PFAS delay column was used to minimize interferences from system contamination, post-injection contamination from poly(tetrafluoroethylene) (PTFE) tubing was still possible leading to the high baseline signal for some analytes. To achieve lower MDLs in PFAS analysis, PTFE tubing should be replaced with stainless steel and polyetheretherketone (PEEK) tubing. A greater source of contamination for most of these analytes with high MDLs was likely PTFE and other fluoropolymers present in laboratory products[64] such as reagents used in sample preparation or Teflon seals in solvent bottle caps. Nevertheless, MDLs achieved in this study should suffice for measurements in wastewater where concentrations typically range from 1-6 orders of magnitude (ng/L).[15-17]

Acceptable recoveries, defined as 70-125%,[51] were achieved for 9 analytes. High recoveries (>150%) were seen for the C6-C8 PFCAs and were most likely due to the contamination issues previously discussed. ADONA also had a high recovery of 143% but

it was not present in method blanks. In this case, the cause could be coextracted compounds that enhance ADONA's ionization (i.e., matrix effects), which are observed even in ultrapure water.[65] Longer chain PFCAs (C11-C13), FOSA and 8:2 Cl-PFESA had lower recoveries between 38 to 60%. This is consistent with previous studies[66, 67] and can be attributed to the higher hydrophobicity of these compounds that result in sorption losses during SPE extraction.[67] To correct for these less-than-ideal recoveries as well as possible ion enhancement/suppression due to matrix effects,[68] two mass-labelled internal standards (IS) were used. However, even the $^{13}C_4$-PFOA IS was not spared. Figure B.4 demonstrates a major suppression event that occurred at the retention time for $^{13}C_4$-PFOA

Table 3.2. Method performance characteristics for wastewater analysis via SPE and LC-ESI-cIM-MS (n=3).

Compound	Recovery (%)	RSD (%)	Accuracy (%)	RSD (%)	MDL (ng/L)	Linearity (R^2)	Linear range (pg/uL)	# of standards
PFHxA	170.3	94.2	178.1	50.5	4.0	0.9962	2.0-25.0	3
PFHpA	282.6	78.2	315.3	78.1	17.2	1.0000	2.0-25.0	3
PFOA	2748.4	134.8	46543.9	154.1	12282.0	0.9990	0.1-25.0	5
PFNA	89.5	24.5	103.0	28.7	0.8	0.9996	0.4-25.0	4
PFDA	112.7	18.0	108.9	22.2	0.8	0.9995	0.4-25.0	4
PFUdA	50.7	10.6	47.9	15.0	0.4	0.9985	0.1-23.8	5
PFDoA	44.6	73.8	52.3	22.8	0.1	0.9979	0.1-25.0	5
PFTrDA	59.8	95.9	55.8	27.6	2.1	0.9981	0.1-25.0	5
PFTeDA	126.5	133.7	63.7	33.8	2.5	0.9966	0.1-25.0	5
L-PFBS	87.7	12.0	103.4	12.5	0.2	1.0000	0.1-8.0	4
L-PFHxS	88.1	12.2	95.7	35.5	7.1	0.9993	0.1-7.0	4
L-PFOS	90.5	23.8	77.4	17.4	3.1	0.9993	0.1-5.7	4
N-EtFOSAA	96.7	53.2	114.0	19.8	1.1	0.9997	0.1-23.8	5
N-MeFOSAA	83.1	29.8	93.3	12.6	1.6	0.9995	0.1-25.0	5
HFPO-DA	97.8	20.1	180.1	13.7	8.0	0.9982	2.0-23.8	3
8:2 Cl-PFESA	37.8	65.8	47.0	45.1	0.4	0.9999	0.1-25.0	5
6:2 Cl-PFESA	80.6	19.2	99.3	19.1	0.4	0.9997	0.1-8.0	4
ADONA	143.3	27.1	151.5	27.7	1.6	0.9993	0.4-25.0	4
FOSA	51.0	37.2	65.4	22.7	0.6	0.9999	0.1-23.8	5

(14.10 min) leading to no analyte signal in the 3rd blank and spiked sample. Initially, $^{13}C_4$-PFOA was being used as the IS for the PFCAs and other monoether-PFCAs. However, because of this suppression, only 2 blank and spiked replicates would be available for method performance evaluation. Therefore, $^{13}C_4$-PFOS was used as the IS for all analytes. Unfortunately, this resulted in only a slight increase in the recoveries for some compounds, which previously had lower recoveries and had no effect on that of ADONA.

Inclusion of the IS did however improve the reproducibility or precision expressed as percent relative standard deviation (RSD) for the C11-C14 PFCAs, FOSA, 8:2 Cl-PFESA, *N*-MeFOSAA and *N*-EtFOSAA. Following IS correction, acceptable precision (<35%) was obtained for 15 of 19 analytes. For HFPO-DA, using the IS changed the recovery from 98 to 180% suggesting that $^{13}C_4$-PFOS was an unsuitable IS for it. Gremmel et al.[65] noted that structural differences between IS and analyte may lead to recoveries that are too high or too low. In the absence of structurally identical or similar IS to improve accuracies, the method can be used to provide semiquantitative results for C11-C14 PFCAs, FOSA, 8:2 Cl-PFESA and ADONA. Quantitative results can be acquired for HFPO-DA through external calibration since its absolute recovery and reproducibility are within limits. The method should not be used to quantify the C6-C8 PFCAs in samples until sources of contamination are investigated and reduced.

3.4. Conclusion

Wastewater samples from several industrial sectors of Ontario, Canada were subjected to a novel NTS strategy based on CCS and *m/z* to detect and identify unknown PFAS. A total of 30 PFAS were tentatively identified through preliminary analyses but the

presence of over 100 more were indicated. Roughly two times more PFAS were identified by NTS when compared to suspect screening suggesting the possible existence of compounds not present in the largest PFAS database. Further investigations are warranted to determine the structures, uses, sources and distribution of these compounds in the Ontario environment. The success of the CCS-*m/z* filtering strategy with LC-ESI-cIM-MS data in this study opens doors for its applicability to PFAS discovery in other biological and environmental matrices. Although LC is the separation method of choice for PFAS analysis, the results obtained here show that GC also has a great deal of potential. The analytical method developed in this study can be used for the quantification of 9 analytes, semi quantitation of another 7 and is well suited to the extraction and detection of unknown PFAS in wastewater.

3.5. References

1. Giesy, J. P.; Kannan, K., Global distribution of perfluorooctane sulfonate in wildlife. *Environmental Science & Technology* **2001,** *35* (7), 1339-42.
2. Murakami, M.; Adachi, N.; Saha, M.; Morita, C.; Takada, H., Levels, Temporal Trends, and Tissue Distribution of Perfluorinated Surfactants in Freshwater Fish from Asian Countries. *Archives of Environmental Contamination and Toxicology* **2011,** *61* (4), 631-641.
3. Rigét, F.; Bossi, R.; Sonne, C.; Vorkamp, K.; Dietz, R., Trends of perfluorochemicals in Greenland ringed seals and polar bears: Indications of shifts to decreasing trends. *Chemosphere* **2013,** *93* (8), 1607-1614.
4. Eriksson, U.; Roos, A.; Lind, Y.; Hope, K.; Ekblad, A.; Kärrman, A., Comparison of PFASs contamination in the freshwater and terrestrial environments by analysis of eggs from osprey (Pandion haliaetus), tawny owl (Strix aluco), and common kestrel (Falco tinnunculus). *Environmental Research* **2016,** *149*, 40-47.
5. Guo, R.; Reiner, E. J.; Bhavsar, S. P.; Helm, P. A.; Mabury, S. A.; Braekevelt, E.; Tittlemier, S. A., Determination of polyfluoroalkyl phosphoric acid diesters, perfluoroalkyl phosphonic acids, perfluoroalkyl phosphinic acids, perfluoroalkyl carboxylic acids, and perfluoroalkane sulfonic acids in lake trout from the Great Lakes region. *Analytical and Bioanalytical Chemistry* **2012,** *404* (9), 2699-2709.
6. Kannan, K.; Corsolini, S.; Falandysz, J.; Fillmann, G.; Kumar, K. S.; Loganathan, B. G.; Mohd, M. A.; Olivero, J.; Wouwe, N. V.; Yang, J. H.; Aldous, K. M., Perfluorooctanesulfonate and Related Fluorochemicals in Human Blood from Several Countries. *Environmental Science & Technology* **2004,** *38* (17), 4489-4495.
7. Yeung, L. W. Y.; Robinson, S. J.; Koschorreck, J.; Mabury, S. A., Part II. A Temporal Study of PFOS and Its Precursors in Human Plasma from Two German Cities in 1982–2009. *Environmental Science & Technology* **2013,** *47* (8), 3875-3882.
8. Kaiser, A.-M.; Aro, R.; Kärrman, A.; Weiss, S.; Hartmann, C.; Uhl, M.; Forsthuber, M.; Gundacker, C.; Yeung, L. W. Y., Comparison of extraction methods for per- and polyfluoroalkyl substances (PFAS) in human serum and placenta samples—insights into extractable organic fluorine (EOF). *Analytical and Bioanalytical Chemistry* **2021,** *413* (3), 865-876.
9. Eriksson, U.; Mueller, J. F.; Toms, L.-M. L.; Hobson, P.; Kärrman, A., Temporal trends of PFSAs, PFCAs and selected precursors in Australian serum from 2002 to 2013. *Environmental Pollution* **2017,** *220*, 168-177.
10. Guy, W. S.; Taves, D. R.; Brey, W. S. J., Organic Fluorocompounds in Human Plasma: Prevalence and Characterization. In *Biochemistry Involving Carbon-Fluorine Bonds*, AMERICAN CHEMICAL SOCIETY: 1976; Vol. 28, pp 117-134.
11. Lange, F. T.; Wenz, M.; Schmidt, C. K.; Brauch, H. J., Occurrence of perfluoroalkyl sulfonates and carboxylates in German drinking water sources compared to other countries. *Water Science and Technology* **2007,** *56* (11), 151-158.

12. Chow, S. J.; Ojeda, N.; Jacangelo, J. G.; Schwab, K. J., Detection of ultrashort-chain and other per- and polyfluoroalkyl substances (PFAS) in U.S. bottled water. *Water Research* **2021,** *201*, 117292.
13. Schwanz, T. G.; Llorca, M.; Farré, M.; Barceló, D., Perfluoroalkyl substances assessment in drinking waters from Brazil, France and Spain. *Science of The Total Environment* **2016,** *539*, 143-152.
14. Munoz, G.; Liu, M.; Vo Duy, S.; Liu, J.; Sauvé, S., Target and nontarget screening of PFAS in drinking water for a large-scale survey of urban and rural communities in Québec, Canada. *Water Research* **2023,** *233*, 119750.
15. Coggan, T. L.; Anumol, T.; Pyke, J.; Shimeta, J.; Clarke, B. O., A single analytical method for the determination of 53 legacy and emerging per- and polyfluoroalkyl substances (PFAS) in aqueous matrices. *Analytical and Bioanalytical Chemistry* **2019,** *411* (16), 3507-3520.
16. Kim, K. Y.; Ndabambi, M.; Choi, S.; Oh, J.-E., Legacy and novel perfluoroalkyl and polyfluoroalkyl substances in industrial wastewater and the receiving river water: Temporal changes in relative abundances of regulated compounds and alternatives. *Water Research* **2021,** *191*, 116830.
17. Loos, R.; Carvalho, R.; António, D. C.; Comero, S.; Locoro, G.; Tavazzi, S.; Paracchini, B.; Ghiani, M.; Lettieri, T.; Blaha, L.; Jarosova, B.; Voorspoels, S.; Servaes, K.; Haglund, P.; Fick, J.; Lindberg, R. H.; Schwesig, D.; Gawlik, B. M., EU-wide monitoring survey on emerging polar organic contaminants in wastewater treatment plant effluents. *Water Research* **2013,** *47* (17), 6475-6487.
18. Stroski, K. M.; Luong, K. H.; Challis, J. K.; Chaves-Barquero, L. G.; Hanson, M. L.; Wong, C. S., Wastewater sources of per- and polyfluorinated alkyl substances (PFAS) and pharmaceuticals in four Canadian Arctic communities. *Science of The Total Environment* **2020,** *708*, 134494.
19. Muir, D.; Bossi, R.; Carlsson, P.; Evans, M.; De Silva, A.; Halsall, C.; Rauert, C.; Herzke, D.; Hung, H.; Letcher, R.; Rigét, F.; Roos, A., Levels and trends of poly- and perfluoroalkyl substances in the Arctic environment – An update. *Emerging Contaminants* **2019,** *5*, 240-271.
20. Vento, S. D.; Halsall, C.; Gioia, R.; Jones, K.; Dachs, J., Volatile per- and polyfluoroalkyl compounds in the remote atmosphere of the western Antarctic Peninsula: an indirect source of perfluoroalkyl acids to Antarctic waters? *Atmospheric Pollution Research* **2012,** *3* (4), 450-455.
21. Midthaug, H. K.; Hitchcock, D. J.; Bustnes, J. O.; Polder, A.; Descamps, S.; Tarroux, A.; Soininen, E. M.; Borgå, K., Within and between breeding-season changes in contaminant occurrence and body condition in the Antarctic breeding south polar skua. *Environmental Pollution* **2021,** *284*, 117434.
22. Wang, Z.; DeWitt, J. C.; Higgins, C. P.; Cousins, I. T., A Never-Ending Story of Per- and Polyfluoroalkyl Substances (PFASs)? *Environmental Science & Technology* **2017,** *51* (5), 2508-2518.
23. Nakayama, S. F.; Yoshikane, M.; Onoda, Y.; Nishihama, Y.; Iwai-Shimada, M.; Takagi, M.; Kobayashi, Y.; Isobe, T., Worldwide trends in tracing poly- and perfluoroalkyl

substances (PFAS) in the environment. *TrAC Trends in Analytical Chemistry* **2019,** *121*, 115410.
24. Arp, H. P. H.; Aurich, D.; Schymanski, E. L.; Sims, K.; Hale, S. E., Avoiding the Next Silent Spring: Our Chemical Past, Present, and Future. *Environmental Science & Technology* **2023,** *57* (16), 6355-6359.
25. Joerss, H.; Menger, F.; Tang, J.; Ebinghaus, R.; Ahrens, L., Beyond the Tip of the Iceberg: Suspect Screening Reveals Point Source-Specific Patterns of Emerging and Novel Per- and Polyfluoroalkyl Substances in German and Chinese Rivers. *Environmental Science & Technology* **2022,** *56* (9), 5456-5465.
26. Miaz, L. T.; Plassmann, M. M.; Gyllenhammar, I.; Bignert, A.; Sandblom, O.; Lignell, S.; Glynn, A.; Benskin, J. P., Temporal trends of suspect-and target-per/polyfluoroalkyl substances (PFAS), extractable organic fluorine (EOF) and total fluorine (TF) in pooled serum from first-time mothers in Uppsala, Sweden, 1996–2017. *Environmental Science: Processes & Impacts* **2020,** *22* (4), 1071-1083.
27. Yeung, L. W.; De Silva, A. O.; Loi, E. I.; Marvin, C. H.; Taniyasu, S.; Yamashita, N.; Mabury, S. A.; Muir, D. C.; Lam, P. K., Perfluoroalkyl substances and extractable organic fluorine in surface sediments and cores from Lake Ontario. *Environment International* **2013,** *59*, 389-397.
28. Liu, Y.; Qian, M.; Ma, X.; Zhu, L.; Martin, J. W., Nontarget Mass Spectrometry Reveals New Perfluoroalkyl Substances in Fish from the Yangtze River and Tangxun Lake, China. *Environmental Science & Technology* **2018,** *52* (10), 5830-5840.
29. Myers, A. L.; Jobst, K. J.; Mabury, S. A.; Reiner, E. J., Using mass defect plots as a discovery tool to identify novel fluoropolymer thermal decomposition products. *Journal of Mass Spectrometry* **2014,** *49* (4), 291-296.
30. Liu, Y.; D'Agostino, L. A.; Qu, G.; Jiang, G.; Martin, J. W., High-resolution mass spectrometry (HRMS) methods for nontarget discovery and characterization of poly- and per-fluoroalkyl substances (PFASs) in environmental and human samples. *TrAC Trends in Analytical Chemistry* **2019,** *121*, 115420.
31. Hollender, J.; Schymanski, E. L.; Singer, H. P.; Ferguson, P. L., Nontarget Screening with High Resolution Mass Spectrometry in the Environment: Ready to Go? *Environmental Science & Technology* **2017,** *51* (20), 11505-11512.
32. Charbonnet, J. A.; McDonough, C. A.; Xiao, F.; Schwichtenberg, T.; Cao, D.; Kaserzon, S.; Thomas, K. V.; Dewapriya, P.; Place, B. J.; Schymanski, E. L.; Field, J. A.; Helbling, D. E.; Higgins, C. P., Communicating Confidence of Per- and Polyfluoroalkyl Substance Identification via High-Resolution Mass Spectrometry. *Environmental Science & Technology Letters* **2022,** *9* (6), 473-481.
33. Place, B. J.; Field, J. A., Identification of Novel Fluorochemicals in Aqueous Film-Forming Foams Used by the US Military. *Environmental Science & Technology* **2012,** *46* (13), 7120-7127.
34. D'Agostino, L. A.; Mabury, S. A., Identification of Novel Fluorinated Surfactants in Aqueous Film Forming Foams and Commercial Surfactant Concentrates. *Environmental Science & Technology* **2014,** *48* (1), 121-129.

35. Trier, X.; Granby, K.; Christensen, J. H., Tools to discover anionic and nonionic polyfluorinated alkyl surfactants by liquid chromatography electrospray ionisation mass spectrometry. *Journal of Chromatography A* **2011,** *1218* (40), 7094-7104.
36. Bugsel, B.; Zwiener, C., LC-MS screening of poly- and perfluoroalkyl substances in contaminated soil by Kendrick mass analysis. *Analytical and Bioanalytical Chemistry* **2020,** *412* (20), 4797-4805.
37. Strynar, M.; Dagnino, S.; McMahen, R.; Liang, S.; Lindstrom, A.; Andersen, E.; McMillan, L.; Thurman, M.; Ferrer, I.; Ball, C., Identification of Novel Perfluoroalkyl Ether Carboxylic Acids (PFECAs) and Sulfonic Acids (PFESAs) in Natural Waters Using Accurate Mass Time-of-Flight Mass Spectrometry (TOFMS). *Environmental Science & Technology* **2015,** *49* (19), 11622-11630.
38. Rotander, A.; Kärrman, A.; Toms, L.-M. L.; Kay, M.; Mueller, J. F.; Gómez Ramos, M. J., Novel Fluorinated Surfactants Tentatively Identified in Firefighters Using Liquid Chromatography Quadrupole Time-of-Flight Tandem Mass Spectrometry and a Case-Control Approach. *Environmental Science & Technology* **2015,** *49* (4), 2434-2442.
39. Baduel, C.; Mueller, J. F.; Rotander, A.; Corfield, J.; Gomez-Ramos, M.-J., Discovery of novel per- and polyfluoroalkyl substances (PFASs) at a fire fighting training ground and preliminary investigation of their fate and mobility. *Chemosphere* **2017,** *185*, 1030-1038.
40. MacNeil, A.; Li, X.; Amiri, R.; Muir, D. C. G.; Simpson, A.; Simpson, M. J.; Dorman, F. L.; Jobst, K. J., Gas Chromatography-(Cyclic) Ion Mobility Mass Spectrometry: A Novel Platform for the Discovery of Unknown Per-/Polyfluoroalkyl Substances. *Analytical Chemistry* **2022,** *94* (31), 11096-11103.
41. Hinnenkamp, V.; Klein, J.; Meckelmann, S. W.; Balsaa, P.; Schmidt, T. C.; Schmitz, O. J., Comparison of CCS Values Determined by Traveling Wave Ion Mobility Mass Spectrometry and Drift Tube Ion Mobility Mass Spectrometry. *Analytical Chemistry* **2018,** *90* (20), 12042-12050.
42. Steeves, K. L.; Bissram, M. J.; Kleywegt, S.; Stevens, D.; Dorman, F. L.; Simpson, A. J.; Simpson, M. J.; Cahill, L. S.; Jobst, K. J., Nontargeted screening reveals fluorotelomer ethoxylates in indoor dust and industrial wastewater. *Environment International* **2023,** *171*, 107634.
43. Mullin, L.; Jobst, K.; DiLorenzo, R. A.; Plumb, R.; Reiner, E. J.; Yeung, L. W. Y.; Jogsten, I. E., Liquid chromatography-ion mobility-high resolution mass spectrometry for analysis of pollutants in indoor dust: Identification and predictive capabilities. *Analytica Chimica Acta* **2020,** *1125*, 29-40.
44. Celma, A.; Ahrens, L.; Gago-Ferrero, P.; Hernández, F.; López, F.; Lundqvist, J.; Pitarch, E.; Sancho, J. V.; Wiberg, K.; Bijlsma, L., The relevant role of ion mobility separation in LC-HRMS based screening strategies for contaminants of emerging concern in the aquatic environment. *Chemosphere* **2021,** *280*, 130799.
45. Belova, L.; Caballero-Casero, N.; van Nuijs, A. L. N.; Covaci, A., Ion Mobility-High-Resolution Mass Spectrometry (IM-HRMS) for the Analysis of Contaminants of Emerging Concern (CECs): Database Compilation and Application to Urine Samples. *Analytical Chemistry* **2021,** *93* (16), 6428-6436.

46. Celma, A.; Sancho, J. V.; Schymanski, E. L.; Fabregat-Safont, D.; Ibáñez, M.; Goshawk, J.; Barknowitz, G.; Hernández, F.; Bijlsma, L., Improving Target and Suspect Screening High-Resolution Mass Spectrometry Workflows in Environmental Analysis by Ion Mobility Separation. *Environmental Science & Technology* **2020,** *54* (23), 15120-15131.
47. Dodds, J. N.; Hopkins, Z. R.; Knappe, D. R. U.; Baker, E. S., Rapid Characterization of Per- and Polyfluoroalkyl Substances (PFAS) by Ion Mobility Spectrometry–Mass Spectrometry (IMS-MS). *Analytical Chemistry* **2020,** *92* (6), 4427-4435.
48. Stephan, S.; Hippler, J.; Köhler, T.; Deeb, A. A.; Schmidt, T. C.; Schmitz, O. J., Contaminant screening of wastewater with HPLC-IM-qTOF-MS and LC+LC-IM-qTOF-MS using a CCS database. *Analytical and Bioanalytical Chemistry* **2016,** *408* (24), 6545-6555.
49. Deeb, A. A.; Schmidt, T. C., Tandem anion and cation exchange solid phase extraction for the enrichment of micropollutants and their transformation products from ozonation in a wastewater treatment plant. *Analytical and Bioanalytical Chemistry* **2016,** *408* (16), 4219-4232.
50. Schymanski, E. L.; Singer, H. P.; Longrée, P.; Loos, M.; Ruff, M.; Stravs, M. A.; Ripollés Vidal, C.; Hollender, J., Strategies to Characterize Polar Organic Contamination in Wastewater: Exploring the Capability of High Resolution Mass Spectrometry. *Environmental Science & Technology* **2014,** *48* (3), 1811-1818.
51. ISO/FDIS 21675:2019(E). Water quality — Determination of perfluoroalkyl and polyfluoroalkyl substances (PFAS) in water — Method using solid phase extraction and liquid chromatography-tandem mass spectrometry (LC-MS/MS). International Organization for Standardization: 2019.
52. Barco-Bonilla, N.; Romero-González, R.; Plaza-Bolaños, P.; Garrido Frenich, A.; Martínez Vidal, J. L., Analysis and study of the distribution of polar and non-polar pesticides in wastewater effluents from modern and conventional treatments. *Journal of Chromatography A* **2010,** *1217* (50), 7817-7825.
53. Köke, N.; Zahn, D.; Knepper, T. P.; Frömel, T., Multi-layer solid-phase extraction and evaporation—enrichment methods for polar organic chemicals from aqueous matrices. *Analytical and Bioanalytical Chemistry* **2018,** *410* (9), 2403-2411.
54. USEPA, CompTox Chemicals Dashboard | PFASMASTER Chemicals. https://comptox.epa.gov/dashboard/chemical-lists/ (accessed July 2022).
55. Zhang, X.; Di Lorenzo, R. A.; Helm, P. A.; Reiner, E. J.; Howard, P. H.; Muir, D. C. G.; Sled, J. G.; Jobst, K. J., Compositional space: A guide for environmental chemists on the identification of persistent and bioaccumulative organics using mass spectrometry. *Environment International* **2019,** *132*, 104808.
56. Schymanski, E. L.; Jeon, J.; Gulde, R.; Fenner, K.; Ruff, M.; Singer, H. P.; Hollender, J., Identifying Small Molecules via High Resolution Mass Spectrometry: Communicating Confidence. *Environmental Science & Technology* **2014,** *48* (4), 2097-2098.
57. PubChem. https://pubchem.ncbi.nlm.nih.gov/ (accessed May 2023).

58. Zhou, Z.; Luo, M.; Chen, X.; Yin, Y.; Xiong, X.; Wang, R.; Zhu, Z.-J., Ion mobility collision cross-section atlas for known and unknown metabolite annotation in untargeted metabolomics. *Nature Communications* **2020,** *11* (1), 4334.
59. Sparkman, O. D.; Penton, Z. E.; Kitson, F. G., *Gas Chromatography and Mass Spectrometry: A Practical Guide*. Second ed.; Academic Press: 2011.
60. Gaskell, S. J., Electrospray: Principles and Practice. *Journal of Mass Spectrometry* **1997,** *32* (7), 677-688.
61. Sproß, J.; Muck, A.; Gröger, H., Detection and fragmentation of doubly charged peptide ions in MALDI-Q-TOF-MS by ion mobility spectrometry for improved protein identification. *Analytical and Bioanalytical Chemistry* **2019,** *411* (24), 6275-6285.
62. Vakhrushev, S. Y.; Langridge, J.; Campuzano, I.; Hughes, C.; Peter-Katalinić, J., Ion Mobility Mass Spectrometry Analysis of Human Glycourinome. *Analytical Chemistry* **2008,** *80* (7), 2506-2513.
63. Raposo, F.; Ibelli-Bianco, C., Performance parameters for analytical method validation: Controversies and discrepancies among numerous guidelines. *TrAC Trends in Analytical Chemistry* **2020,** *129*, 115913.
64. Yamashita, N.; Kannan, K.; Taniyasu, S.; Horii, Y.; Okazawa, T.; Petrick, G.; Gamo, T., Analysis of perfluorinated acids at parts-per-quadrillion levels in seawater using liquid chromatography-tandem mass spectrometry. *Environmental Science & Technology* **2004,** *38* (21), 5522-5528.
65. Gremmel, C.; Frömel, T.; Knepper, T. P., HPLC–MS/MS methods for the determination of 52 perfluoroalkyl and polyfluoroalkyl substances in aqueous samples. *Analytical and Bioanalytical Chemistry* **2017,** *409* (6), 1643-1655.
66. Joerss, H.; Apel, C.; Ebinghaus, R., Emerging per- and polyfluoroalkyl substances (PFASs) in surface water and sediment of the North and Baltic Seas. *Science of The Total Environment* **2019,** *686*, 360-369.
67. Kaboré, H. A.; Vo Duy, S.; Munoz, G.; Méité, L.; Desrosiers, M.; Liu, J.; Sory, T. K.; Sauvé, S., Worldwide drinking water occurrence and levels of newly-identified perfluoroalkyl and polyfluoroalkyl substances. *Science of The Total Environment* **2018,** *616-617*, 1089-1100.
68. Winchell, L. J.; Wells, M. J. M.; Ross, J. J.; Fonoll, X.; Norton, J. W.; Kuplicki, S.; Khan, M.; Bell, K. Y., Analyses of per- and polyfluoroalkyl substances (PFAS) through the urban water cycle: Toward achieving an integrated analytical workflow across aqueous, solid, and gaseous matrices in water and wastewater treatment. *Science of The Total Environment* **2021,** *774*, 145257.

Chapter 4. Conclusion and Future Work

Industrial wastewater contains a plethora of chemicals, some of which are known to be harmful to the environment and human health, and some of which are yet to be detected, much less studied. In this thesis, wastewater samples from more than 10 industrial sectors in Ontario were analyzed for halogenated POPs using both gas chromatographic and liquid chromatographic cyclic ion mobility mass spectrometry (GC/LC-cIM-MS) methods. Comprehensive screening was achieved via targeted, suspect and non-targeted methods. NTS was performed using an innovative method that was previously established by our group to differentiate PFAS and other halogenated compounds from non-halogenated ones based on the ratio of their CCS and mass. This data prioritization strategy for identifying halogenated chemicals was simple and effective leading to an approximately 50- and 80-fold reduction in compounds for LC and GC, respectively. When combined with suspect screening, a large proportion (48-55%) of the compounds filtered by NTS remained unmatched by a PFAS suspect screening database. The implication of this is that the chemical identities of several PFAS existing in the Ontario environment today are unknown.

Although LC-ESI-MS is favored for PFAS analysis, GC-APCI-MS was shown to be a valuable and complementary technique for the detection of PFAS. GC results revealed 19 suspected PFAS, including 2 classes that were detected in the environment for the first time. Targeted analyses showed that legacy pollutants such as PBDEs, PCBs, PCNs, and OCPs were either not detected or present at low levels. Industrial sectors such as electroplating, textiles, containerboard manufacturing and petrochemical were found to be

important emitters of PFAS to the aquatic environment. The novel data prioritization approach using CCS and *m/z*, having been developed and validated on GC-APCI-cIM-MS data, was also found to be applicable to PFAS discovery in complex samples when analyzed by LC-ESI-cIM-MS despite the presence of multiply charged ions. A limitation of this was found to be whether CCS or raw DTs were used in data processing. As such, additional work needs to be performed to better characterize how data filtering is affected by using DT instead of CCS. Furthermore, the CCS calibration procedure should be extended to include multiply charged calibrants, which would enable the acquisition of more accurate CCS values for multiply charged sample ions. Nevertheless, 30 PFAS were tentatively identified using the NTS workflow. A quantitative method was also developed and validated for the targeted analysis of 16 PFAS and can be used in the future to determine the concentrations of these analytes in the wastewater samples.

In both the LC and GC analyses several PFAS were tentatively identified. Besides those pointed out, more than a hundred others prioritized by NTS remained unexamined. Several chlorinated/brominated compounds were detected as well. Future work should focus on establishing the identity of those present at high levels and/or with high detection frequencies. For the GC work, cleaner mass spectra are required for structural analysis. This could be achieved by performing sample cleanup, extending the chromatographic run time or acquiring software to make use of DT alignment. Analytical standards may then need to be purchased or synthesized to perform more targeted quantifications of the widely distributed contaminants. This would enable a more informed discussion on possible sources and uses, and then facilitate attempts to minimize emissions from specific sources.

After that, their occurrence in other environmental matrices and possibly different geographical regions could be investigated to determine their relative importance for continued research into their persistence, bioaccumulation, LRTP and toxicity.

Overall, this study highlighted the importance of regular monitoring campaigns to detect new, possibly hazardous chemicals being released by different industrial sectors. Through the use of advanced analytical techniques and data processing strategies, we were able to gain a better understanding of the types and levels of pollutants present in the industrial wastewaters of Ontario, which should ultimately lead to more effective strategies for pollution prevention and control.

Appendices

A. Appendix A

Table A.1. List of native standards with supplier information, purity and concentration.

Compound	Acronym	Supplier, purity and concentration
2-(N-ethylperfluoro-1-octanesulfonamido)-ethanol	*N*-EtFOSE	Wellington, 98%, 50 µg/mL
1,2,3,4,5,7-hexachloronaphthalene	PCN-64	Cambridge Isotope Laboratories, 100 µg/mL
1,2,3,4,5,6,7-heptachloronaphthalene	PCN-73	Cambridge Isotope Laboratories, 100 µg/mL
2,4,4'-Trichlorobiphenyl	PCB-28	BP-D7 (mixture), Wellington Laboratories, 10 µg/mL each
2,2',5,5'-Tetrachlorobiphenyl	PCB-52	
2,2',4,5,5'-Pentachlorobiphenyl	PCB-101	
2,3',4,4',5-Pentachlorobiphenyl	PCB-118	
2,2',4,4',5,5'-Hexachlorobiphenyl	PCB-153	
2,2',3,4,4',5'-Hexachlorobiphenyl	PCB-138	
2,2',3,4,4',5,5'-Heptachlorobiphenyl	PCB-180	
Phenanthrene	-	Cambridge Isotope Laboratories, 200 µg/mL
2,2',4,4'-Tetrabromodiphenyl ether	BDE-47	BDE-MXA (mixture), Wellington Laboratories, 5 µg/mL each
2,2',4,4'-Tetrabromodiphenyl ether	BDE-99	
2,2',4,4',5,5'-Hexabromodiphenyl ether	BDE-153	
Tris(1,3-dichloro-2-propyl)phosphate	TDCPP	Wellington Laboratories, 50 µg/mL
Bis(2-ethylhexyl)-3,4,5,6-tetrabromo-phthalate	BEHTBP	Wellington Laboratories, 50 µg/mL
Gamma-1,2,3,4,5,6-hexachlorocyclohexane	gamma-HCH	Cambridge Isotope Laboratories, 100 µg/mL
cis-Chlordane	-	Cambridge Isotope Laboratories, 100 µg/mL
1,1-Dichloro-2,2-bis(4-chlorophenyl)ethene	4,4'-DDE	Cambridge Isotope Laboratories, 100 µg/mL

Table A.2. List of isotopically labeled standards with supplier information, purity and concentration/amount.

Compound	Supplier, purity and concentration
$^{13}C_{10}$-PCN-64	Cambridge Isotope Laboratories, 99% $^{13}C_{10}$, 10 µg/mL
$^{13}C_{10}$-PCN-73	Cambridge Isotope Laboratories, 98% $^{13}C_{10}$, 10 µg/mL
$^{13}C_{12}$-PCB 28	MBP-D7 (mixture), Wellington Laboratories, 99% $^{13}C_{12}$, 5 µg/mL each
$^{13}C_{12}$-PCB 52	
$^{13}C_{12}$-PCB 101	
$^{13}C_{12}$-PCB 118	
$^{13}C_{12}$-PCB 153	
$^{13}C_{12}$-PCB 138	
$^{13}C_{12}$-PCB 180	
$^{13}C_{12}$-BDE 47	MBDE-MXA (mixture), Wellington Laboratories, 99% $^{13}C_{12}$, 5 µg/mL each
$^{13}C_{12}$-BDE 99	
$^{13}C_{12}$-BDE 153	
$^{13}C_{6}$-BTBPE	Wellington Laboratories, 99% $^{13}C_{6}$, 50 µg/mL
$^{13}C_{6}$-gamma HCH	Cambridge Isotope Laboratories, 99% $^{13}C_{6}$, 100 µg/mL
$^{13}C_{10}$-chlordane	Cambridge Isotope Laboratories, 99% $^{13}C_{10}$, 100 µg/mL
$^{13}C_{12}$-DDE	Cambridge Isotope Laboratories, 99% $^{13}C_{12}$, 100 µg/mL
Phenanthrene-D10	Cambridge Isotope Laboratories, D10 98%, 200 µg/mL

Table A.3. Summary of details for sampling sites in Ontario, Canada.

Sample ID	Sector	Sampling Date
R1A	Other (Printing ink)	15/09/2021
R1B	Electroplating	24/11/2021
R1C	Plastic manufacturing/recycling	29/11/2021
R1D	Other (Automotive)	?
R1E	Electroplating	01/12/2021
R1F	Computers/semiconductors	20/10/2021
R1G	Other (Cannabis production)	27/10/2021
R1H	Foam insulation	03/11/2021
R1I	Foam insulation	10/11/2021
R1J	Containerboard manufacturing	17/11/2021
WWTP (E2)	WWTPs (E)	13/09/2021
WWTP (E1)	WWTPs (E)	13/09/2021
WWTP (I2)	WWTPs (I)	13/09/2021
WWTP (I1)	WWTPs (I)	13/09/2021
R2A	Electroplating	13/09/2021
R2I	Cosmetics & personal care products	13/09/2021
R2E	Petrochemical	13/09/2021
R2F	Containerboard manufacturing	13/09/2021
R2B	Chemical manufacturing	13/09/2021
R2G	Containerboard manufacturing	13/09/2021
R2H	Textile	13/09/2021
R2D	Truck washing	13/09/2021
R2C	Chemical manufacturing	13/09/2021
R3A	Truck washing	20/09/2021
R3B	Truck washing	20/09/2021
R3C	Plastic manufacturing/recycling	21/09/2021
R3D	Other (Refrigeration)	21/09/2021
R3E	Chemical manufacturing	21/09/2021
R3F	Petrochemical	05/10/2021
R3G	Chemical manufacturing	19/10/2021
R3I	Other (Storm discharge)	19/10/2021
R4A	Computers/semiconductors	19/10/2021
R4B	Electroplating	19/10/2021
R4C	Electroplating	19/10/2021
R4D	Textile	22/10/2021
R4E	Computers/semiconductors	22/10/2021
R4F	Cosmetics & personal care products	19/10/2021

Table A.4. Method performance data for wastewater analysis via LLE and GC-HRMS (n=3).

Compound	Recovery (%)	RSD (%)	Accuracy (%)	RSD (%)	MDL (ng/L)	Linearity (R^2)	Linear range (pg/uL)
PCN-64	46.5	35.6	93.4	13.0	2.4	0.998	0.32-200
PCN-73	24.2	30.7	142.4	45.3	3.5	0.997	0.32-200
PCB 28	72.0	19.8	106.0	33.3	2.1	0.999	0.32-200
PCB 52	49.2	32.1	87.0	8.8	3.2	0.999	0.32-200
PCB 101	51.2	35.5	88.7	14.7	2.6	0.996	0.32-200
PCB 118	57.3	31.0	95.3	22.9	1.8	0.997	0.32-200
PCB 153	60.8	26.3	75.6	14.3	2.3	0.999	0.32-200
PCB 138	49.0	17.9	74.6	19.9	1.9	0.999	0.32-200
PCB 180	47.2	41.4	100.2	27.5	2.2	0.996	0.32-200
Phenanthrene	65.3	29.6	162.8	16.2	71.3	0.999	0.32-200
BDE-47	48.7	43.5	70.8	14.0	2.0	0.999	0.256-160
BDE-99	39.3	53.7	81.4	7.3	4.2	0.991	0.256-160
TDCPP	46.1	34.5	64.0	34.7	1.3	0.999	0.256-160
BEHTBP	48.1	30.4	59.4	22.7	2.8	0.990	0.256-160
gamma-HCH	51.4	31.0	88.7	7.9	10.8	0.999	0.32-200
cis-Chlordane	61.9	30.5	93.4	23.2	0.4	0.997	0.32-200
4,4'-DDE	27.4	36.8	84.4	8.1	3.0	0.999	0.32-200
BDE153	48.2	53.6	118.8	45.9	2.9	0.998	0.32-200

Table A.5. Method performance data for filter analysis via ASE and GC-HRMS (n=3).

Compound	Recovery (%)	RSD (%)	Accuracy (%)	RSD (%)	MDL (ng/L)	Linearity (R^2)	Linear range (pg/uL)
PCN-64	59.0	22.6	79.8	6.8	1.0	0.999	0.32-200
PCN-73	72.4	19.0	89.3	21.5	1.6	0.998	0.32-200
PCB 28	91.3	23.1	73.9	10.6	1.2	0.999	0.32-200
PCB 52	36.4	23.3	79.8	16.9	2.6	0.994	0.32-200
PCB 101	48.3	29.7	102.4	9.2	1.5	0.999	0.32-200
PCB 118	67.9	59.1	100.6	9.9	1.5	0.998	0.32-200
PCB 153	85.5	30.1	110.1	12.4	2.2	1.000	0.32-200
PCB 138	69.0	23.4	109.1	13.6	2.2	1.000	0.32-200
PCB 180	14.0	65.5	109.7	16.3	2.2	0.998	0.32-200
BDE-47	11.7	81.3	76.5	8.2	2.7	1.000	0.256-160
BDE-99	109.6	60.4	83.0	18.4	2.1	0.993	0.256-160
TDCPP	158.2	51.5	17.5	52.6	0.4	0.999	0.256-160
BEHTBP	81.7	40.8	64.7	17.5	1.7	0.990	0.256-160
gamma-HCH	33.0	25.4	119.1	30.7	11.5	0.998	0.32-200
cis-Chlordane	75.5	36.5	103.3	3.9	1.7	0.997	0.32-200
4,4'-DDE	80.3	43.8	95.0	5.9	1.4	0.999	0.32-200
BDE153	91.6	13.5	99.7	20.3	1.4	0.998	0.32-200

Table A.6. Concentration of targeted analytes in wastewater (ng/L) across industrial sites (n=37). Values marked by * are in between estimated MDLs and LOQs.

Compound	WWTP (E1)	WWTP (E2)	WWTP (I1)	WWTP (I2)	R2E	R2A	R2G	R2C	R2F	R2H	R2B	R2I	R2D	R3A	R3B	R3C	R3D	R3E	R3F	R3G	R3I	R1A	R1B	R1C	R1D	R1E	R1F	R1G	R1H	R1I	R1J	R4A	R4B	R4C	R4D	R4E	R4F
PCN-64	<2.4	<2.4	<2.4	<2.4	<2.4	<2.4	<2.4	<2.4	<2.4	<2.4	<2.4	<2.4	<2.4	<2.4	<2.4	<2.4	<2.4	<2.4	<2.4	<2.4	<2.4	<2.4	<2.4	<2.4	<2.4	<2.4	<2.4	<2.4	<2.4	<2.4	<2.4	<2.4	<2.4	<2.4	<2.4	<2.4	<2.4
PCN-73	<3.5	<3.5	<3.5	<3.5	<3.5	<3.5	<3.5	<3.5	<3.5	<3.5	<3.5	<3.5	<3.5	<3.5	<3.5	<3.5	<3.5	<3.5	<3.5	<3.5	<3.5	<3.5	<3.5	<3.5	<3.5	<3.5	<3.5	<3.5	<3.5	<3.5	<3.5	<3.5	<3.5	<3.5	<3.5	<3.5	<3.5
PCB-28	<2.1	<2.1	<2.1	<2.1	<2.1	<2.1	<2.1	<2.1	<2.1	<2.1	<2.1	<2.1	<2.1	<2.1	<2.1	<2.1	<2.1	<2.1	<2.1	<2.1	<2.1	<2.1	<2.1	<2.1	<2.1	<2.1	<2.1	<2.1	<2.1	<2.1	<2.1	<2.1	<2.1	<2.1	<2.1	<2.1	<2.1
PCB-52	<3.2	<3.2	<3.2	<3.2	<3.2	<3.2	<3.2	<3.2	<3.2	<3.2	<3.2	<3.2	<3.2	<3.2	<3.2	<3.2	<3.2	<3.2	<3.2	<3.2	<3.2	<3.2	<3.2	<3.2	<3.2	<3.2	4175.6	<3.2	<3.2	<3.2	<3.2	<3.2	<3.2	16.6	<3.2	<3.2
PCB-101	<2.6	<2.6	<2.6	<2.6	<2.6	<2.6	<2.6	<2.6	<2.6	<2.6	<2.6	<2.6	<2.6	<2.6	<2.6	<2.6	<2.6	<2.6	<2.6	<2.6	<2.6	<2.6	<2.6	<2.6	<2.6	<2.6	99.0	<2.6	<2.6	<2.6	<2.6	<2.6	<2.6	<2.6	<2.6	<2.6
PCB-118	<1.8	<1.8	<1.8	<1.8	<1.8	<1.8	<1.8	<1.8	<1.8	<1.8	<1.8	<1.8	<1.8	<1.8	<1.8	<1.8	<1.8	<1.8	<1.8	<1.8	<1.8	<1.8	<1.8	<1.8	<1.8	<1.8	<1.8	<1.8	<1.8	<1.8	<1.8	<1.8	<1.8	<1.8	<1.8	<1.8
PCB-153	<2.3	<2.3	<2.3	<2.3	<2.3	<2.3	<2.3	<2.3	<2.3	<2.3	<2.3	<2.3	<2.3	<2.3	<2.3	<2.3	<2.3	<2.3	<2.3	<2.3	<2.3	<2.3	<2.3	<2.3	<2.3	<2.3	<2.3	<2.3	<2.3	<2.3	<2.3	<2.3	<2.3	<2.3	<2.3	<2.3
PCB-138	<1.9	<1.9	<1.9	<1.9	<1.9	<1.9	<1.9	<1.9	<1.9	<1.9	<1.9	<1.9	<1.9	<1.9	<1.9	<1.9	<1.9	<1.9	<1.9	<1.9	<1.9	<1.9	<1.9	<1.9	<1.9	<1.9	<1.9	<1.9	<1.9	<1.9	<1.9	<1.9	<1.9	<1.9	<1.9	<1.9
PCB-180	<2.2	<2.2	<2.2	<2.2	<2.2	<2.2	<2.2	<2.2	<2.2	<2.2	<2.2	<2.2	<2.2	<2.2	<2.2	<2.2	<2.2	<2.2	<2.2	<2.2	<2.2	<2.2	<2.2	<2.2	<2.2	<2.2	<2.2	<2.2	<2.2	<2.2	<2.2	<2.2	<2.2	<2.2	<2.2	<2.2
Phenanthrene	<71.3	<71.3	<71.3	<71.3	<71.3	<71.3	<71.3	<71.3	<71.3	<71.3	<71.3	<71.3	<71.3	71.4*	<71.3	<71.3	<71.3	<71.3	<71.3	<71.3	<71.3	<71.3	<71.3	<71.3	<71.3	<71.3	2.5E+04	<71.3	<71.3	<71.3	<71.3	<71.3	<71.3	448.9	<71.3	<71.3
BDE-47	<2.0	<2.0	2.0*	3.6*	<2.0	<2.0	<2.0	<2.0	<2.0	<2.0	<2.0	<2.0	<2.0	<2.0	<2.0	9.8	<2.0	<2.0	<2.0	<2.0	<2.0	<2.0	<2.0	<2.0	<2.0	<2.0	<2.0	<2.0	<2.0	<2.0	<2.0	<2.0	<2.0	<2.0	<2.0	<2.0	<2.0
BDE-99	<4.2	<4.2	<4.2	4.3*	<4.2	<4.2	<4.2	<4.2	<4.2	<4.2	<4.2	<4.2	<4.2	<4.2	<4.2	10.9*	<4.2	<4.2	<4.2	<4.2	<4.2	<4.2	<4.2	<4.2	<4.2	<4.2	<4.2	<4.2	<4.2	<4.2	<4.2	<4.2	<4.2	<4.2	<4.2	<4.2	<4.2
TDCPP	201.6	85.0	98.6	17.6	2.5*	6.8	14.9	7.3	6.4	18.7	<1.3	<1.3	<1.3	3.9*	<1.3	40.4	3.6*	42.6	1.4*	3.1*	4.9	18.6	2.3*	11.2	4.5	3.5*	<1.3	<1.3	74.2	<1.3	<1.3	27.4	8.9	70.0	<1.3	35.2	11.5
BEHTBP	<2.8	<2.8	<2.8	<2.8	<2.8	<2.8	<2.8	<2.8	<2.8	<2.8	<2.8	<2.8	<2.8	<2.8	<2.8	<2.8	<2.8	<2.8	<2.8	<2.8	<2.8	<2.8	<2.8	<2.8	<2.8	<2.8	<2.8	<2.8	<2.8	<2.8	<2.8	<2.8	<2.8	<2.8	<2.8	<2.8	<2.8
gamma-HCH	<10.8	<10.8	<10.8	<10.8	<10.8	<10.8	<10.8	<10.8	<10.8	<10.8	<10.8	<10.8	<10.8	<10.8	<10.8	<10.8	<10.8	<10.8	<10.8	<10.8	<10.8	<10.8	<10.8	<10.8	<10.8	<10.8	<10.8	<10.8	<10.8	<10.8	<10.8	<10.8	<10.8	<10.8	<10.8	<10.8	<10.8
cis-Chlordane	<0.4	<0.4	<0.4	<0.4	<0.4	<0.4	<0.4	<0.4	<0.4	<0.4	<0.4	<0.4	<0.4	<0.4	<0.4	<0.4	<0.4	<0.4	<0.4	<0.4	<0.4	<0.4	<0.4	<0.4	<0.4	<0.4	<0.4	<0.4	<0.4	<0.4	<0.4	<0.4	<0.4	<0.4	<0.4	<0.4	<0.4
4,4'-DDE	<3.0	<3.0	<3.0	<3.0	<3.0	<3.0	<3.0	<3.0	<3.0	<3.0	<3.0	<3.0	<3.0	<3.0	<3.0	<3.0	<3.0	<3.0	<3.0	<3.0	<3.0	<3.0	<3.0	<3.0	<3.0	<3.0	<3.0	<3.0	<3.0	<3.0	<3.0	<3.0	<3.0	<3.0	<3.0	<3.0	<3.0
BDE153	<2.9	<2.9	<2.9	<2.9	<2.9	<2.9	<2.9	<2.9	<2.9	<2.9	<2.9	<2.9	<2.9	<2.9	<2.9	<2.9	<2.9	<2.9	<2.9	<2.9	<2.9	<2.9	<2.9	<2.9	<2.9	<2.9	<2.9	<2.9	<2.9	<2.9	<2.9	<2.9	<2.9	<2.9	<2.9	<2.9	<2.9

Table A.7. Approximate concentrations of targeted analytes in filter papers (ng/L) across industrial sites (n=31). These estimates were obtained by normalizing analyte concentrations in extracts to approximate volume of water filtered through each filter paper. Values marked by * are in between estimated MDLs and LOQs.

Compound	WWTP (E1)	WWTP (E2)	WWTP (I1)	WWTP (I2)	R2E	R2A	R2G	R2C	R2F	R2H	R2B	R2I	R2D	R3A	R3B	R3C	R3D	R3E	R3F	R3G	R3I	R1A	R1B	R1C	R1D	R1H	R1I	R1J	R4B	R4C	R4D
PCN-64	<1.0	<1.0	<1.0	<1.0	<1.0	<1.0	<1.0	<1.0	<1.0	<1.0	<1.0	<1.0	<1.0	<1.0	<1.0	<1.0	<1.0	<1.0	<1.0	<1.0	<1.0	<1.0	<1.0	<1.0	<1.0	<1.0	<1.0	<1.0	<1.0	<1.0	<1.0
PCN-73	<1.6	<1.6	<1.6	<1.6	<1.6	<1.6	<1.6	<1.6	<1.6	<1.6	<1.6	<1.6	<1.6	<1.6	<1.6	<1.6	<1.6	<1.6	<1.6	<1.6	<1.6	<1.6	<1.6	<1.6	<1.6	<1.6	<1.6	<1.6	<1.6	<1.6	<1.6
PCB-28	<1.2	<1.2	<1.2	<1.2	<1.2	<1.2	<1.2	<1.2	<1.2	<1.2	<1.2	<1.2	<1.2	<1.2	<1.2	<1.2	<1.2	<1.2	<1.2	<1.2	<1.2	<1.2	<1.2	<1.2	<1.2	<1.2	<1.2	<1.2	<1.2	<1.2	<1.2
PCB-52	<2.6	<2.6	<2.6	<2.6	<2.6	<2.6	<2.6	<2.6	<2.6	<2.6	<2.6	<2.6	<2.6	<2.6	<2.6	<2.6	<2.6	<2.6	<2.6	<2.6	<2.6	<2.6	<2.6	<2.6	3.6*	<2.6	<2.6	<2.6	<2.6	<2.6	<2.6
PCB-101	<1.5	<1.5	<1.5	<1.5	<1.5	<1.5	<1.5	<1.5	<1.5	<1.5	<1.5	<1.5	<1.5	<1.5	<1.5	<1.5	<1.5	<1.5	<1.5	<1.5	<1.5	<1.5	<1.5	<1.5	18.5	<1.5	<1.5	<1.5	<1.5	<1.5	<1.5
PCB-118	<1.5	<1.5	<1.5	<1.5	<1.5	<1.5	2.0*	<1.5	<1.5	<1.5	<1.5	<1.5	<1.5	<1.5	<1.5	<1.5	<1.5	<1.5	<1.5	<1.5	<1.5	<1.5	<1.5	<1.5	7.5	<1.5	<1.5	<1.5	<1.5	<1.5	<1.5
PCB-153	<2.2	<2.2	<2.2	<2.2	<2.2	<2.2	<2.2	<2.2	<2.2	<2.2	<2.2	<2.2	<2.2	<2.2	<2.2	<2.2	<2.2	<2.2	<2.2	<2.2	<2.2	<2.2	<2.2	<2.2	16.6	<2.2	<2.2	<2.2	<2.2	<2.2	<2.2
PCB-138	<2.2	<2.2	<2.2	<2.2	5.2*	<2.2	4.0*	<2.2	<2.2	<2.2	<2.2	<2.2	<2.2	<2.2	<2.2	<2.2	<2.2	<2.2	<2.2	<2.2	<2.2	<2.2	<2.2	<2.2	22.6	<2.2	<2.2	<2.2	<2.2	<2.2	<2.2
PCB-180	<2.2	<2.2	<2.2	<2.2	<2.2	<2.2	<2.2	<2.2	<2.2	<2.2	<2.2	<2.2	<2.2	<2.2	<2.2	<2.2	<2.2	<2.2	<2.2	<2.2	<2.2	<2.2	<2.2	<2.2	<2.2	<2.2	<2.2	<2.2	<2.2	<2.2	<2.2
BDE-47	<2.7	<2.7	<2.7	<2.7	31.6	<2.7	16.0	<2.7	13.8	6.2*	<2.7	<2.7	<2.7	<2.7	<2.7	<2.7	<2.7	<2.7	<2.7	<2.7	<2.7	<2.7	<2.7	<2.7	<2.7	<2.7	<2.7	<2.7	<2.7	<2.7	<2.7
BDE-99	<2.0	<2.0	<2.0	<2.0	<2.0	<2.0	<2.0	<2.0	<2.0	6.8	<2.0	<2.0	<2.0	<2.0	<2.0	<2.0	<2.0	<2.0	<2.0	<2.0	<2.0	<2.0	<2.0	<2.0	<2.0	<2.0	<2.0	<2.0	<2.0	<2.0	<2.0
TDCPP	<0.4	0.7*	<0.4	<0.4	<0.4	<0.4	<0.4	<0.4	<0.4	1.3*	<0.4	<0.4	<0.4	<0.4	<0.4	<0.4	<0.4	<0.4	<0.4	<0.4	<0.4	<0.4	<0.4	<0.4	<0.4	3.0	<0.4	2.4	<0.4	<0.4	<0.4
BEHTBP	<1.7	<1.7	<1.7	<1.7	<1.7	<1.7	<1.7	<1.7	<1.7	<1.7	<1.7	<1.7	<1.7	<1.7	<1.7	<1.7	<1.7	<1.7	<1.7	<1.7	<1.7	<1.7	<1.7	<1.7	<1.7	<1.7	<1.7	<1.7	<1.7	<1.7	<1.7
gamma-HCH	<11.5	<11.5	<11.5	<11.5	<11.5	<11.5	<11.5	<11.5	<11.5	<11.5	<11.5	<11.5	<11.5	<11.5	<11.5	<11.5	<11.5	<11.5	<11.5	<11.5	<11.5	<11.5	<11.5	<11.5	<11.5	<11.5	<11.5	<11.5	<11.5	<11.5	<11.5
cis-Chlordane	<1.7	<1.7	<1.7	<1.7	<1.7	<1.7	<1.7	<1.7	<1.7	<1.7	<1.7	<1.7	<1.7	<1.7	<1.7	<1.7	<1.7	<1.7	<1.7	<1.7	<1.7	<1.7	<1.7	<1.7	<1.7	<1.7	<1.7	<1.7	<1.7	<1.7	<1.7
4,4'-DDE	<1.4	<1.4	<1.4	<1.4	<1.4	<1.4	<1.4	<1.4	<1.4	<1.4	<1.4	<1.4	<1.4	<1.4	<1.4	<1.4	<1.4	<1.4	<1.4	<1.4	<1.4	<1.4	<1.4	<1.4	<1.4	<1.4	<1.4	<1.4	<1.4	<1.4	<1.4
BDE153	<1.4	<1.4	<1.4	<1.4	<1.4	<1.4	<1.4	<1.4	<1.4	<1.4	<1.4	<1.4	<1.4	<1.4	<1.4	<1.4	<1.4	<1.4	<1.4	<1.4	<1.4	<1.4	<1.4	<1.4	<1.4	<1.4	<1.4	<1.4	<1.4	<1.4	<1.4

Table A.8. Summary of descriptive statistics for concentrations of analytes in wastewater (ng/L) with DF ≥ 1. For DF=1, minimum value is the estimated MDL.

Compound	Min	Q1	Median	Mean	Q3	Max	DF
PCB-52	16.6	1056.3	2096.1	2096.1	3135.9	4175.6	2
PCB-101	2.6	-	-	-	-	99.0	1
Phenanthrene	71.4	260.2	448.9	8604.5	12871.1	25293.3	3
BDE-47	2.0	2.8	3.6	5.1	6.7	9.8	3
BDE-99	4.3	6.0	7.6	7.6	9.2	10.9	2
TDCPP	1.4	4.3	11.4	29.5	36.5	201.6	28

Table A.9. Summary of descriptive statistics for concentrations of analytes in filter papers (ng/L) with DF ≥ 1. For DF=1, minimum value is the estimated MDL.

Compound	Min	Q1	Median	Mean	Q3	Max	DF
PCB-52	2.6	-	-	-	-	3.6	1
PCB-101	1.5	-	-	-	-	18.5	1
PCB-118	2.0	3.4	4.8	4.8	6.1	7.5	2
PCB-153	2.2	-	-	-	-	16.6	1
PCB-138	4.0	4.6	5.2	10.6	13.9	22.6	3
BDE-47	6.2	11.9	14.9	16.9	19.9	31.6	4
BDE-99	2.0	-	-	-	-	6.8	1
TDCPP	0.7	1.2	1.9	1.8	2.5	3.0	4

B. Appendix B

Table B.1. List of native and isotopically standards with supplier information, purity and concentration.

Type	Compound	Abbreviation	Supplier	Purity (%)	Concentration (ug/mL)	CAS Number
Native	Perfluorohexanoic acid	PFHxA	Chromatographic Specialties Inc	100	2.012	307-24-4
Native	Perfluoroheptanoic acid	PFHpA		99	2.016	375-85-9
Native	Perfluorooctanoic acid	PFOA		100	2.004	335-67-1
Native	Perfluorononanoic acid	PFNA		97	2.018	375-95-1
Native	Perfluorodecanoic acid	PFDA		98	1.976	335-76-2
Native	Perfluoroundecanoic acid	PFUdA		95	2.01	2058-94-8
Native	Perfluorododecanoic acid	PFDoA		100	2.02	307-55-1
Native	Perfluorotridecanoic acid	PFTrDA		100	2.032	72629-94-8
Native	Perfluorotetradecanoic acid	PFTeDA		97	2.01	376-06-7
Native	Perfluorobutane sulfonic acid	PFBS		100	2.032	375-73-5
Native	Perfluorohexane sulfonic acid (Linear 88% and Branched 12%)	PFHxS		100	2.012	355-46-4
Native	Perfluorooctane sulfonic acid (Linear 71% and Branched 29%)	PFOS		100	2.04	1763-23-1
Native	N-ethylperfluorooctanesulfonamidoacetic acid (linear)	N-EtFOSAA		94.4	2.009	2991-50-6
Native	N-methylperfluorooctanesulfonamidoacetic acid (linear)	N-MeFOSAA		99.6	2.02	2355-31-9
Native	4,8-Dioxa-3H-perfluorononanoic acid (PFECAs)	ADONA		98	2.031	919005-14-4
Native	11-Chloroeicosafluoro-3-oxaundecane sulfonic acid	8:2 Cl-PFESA		98	2.023	763051-92-9
Native	9-Chlorohexadecafluoro-3-oxanone sulfonic acid	6:2 Cl-PFESA		98	2.002	756426-58-1
Native	Perfluoro(2-methyl-3-oxahexanoic) acid (PFECAs)	HFPO-DA/Gen X		95.7	2.029	13252-13-6
Native	Perfluorooctane sulfonamide	FOSA	TRC	95	-	754-91-6
Surrogate	Sodium perfluoro-1-[1,2,3,4-13C4]-octanesulfonate	13C4-PFOS	Wellington	98	50	960315-53-1
Surrogate	Perfluoro-n-[1,2,3,4-13C4]octanoic acid	13C4-PFOA	Wellington	98	50	960315-48-4
Injection	Sodium perfluoro-1-[1,2,3-13C3]-hexanesulfonate	13C3-PFHxS	Wellington	>99	50	2708218-86-2

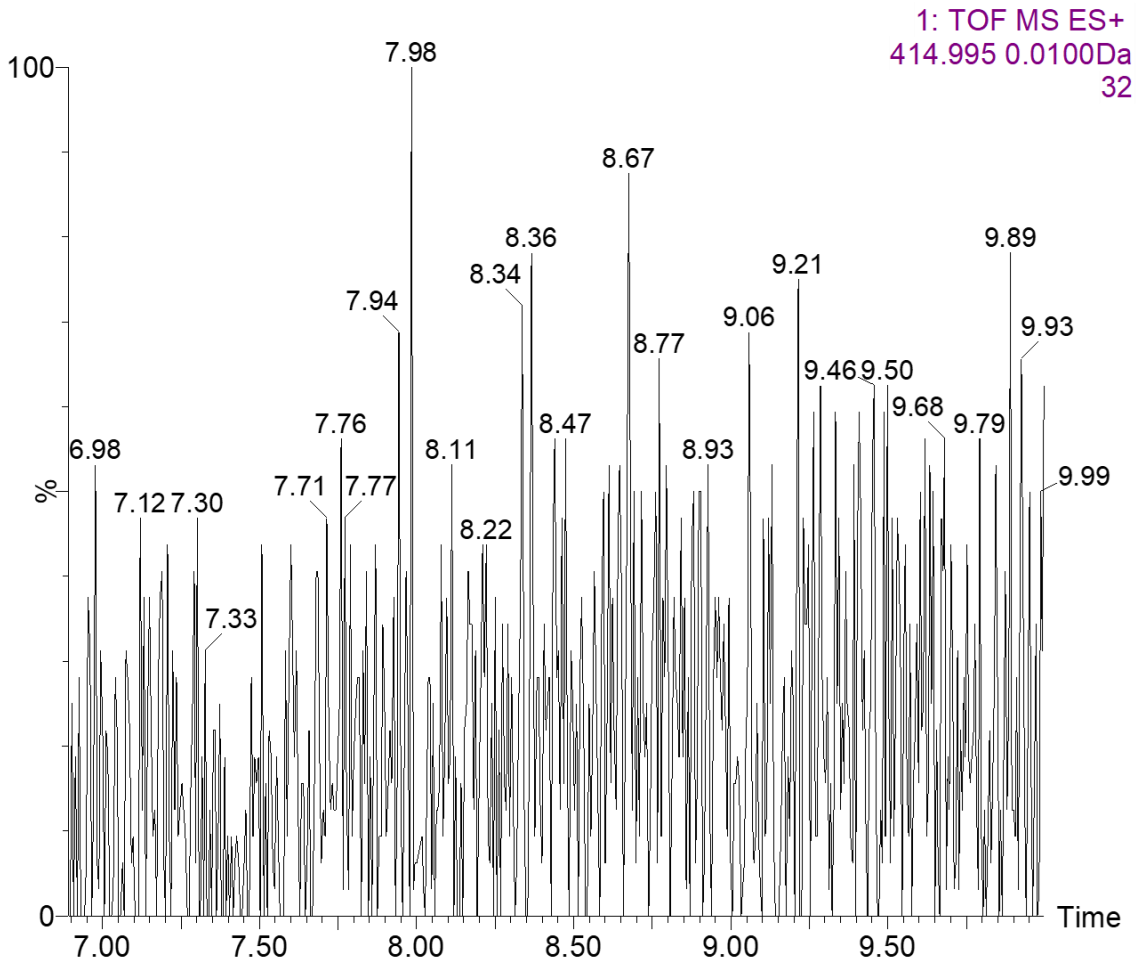

Figure B.1. Extracted ion chromatogram (XIC) for a background signal (8.23_414.9953m/z) remaining after blank subtraction in the GC-APCI-cIM-MS dataset**.**

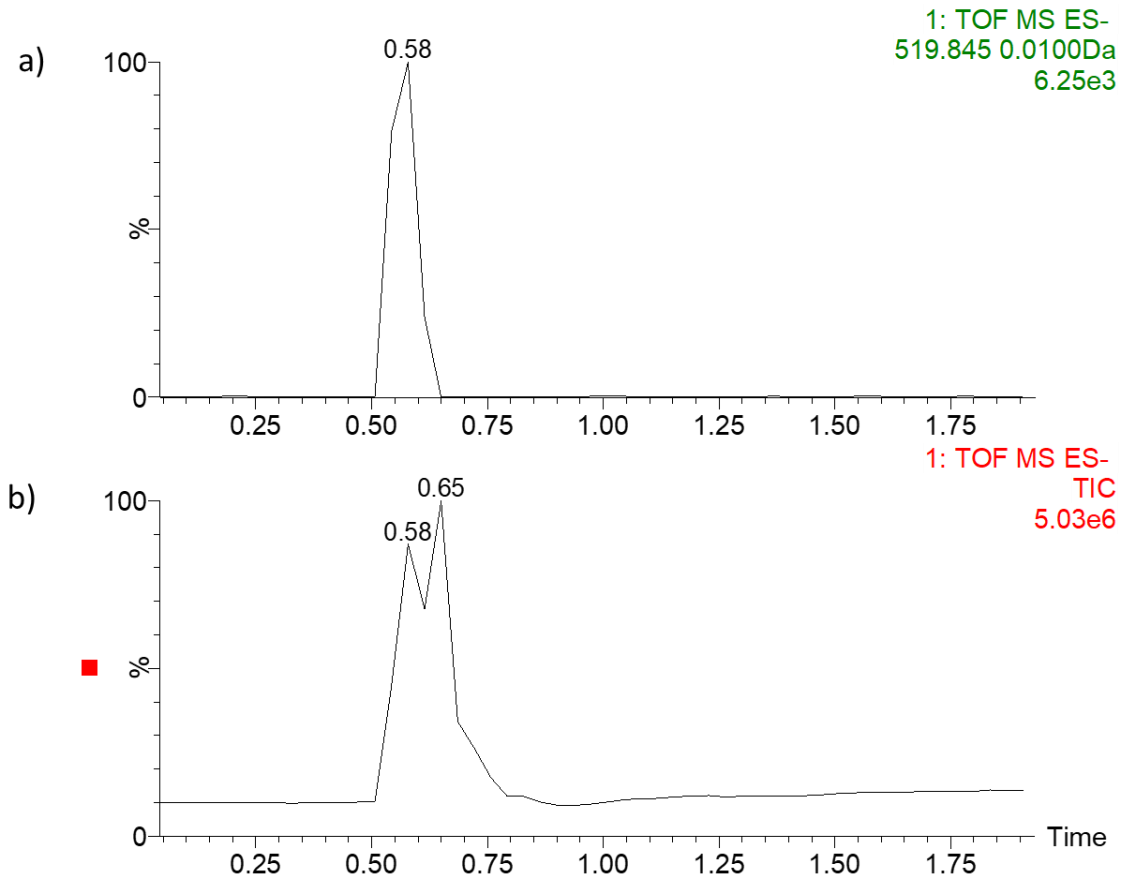

Figure B.2. (a) Extracted ion chromatogram (XIC) for a background signal (0.54_519.8446m/z) remaining after blank subtraction in the LC-APCI-cIM-MS dataset **(b)** Total ion chromatogram showing the ion's likely origin from the solvent peak.

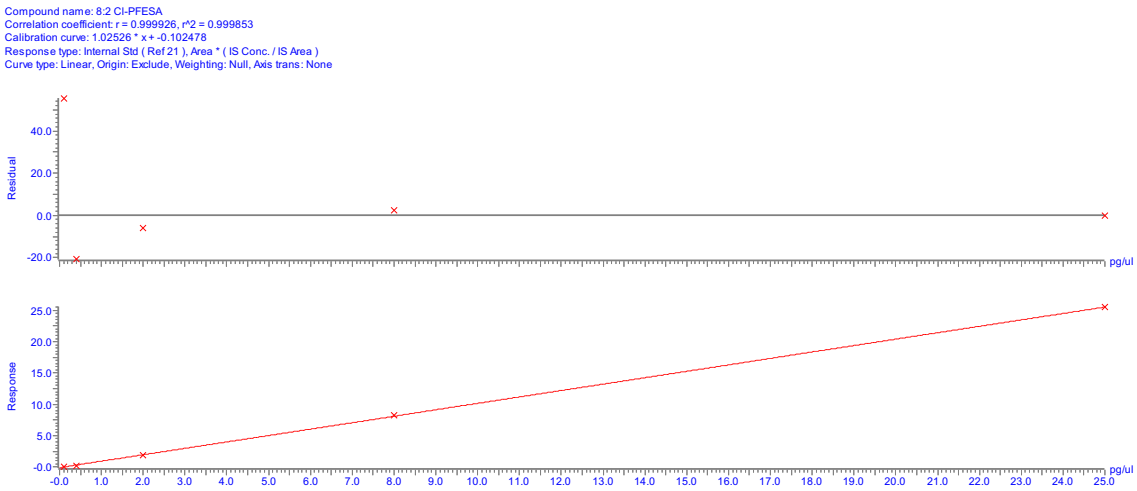

Figure B.3. Internal standard calibration curve for the emerging and replacement PFAS 8:2 Cl-PFESA (8:2 Chlorinated perfluoroether sulfonic acid)**.**

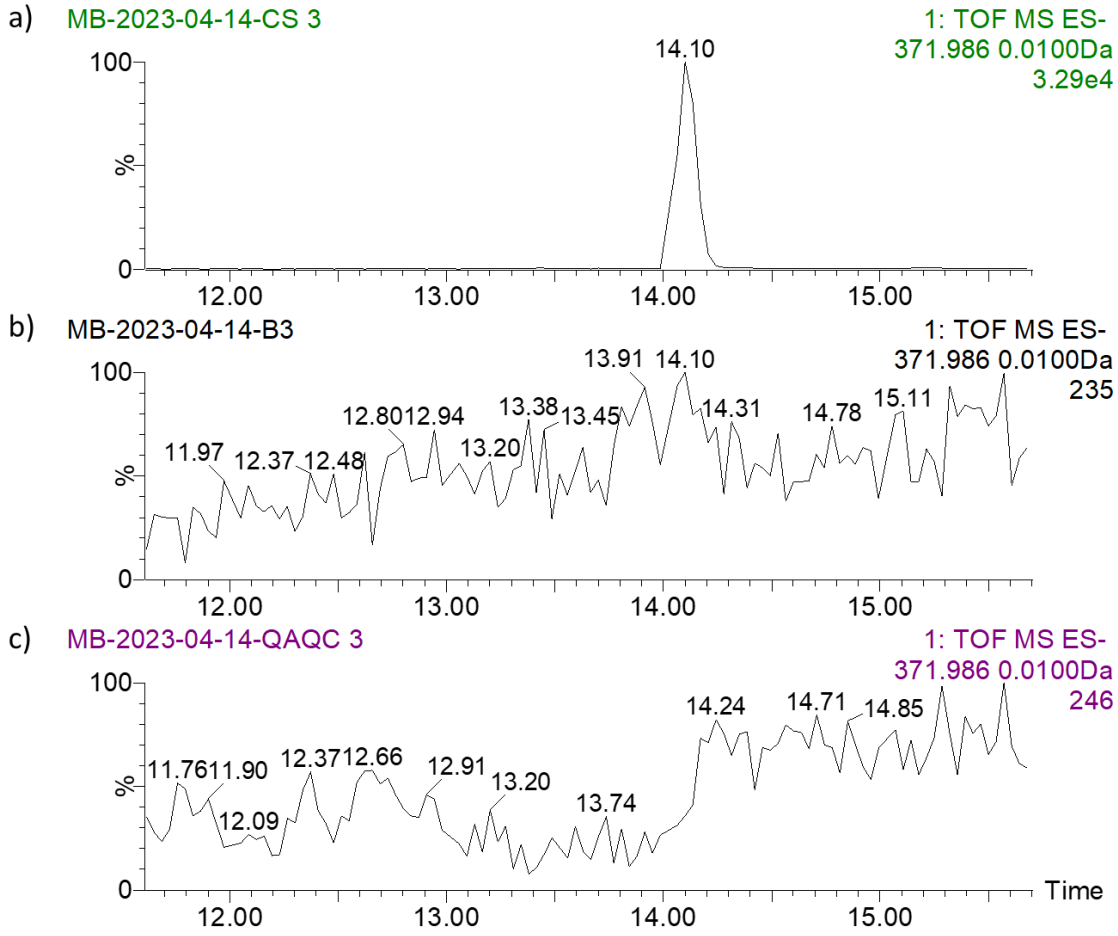

Figure B.4. Extracted ion chromatogram (XIC) for $^{13}C_4$-PFOA (14.10_371.986) in (a) Recovery standard 2 pg/µL (b) Blank 3 and (c) Spiked sample 3 showing signal suppression.